Effects of extrusion conditions on "Die Pick-Up" formed during extrusion of aluminium alloy AA6060

Robbie Gavin Peris

Thesis submitted in partial fulfilment
of Master of Engineering

AUT University
Auckland

March, 2007

Acknowledgments

I would like to take this opportunity to thank the following individuals for their contribution towards the success of this project.

Firstly I would like to thank my supervisor Associate Professor Dr. Zhan Chen for his guidance, patience and expertise which was a great help right throughout the project duration.

Then I would like to thank Mr. Cliff Hand, Operations Manager and Mr. Sen Chen, Product Development Manager at Fletcher Aluminium for providing me the opportunity to work at Fletcher Aluminium and for their guidance throughout the project.
Research fellow Dr. Timotius Pasang was a great help for his knowledge on material science.

Next I would like to thank Mr. Josh Mainwaring, Extrusion Manager and Mr. Bill Hayward, Metallurgist at Fletcher Aluminium for their expertise and assistance to complete the experiment for the project.

Then I would like to thank all the technicians and operators at Fletcher Aluminium and the technicians at AUT University for their patience and valuable help.

Finally I would like to thank my parents and my girl friend for their assistant and encouragement during the project period.

Abstract

Extrusion is a continuous solid state deformation process which is widely used in the aluminium industry. The demand for aluminium extrudates are growing and extruders are pressurized to extrude products as fast as possible without lowering the quality of the product. Important extrusion parameters and conditions are exit temperature, extrusion speed and alloy composition. It is widely accepted in extrusion industry that extrusion surface defects increase when the extrusion speed and exit temperature are increased for a constant alloy. One of the major surface defects is the so-called die pick-up and it is presently uncertain if increase with extrusion speed (from a low 25m/min) would result in an increase of the number of die pick-up defect.

Die pick-up appears like a scratch mark or comet on the surface of the extrudate which damages the appearance. Previous research suggests that second phase particles, eutectic reactions (555°C – 600°C), extrusion process conditions and die conditions may influence the cause of die pick-up. However the influencing factors for die pick-up are not well established.

The research started by determining the lowest melting temperature for AA6060 alloy as this temperature limit the highest temperature above which incipient melting starts. This temperature corresponds to the eutectic melting temperature for AA6060 alloy. Eutectic melting was only detected above 610°C and therefore the exit temperature could be increased to a maximum of 610°C. For an AA6xxx alloy system the lowest melting temperature is 555°C if Mg_2Si and excess silicon were present. However as Mg_2Si may have fully dissolved into the solid solution, no $\beta + Mg_2Si \rightarrow Liq$ reaction can take place.

A preliminary investigation was conducted to study the characteristics of the newly installed extrusion control and monitoring system. Through this study the relationship between the set extrusion speed and the actual extrusion speed was established. It was found that the actual extrusion speed was lower than the set extrusion speed and was further complicated by the capacity limit of the extrusion pressure. Exit temperature measurements were accurate, however it was measured about 1m away from the die exit. Experiments

were carried out to estimate the exit temperature drop and hence the exit temperature measurements were corrected accordingly.

Thus, the aim of the present research was to establish the relationship between die pick-up and extrusion conditions (extrusion speed, exit temperature and die condition) and to propose the likely formation mechanism for die pick-up.

In this research AA6060 alloy was used and was extruded at 25m/min, 30m/min, 35m/min, 40m/min and 45m/min. The exit temperature was found to increases from 542°C to 567°C. Three types of die pick-up was identified which were named as ***normal pick-up***, ***die line pick-up*** and ***lump pick-up***. Normal pick-up occurred regardless of the extrusion speed and exit temperature; however the amount of normal pick-up did not increase when the extrusion speed was increased. Die line pick-up occurred when the extrusion speed was 45m/min and appeared only on the die lines. Lump pick-up is not significant since it was very rare.

AA6060 (0.4%Mg and 0.5%Si) alloy has about 0.27% excess silicon and therefore at 555°C, Mg_2Si particles react with aluminium and excess silicon to form liquid. However normal pick-up and die line pick-up still occurred at temperatures lower and higher than 555°C and therefore it confirms that eutectic reactions do not influence formation of pick-up. Therefore die pick-up is most likely to be caused due to a mechanical process rather than a metallurgical process.

Table of Contents

List of Figures

List of Tables

Statement of Originality

"I hereby declare that this submission is my own work and that, to the best of my knowledge and belief it contains no material previously published or written by another person nor material which to a substantial extent has been accepted for the qualification of any other degree or diploma of a university or other institution of higher learning, except where due acknowledgement is made in the acknowledgements."

……(signed)

...……(date)

1 Introduction

1.1 Introduction to Extrusion

Aluminium is one of the most consumed metals in the world only second to steel since being first produced a century ago. As shown in Figure 1 the global consumption has grown dramatically and is expected to grow at a similar pace. Applications of aluminium vary from household products to aerospace products due to its low weight and excellent strength.

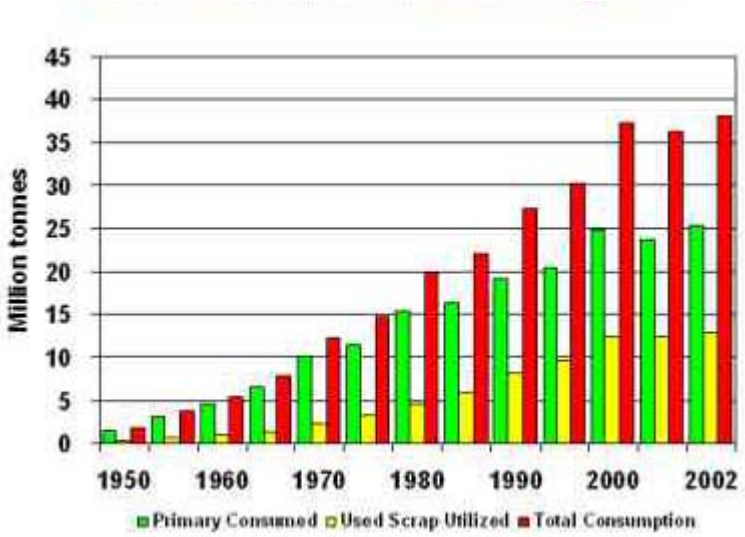

Figure 1 Global Aluminium Consumption [1]

Almost 50% of the aluminium consumed annually is used in the extrusion industry [2]. In the extrusion industry AA6xxx series alloy is the major alloy used due to its high extrudability. Fletcher aluminium is extruder located in Auckland New Zealand. Almost 90% of its production consists of AA6060 alloy. Due to its growing demand, Fletcher aluminium has to increase the production while producing high quality products. The scrap generated at Fletcher aluminium is mainly due to surface defects such as die lines, die pick up, blisters, flow lines and tearing. Extrusion temperature, extrusion speed, homogenization condition, pre heat condition, die bearing condition are some of the causes of these surface defects [3].

This study focused on the effect of extrusion parameters on surface defects. Thus it is very important to know the entire extrusion process at Fletcher aluminium to understand what factors may influence the formation of surface defects. The process consists of casting, homogenization, pre-heating, extruding, stretching, ageing and anodizing.

However the casting and homogenization process are outsourced. Figure 2 shows a typical procedure carried out during an extrusion process.

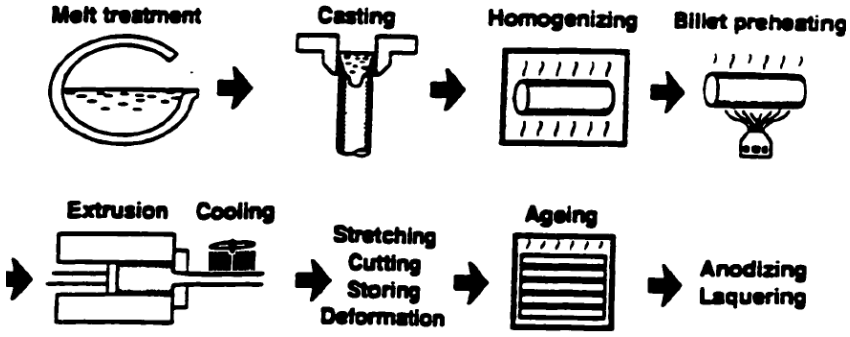

Figure 2 Production of Extrusion [4]

1.1.1 Casting, homogenization and pre-heat process

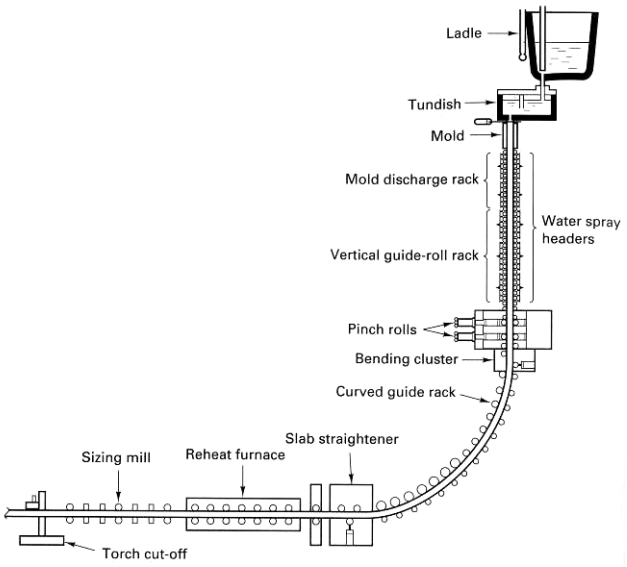

Figure 3 Continuous Casting [5]

Figure 3 shows a schematic diagram of the continuous casting process which is used to produced aluminium billet for extrusion. This process has been developed to overcome many difficulties related to ingot manufacture such as piping, entrapped slag and structure variation along the length [5]. When the aluminium melt has achieved the right composition, the molten metal is flowed from the ladle through the tundish into a bottomless water cooled mould.

Usually this mould is made of copper. The molten metal is cooled in such away that the outside solidifies before the metal exits the mould. This solidifying metal is sent

through a short reheat furnace and cut into desired lengths. These desired lengths are called as logs. At Fletcher aluminium the logs are 7m in length and 202mm in diameter.

Homogenizing is the first thermal treatment applied to extrusion logs to improve the extrudability. The microstructure of the cast condition is quite heterogeneous and has a cored dendritic structure with solute content increasing from centre to edge with an interdendritic distribution of second phase particles [6]. During this process the logs are heated to 565°C – 595°C for 1 – 3 hours. The main outcome of this process is to transform β-AlFeSi into α-AlFeSi [7]. The structure of β-AlFeSi is needle shaped and α-AlFeSi are more globular. Therefore globular α-AlFeSi particles promote better workability. The other outcome of homogenization is to dissolve magnesium silicide (Mg_2Si). Mg_2Si is the principal strengthening agent in AA6xxx alloy. During the homogenization process Mg_2Si may not be fully dissolved in some cases and the sizes of the Mg_2Si particles should be in a state where it could be completely dissolve during the extrusion.

Pre-heating of logs is done just before extrusion. Figure 4 shows logs being loaded on the rollers to be sent to the furnace for pre-heating.

Figure 4 Logs being loaded to the Pre Heat Furnace

Figure 5 shows the pre-heating furnace at Fletcher aluminium which is gas fired and approximately 11m in length.

Figure 5 Pre-Heat Furnace

This pre-heat furnace has a three-stage heating system where the logs are heated up gradually to its desired final temperature. At end of each stage the temperature is measured by a thermocouple probe to give a feedback to the furnace. It takes roughly about 20 – 30 minutes for the pre-heating process to complete. The final pre-heat temperature setting varies between 430°C – 470°C depending on the profile to be extruded. It is general practice at Fletcher to have a high final pre heat temperature for complex geometry to ease the extrusion. The main purpose of pre heating is to lower the strength and to increase the plasticity of the logs before extrusion. Pre-heating is also used to transform any remaining β-AlFeSi into α-AlFeSi and to further dissolve remaining Mg_2Si after the homogenization process.

1.1.2 Extrusion and post extrusion processes

At the end of the pre heating process the logs are sheared to 570mm – 600mm in length. At this stage they are called as billets. The length of the billets depends on the cross sectional area of the profile and length of the extrusion.

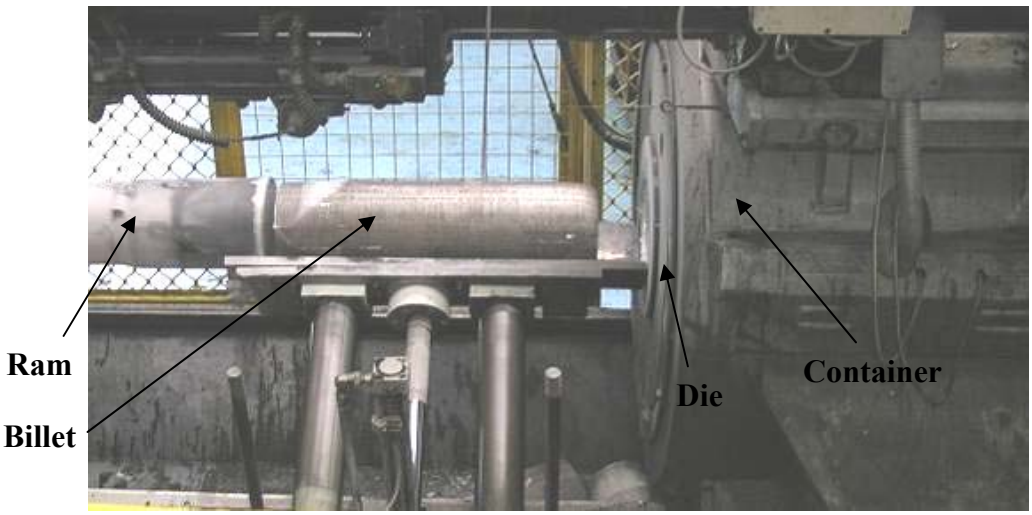

Figure 6 Billet being loaded on to the extrusion press

Figure 6 shows a typical billet being loaded on to the extrusion press. The billet is then pushed into the container where a die is located by the ram. As the ram advances the pressure builds up until the material flows plastically through the die. As the material flows through the die the temperature of the metal increases and stabilizes. Typically the exit temperature could rise up to 565°C depending on the extrusion speed which could be 20m/min – 35m/min. The extrusion speed depends on the profile of the extrusion. The exit temperature always lies between the solvus and solidus temperature and well below the liquidus temperature. Figure 7 shows a typical profile being extruded.

Figure 7 Metal flowing (extrudate) at the exit door

During extrusion it is expected that Mg_2Si particles are fully dissolved for AA6060 alloy and will precipitate if there is inadequate cooling after extrusion. However since there is less Mg_2Si particles present in AA6060 alloy system, air cooling is sufficient to prevent Mg_2Si particles being precipitating.

For quality assurance purposes, samples of the first few extrusions are taken for visual inspection. Surface tearing, flow lines, excessive die lines and excessive die pick up are checked at this stage. Depending on judgement of the operators, it is decided whether the die needs to be changed or not.

Once the extrudates are cooled down to room temperature the products are stretched by 1% - 3%. This process is also known as strain hardening or cold working which increases the yield strength of the extrusion products, but the amount of increase in yield strength is not significant. During the extrusion process the product usually has a slight curvature along the length. Therefore the stretching process is also used to make the product straighter. After the stretching the extrusion product is sent for cutting. The end bits of the extrusion are always discarded because it gets damaged during the stretching. This occurs because the machine clamps the extrusion from each ends with teeth featured grips and squashes the products. The extrusion is cut into 5m lengths and stored on the racks to be sent for ageing.

Ageing process is also known as precipitation heat treatment. During this process the strength of the extrusion product increases. At Fletcher the ageing process varies depending on the strength requirement. Generally the extrusions are heated up to 185°C – 215°C for 2 – 5 hours. Depending on the ageing process parameters the ultimate strength could vary between 180 – 210 MPa for AA6060 alloy. The temperature and time are very critical for this process. If the extrusions are aged for too long the tensile strength will decrease. To get an optimum ageing process Mg_2Si particles have to be fully dissolved during the extrusion process as mentioned in section 1.1.2. During the ageing process Mg_2Si particles precipitates from the solid solution and hence the tensile strength increases. The tensile strength will increase until the Mg_2Si particles grow to certain size. Once the Mg_2Si particles exceed this optimum size the tensile strength decreases. This process is governed by diffusion of Mg and Si elements. Therefore it is very essential to control the temperature and time during the ageing process as well as the size of the Mg_2Si particles during extrusion.

The anodizing or powder coating process is the last treatment the extrusion will undergo after age hardening. The customer requirement determines which process to be used.

Before the extrudates are anodized they are cleaned with weak and strong etching solution (NaOH) alkaline at 50°C±1 and 60°C±5 respectively. Then the extrudates are rinsed with water. Then again the extrudates are etched with strong NaOH at 60°C±5 and rinsed. Next the products are sent through sulphuric (H_2SO_4) and nitric acid (HNO_3) at ambient temperature and rinsed. Then the products are anodized using H_2SO_4 at 18°C±5 and rinsed. If the products are needed to be coloured it is done by using a solution containing sulphuric acid, sulphosalicylic, sulphate stannous and ferrous at 18°C±5 and rinsed. Then it is sealed by using nickel salt and ammonium bifluoride at 22°C±2. Finally the products are hot rinsed at 60°C±5.

Powder coating is done after the extrusions have been etched in NaOH. This process uses an electrostatic powder which is mixed with air from a small fluidized bed in a powder feed hopper. The feed hopper has a vibration motion to prevent clogging of powder before entering into the transport lines. The powder is sent by a hose to the spray gun which has a charged electrode in the nozzle fed by a high dc voltage. The film thickness depends on the powder chemistry, pre heat temperature and dwell time which could vary from 37.5µm to 125µm for cold products and from 500µm to 600µm for preheated products. Once the extrudates are uniformly coated with the powder the extrudates are sent for curing. This is done in an electric furnace. The curing temperature varies at 140°C – 220°C for 15 – 30minutes.
When anodizing or powder coating is completed the extrusion products are sent for packing and dispatched to the customers.

1.2 Thermal Cycles

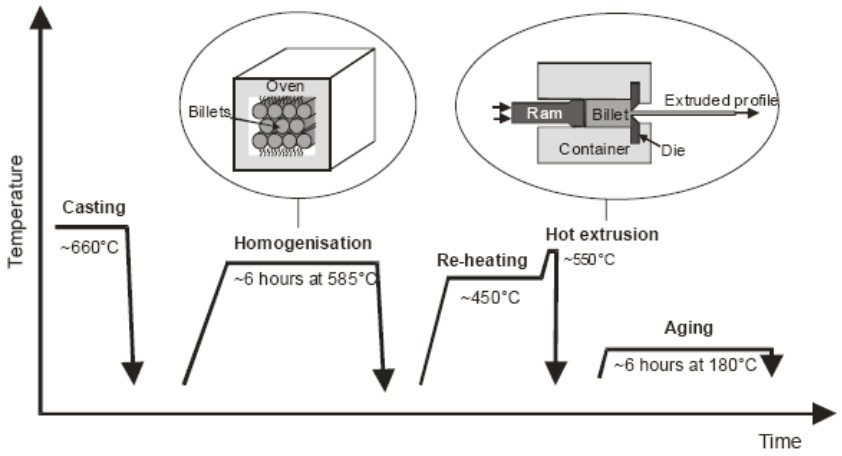

Figure 8 Thermal cycles for extrusion process [8]

Figure 8 illustrates a typical thermal cycle for a hot extrusion process from casting to ageing. The duration and temperature vary depending on the alloy and product profile. As mentioned before, this study is to assess the effects of extrusion parameters on surface defects and hence the temperature variation with time is very important. The extrusion logs (AA6060) supplied to Fletcher aluminium are homogenized at 575°C for 2 hours. However the pre-heat temperature and exit temperature vary depending on the product profile.

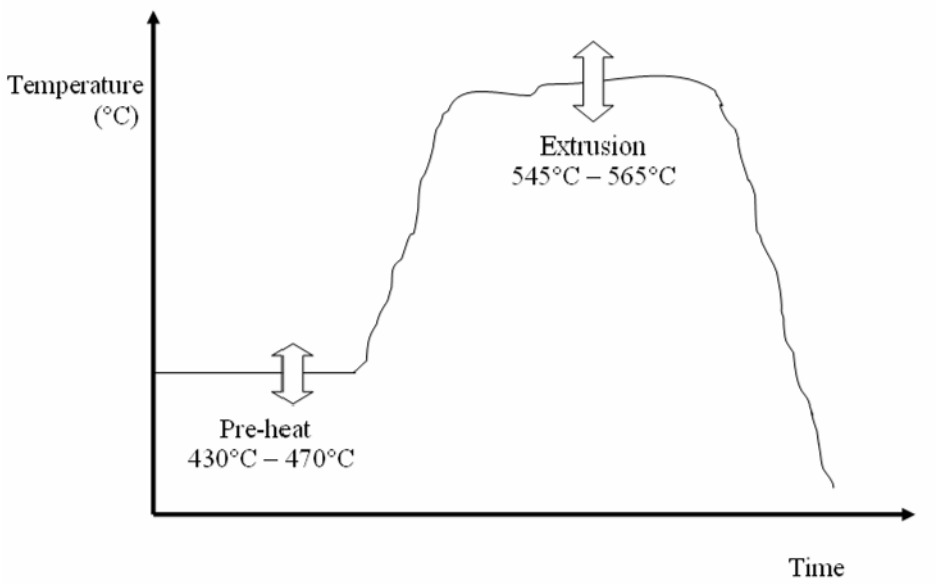

Figure 9 Pre-heat and extrusion thermal cycle

Figure 9 illustrates a typical thermal cycle for pre-heating and extrusion. The pre-heat temperature is varied at 430°C – 470°C and the exit temperature vary between 545°C – 565°C depending on the extrusion speed. The exit temperature increases when the extrusion speed is increased due to the heat generated from shear deformation and friction increases. When the billet is pushed through the die the exit temperature increases rapidly from the pre-heat temperature. Depending on the extrusion speed the exit temperature will increase to a maximum temperature. At this point the extrusion process reaches an equilibrium state where the heat generated and heat loss are balanced and the exit temperature remains constant when the extrusion speed is maintained constant. For a constant extrusion speed, it produces a maximum exit temperature. Therefore the exit temperature is a function of extrusion speed and the extrusion speed is limited due to the exit temperature. The extrusion speed could be increased until the alloy starts to partially melt, which is called incipient melting. At the incipient melting temperature the second phase of the alloy and aluminium reacts and produces liquid. As

mentioned in section 1.3.3 incipient melting causes the product to tear. The incipient melting temperature depends on the amount of alloying elements present in the system. Therefore it is very important to determine this temperature for AA6060 alloy in order to establish the maximum exit temperature could be reached for AA6060.

It is widely accepted that surface defects (see section 1.3) increases when the extrusion speed is increased. Tearing due to friction and incipient melting will definitely increase since the friction and temperature increases with extrusion speed. However the formation of die pick-up, die lines and blisters could not be directly related to the extrusion speed and exit temperature since there are other influencing factors such as homogenization condition, die bearing surface condition etc.

1.3 Extrusion Surface Defects

Surface defects on extrusion products are a common problem among all the extruders worldwide. There are many surface defects found such as die pick-up, die lines, blisters and tearing. Most of these surface defects could be covered up by anodizing and powder coating provided that the defects do not exceed a certain size. Therefore to keep the surface defects at smaller size, extruders mostly extrude products at a slower speed due to the lack of understanding of surface defects. This has directly influence the productivity for extruders.

1.3.1 Die Pick-Up

Die pick up is like a tear drop or comet as shown in Figure 10, parallel to the extrusion direction. Generally the length of the die pick up varies between 0.5mm – 3mm and could be found everywhere on the surface of the extrudates. The severity of the die pick-up depends on the process parameters.

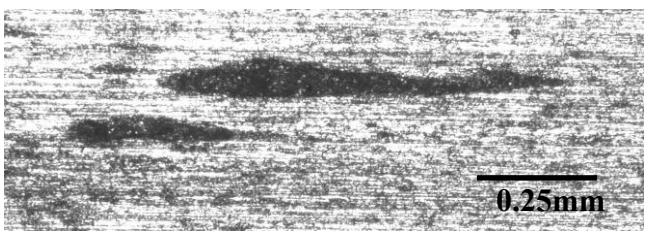

Figure 10 Die Pick Up

This surface defect could be attributed to inclusions in the billet, inadequate homogenization, die deflection, extrusion process parameters, iron oxide and aluminium oxide on the die bearing surface [3, 10].

1.3.2 Die Lines

Die line is a continuous deep groove parallel to the extrusion direction. As shown in Figure 11 and Figure 12, there about 10 lines horizontally.

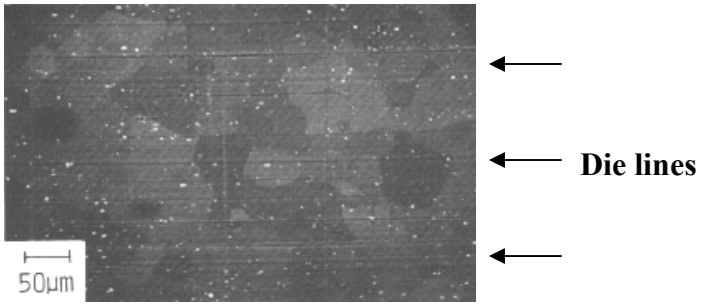

Figure 11 Extruded Surface[3]

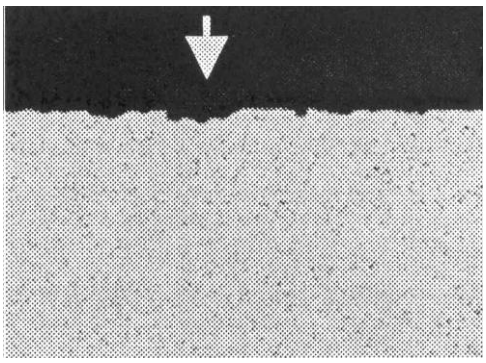

Figure 12 Cross section showing Die lines

These defects could be caused by the interaction of the die land area with intermetallic particles and build up aluminium [3]. It also occurs when the die bearing surface is highly polished and when the die is operating in the optimum chocked condition. Generally the depth of a die line could vary between 0.2µm and 0.5µm and could be inconvenience when the extrudate needs to be anodized.

1.3.3 Tearing

There are two types of tearing which are caused by friction and incipient melting. Figure 13 shows an example of tearing due to excessive friction between the die bearing surface and the flowing metal. During this incident the cohesive strength of the flowing metal is lower than the frictional force, due to less plasticity at high temperature.

Therefore the flowing metal has less strength to hold on and eventually starts to tear. This is often called as mechanical tearing. This tearing usually starts off from the surface of the extrusion and extends almost 100µm into the extrudates as shown in Figure 13.

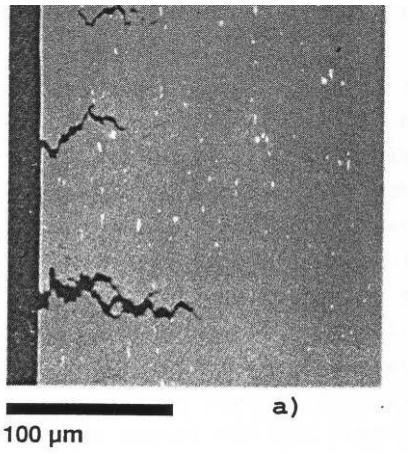

Figure 13 Tearing due to friction [10]

Figure 14 shows a cross section of internal tearing. This could be caused by incipient melting.

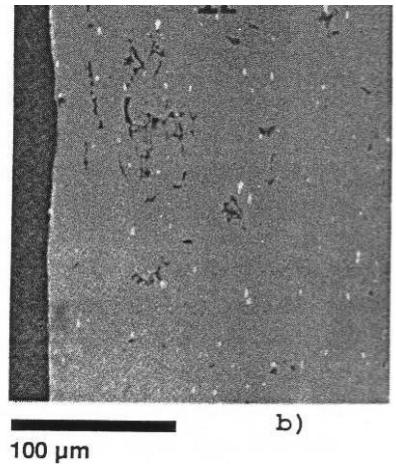

Figure 14 Tearing caused due to incipient melting [10]

In every aluminium alloy there are second phase particles which are formed due to inclusion and alloy elements. In AA6060 there are Mg_2Si and AlFeSi. These compounds react with Si and Al, and form liquid at relatively low temperatures. AA6060 has a melting point of 640°C but due to these reactions AA6060 could melt in the regions of 555°C if excess Si is present. When these isolated liquid starts to solidify dendrites form which are less in strength and cause surface tearing. Therefore it is quite

important to investigate at which temperatures incipient melting occurs for AA6060 alloy system.

1.3.4 Blisters

Figure 15 shows a cross section and the top view of a blister. As shown in the figure it consists of a very thin layer which is on the extrusion surface and being lifted up at a particular location.

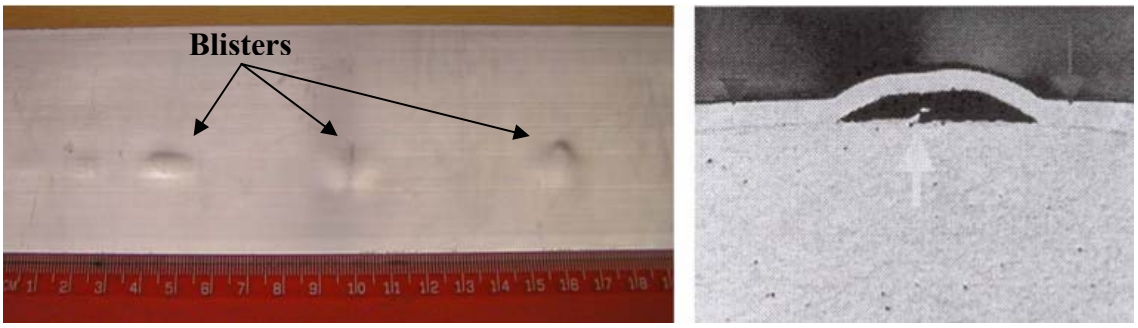

Figure 15 Top view and cross section of blisters

The cause of these defects is not clear but there is a wide acceptance that these are formed due to air and lubricants being trapped during the extrusion process. Since there is a separate layer it could be also formed due to a weak bonding between the oxide layer and the aluminium substrate.

1.4 Aim

The scrap generated at Fletcher aluminium due to surface defects reflects the high quality requirement of its window and door business. As Fletcher aluminium operates their extrusion press at quite low extrusion speeds since it is widely accepted through out the extrusion industry that the surface defects increase when the extrusion speed is increased. Therefore the productivity at Fletcher aluminium is quite stable and may have room for improvement.

The aim of this study is to relate extrusion surface defects (mainly die pick-up) with extrusion parameters such as pre-heat temperature, extrusion speed and exit temperature. The other objective is to determine the incipient melting temperature of AA6060 alloy, since this temperature dictates the maximum exit temperature the alloy could be exposed. Then these data could be used to operate the extrusion press at higher extrusion speeds without increasing the amount of die pick-up.

2 Literature Review

Chapter 1 gave a brief introduction to extrusion, surface defects and thermal cycles. Surface defects could be attributed to inadequate homogenization, process parameters and tooling conditions. This research focused to link the surface defects such as die pick-up with process parameters and die condition. Process parameters are exit temperature, extrusion speed and pre-heat temperature.

2.1 Phase transformations in AA6xxx alloys

Temperature is a main parameter for the extrusion process. Hot extrusion occurs at high temperatures where the microstructure change is quite important. At these temperatures (465°C – 590°C) the alloy undergoes various phase transformations depending on the composition. Figure 16 shows the Al – Mg_2Si quasi binary phase diagram.

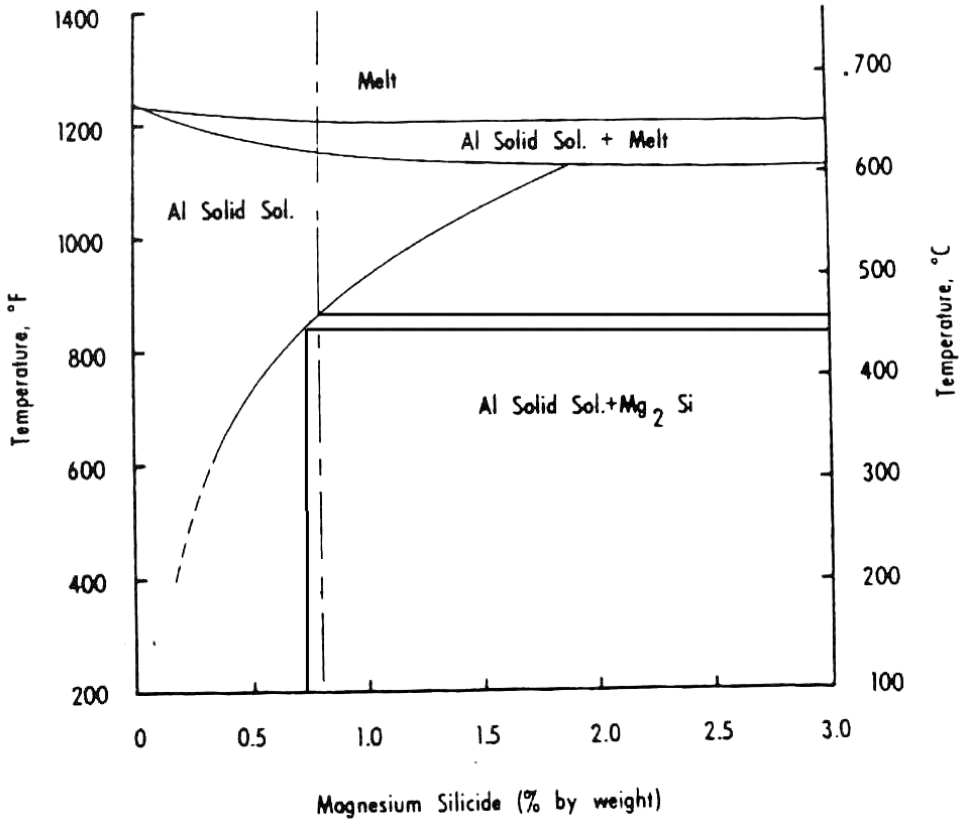

Figure 16 Al-Mg_2Si quasi binary phase diagram [4]

For AA6060 alloy Mg and Si combine to form Mg_2Si compounds and is the primary hardening phase for this alloy. For AA6060 alloy the Mg contents vary between 0.4% and 0.5%. To satisfy the stoichiometric requirement it needs 0.23% to 0.29% of Si. Therefore the amount Mg_2Si varies between 0.73% and 0.79%. According to the phase

diagram the vertical lines for 0.73% and 0.79% intersects the solubility line approximately at about 450°C and 455°C. This means at 450°C and 455°C, Mg_2Si particles starts to dissolve. Phase diagram represent the phases at an equilibrium state, but the Mg_2Si particles do not dissolve instantaneously. Dissolution is a time dependent phenomenon. Experiments conducted on AA6063 alloy (0.3% - 0.5% Mg) shows that large Mg_2Si particles take seven days to fully dissolve [4, 11]. Pre-heating the billets for 20 – 30 minutes does not necessarily mean that Mg_2Si particles are fully dissolved [12-14]. Therefore there may be some remaining Mg_2Si particles within the alloy system. The remaining Mg_2Si particles may influence some eutectic melting.

2.1.1 Eutectic melting

In AA6060 alloy system there are a number of intermetallic phases present. Fe has a very low solubility and as a result it will bind with Al and excess Si to form AlFeSi particles. β-AlFeSi particle are plate like shaped formed during casting [15]. A small fraction of AlFeMnSi particles may also be present and are cubic shaped. Table 1 lists the possible eutectic reactions that could occur in AA6060 alloy. The initial eutectic reaction occurs at 555°C if there is Si and Mg_2Si particles present in the alloy system and these particles are in contact. These reactions occur instantaneously.

Table 1 Incipient melting temperatures of some phases on AA6xxx alloy [4],[16],[15],[7],[17]

Melting temperature	Reaction
555°C	$Al + Mg_2Si + Si \longrightarrow Liquid$
576°C	$Al + Mg_2Si + \beta - AlFeSi \longrightarrow Liquid + \alpha_h - AlFeSi$
577°C	$Al + Si \longrightarrow Liquid$
578°C	$Al + \beta - AlFeSi + Si \longrightarrow Liquid$
587°C	$Al + Mg_2Si \longrightarrow Liquid$
612°C	$Al + \beta - AlFeSi \longrightarrow Liquid + \alpha_h - AlFeMnSi$
630°C	$Al + \beta - AlFeSi \longrightarrow Liquid + Al_3Fe$

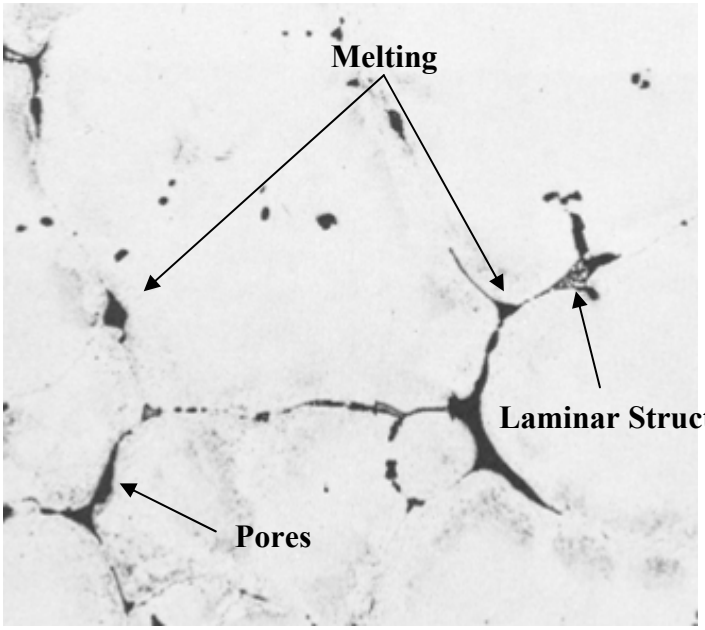

Figure 17 Eutectic melting formed during heat treatment for A712 alloy [18]

Figure 17 shows the typical microstructure of eutectic melting during heat treatment for A712 alloy. However the composition of this alloy (Al-Zn-Mg) is not similar to AA6060 but the micrograph was used to show what eutectic melting looks like. The second phase particles are located at the grain boundary and therefore the eutectic melting occurs at the grain boundary. When the material is heated above the eutectic temperature, the grain boundary melts and liquid starts to form. Upon solidification a laminar structure starts to develop [19]. Due to the volume difference between liquid and solid, generally pores in the grain boundary can be found. The laminar structure and pores are evidence of eutectic melting and incipient melting.

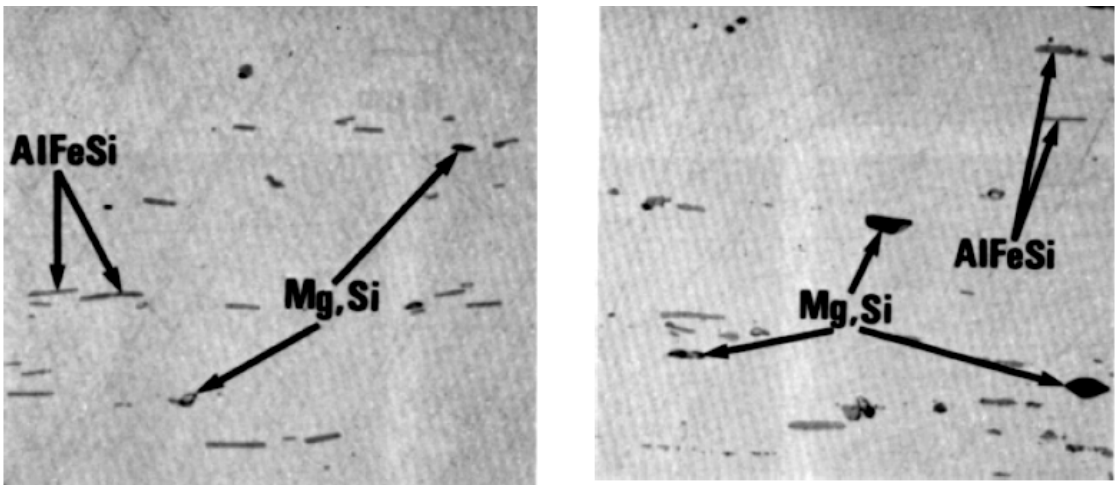

Figure 18 AlFeSi and Mg_2Si Particles [20]

Figure 18 shows the AlFeSi (gray) and Mg_2Si (black) particles in the Al matrix of AA6060 alloy. Due to the presence of these intermetallics and eutectic reactions, a number of side effects could occur. These intermetallics have a weak adhesion to the Al matrix and may loosen from the matrix during extrusion. As a result of this, the particles may stick to the die surface and scratch the surface of the extrudate. Micro-cracks could form due to the presence of intermetallics during deformation and crack the aluminium surface. Eutectic melting may also create die pick-up and tearing on the surface [21].

2.2 Extrusion limitations

There are many limitations for any extrusion profile from extrusion log preparation to fabrication of extrudate. When considering the limitations during the extrusion process the pre-heat temperature, pressure and extrusion speed are very vital. Obviously any extruder would prefer to extrude at high speeds to enable greater productivity. However due to the increase in exit temperature with extrusion speed, the amount of surface defects also increase, which is not desirable. As mentioned in section 2.1.1, exit temperature will definitely influence the eutectic reactions and cause defects. Some of the limitations could be grouped as follows;

- Press capacity (available pressure)
- Complications in metal flow
- Complications in tooling
- Extrusion surface defects (die pick-up, tearing, die lines)

The process limitations in regard to extrusion speed and billet temperature could be represented in an extrusion limit diagram. Figure 19 shows a typical extrusion limit diagram.

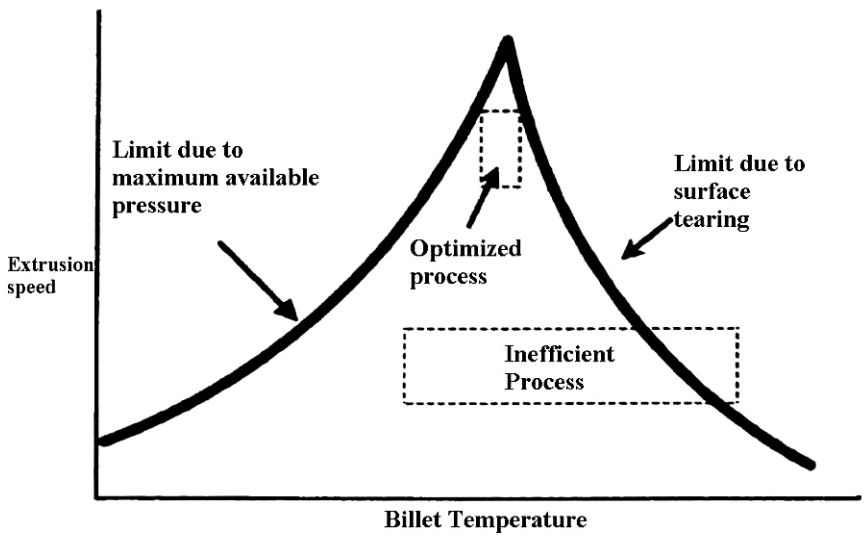

Figure 19 Extrusion limit diagram [22]

The extrusion limit diagram has two curves, the left curve represents the limitation due to pressure and the right curve represents the limitation due to surface tearing. The deformation strength required for aluminium is temperature determinant. At lower billet temperatures the deformation strength is greater and needs more force or pressure to push the billet through the die [23]. Therefore it is much harder to increase the extrusion speed. However if the billet temperature is much higher it is much easier to push the billet through the die since it has less deformation strength and needs less pressure. This does not mean higher billet temperature is much suited. As a result of increasing the extrusion speed the exit temperature also increases (refer section 2.3). As mentioned in section 2.1.1 the eutectic melting temperatures dictates the maximum temperature the extrusion could be exposed. Therefore for higher billet temperatures there is a limitation on how much the extrusion speed could be increased, because the amount the exit temperature could be increased is reduced. Extrusion limit diagrams could be also divided into two categories as shown in Figure 20.

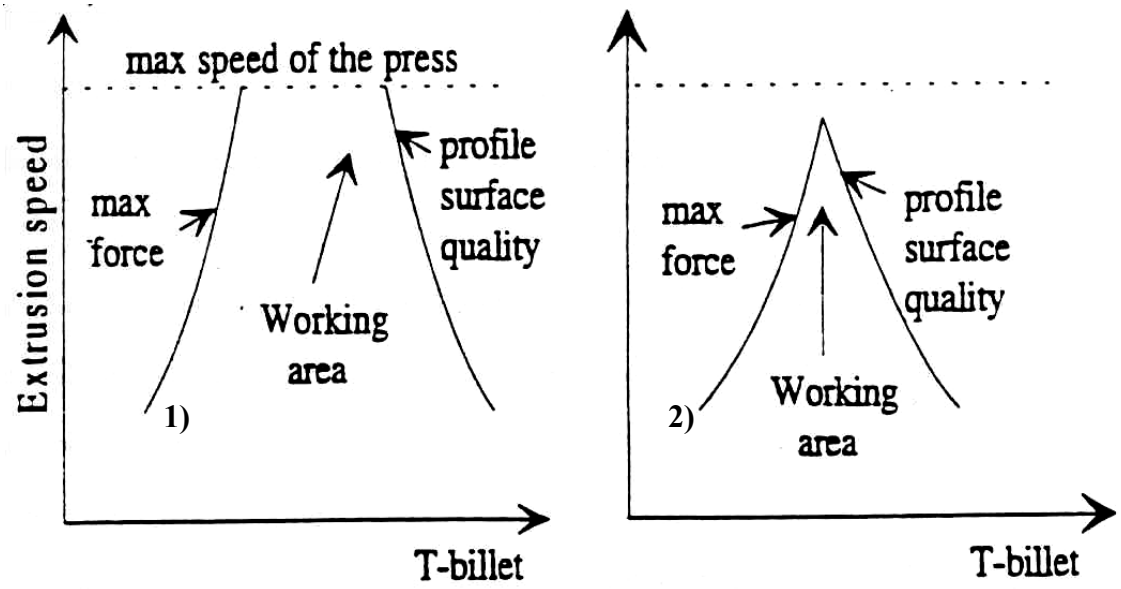

Figure 20 Extrusion limit diagrams 1) Easy to extrude 2) Difficult to extrude [16]

The left graph in Figure 20 represents an alloy which is easy to extrude and on the right graph in Figure 20 represents an alloy which is difficult to extrude. In the left graph, this particular alloy could be extruded at the maximum extrusion speed which the extrusion capable of for a variety of billet temperatures. On the other hand the right graph, the alloy could not be extruded at the maximum extrusion speed. Therefore the right graph has less working area compared to the left graph. In regard to AA6xxx alloys the right graph closely responds, when the Mg concentration is too much in the solid solution. When the Mg concentration is too much in the solid solution, the flow stress of the alloy increases and the extrudability decreases [24]. The right side of the typical extrusion limit diagram could be further modified as in Figure 21.

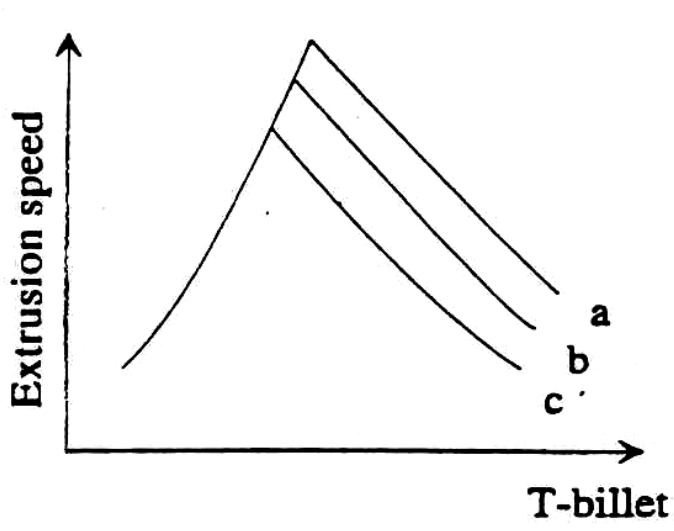

Figure 21 Metallurgical limitations for extrusion limit diagram [16]

The working range could be further increased if the low melting phases are eliminated from the material. The lines a, b and c corresponds the following limitations.

- a – Surface tearing
- b – Die pick-up, die lines
- c – Recrystallization of the surface

Depending on the quality control of the manufacturing process one of these lines could be used for the metallurgical limitations. Figure 22 shows the complete extrusion limit diagram to illustrate how the extrusion could be limited due to a number of factors as mentioned this section.

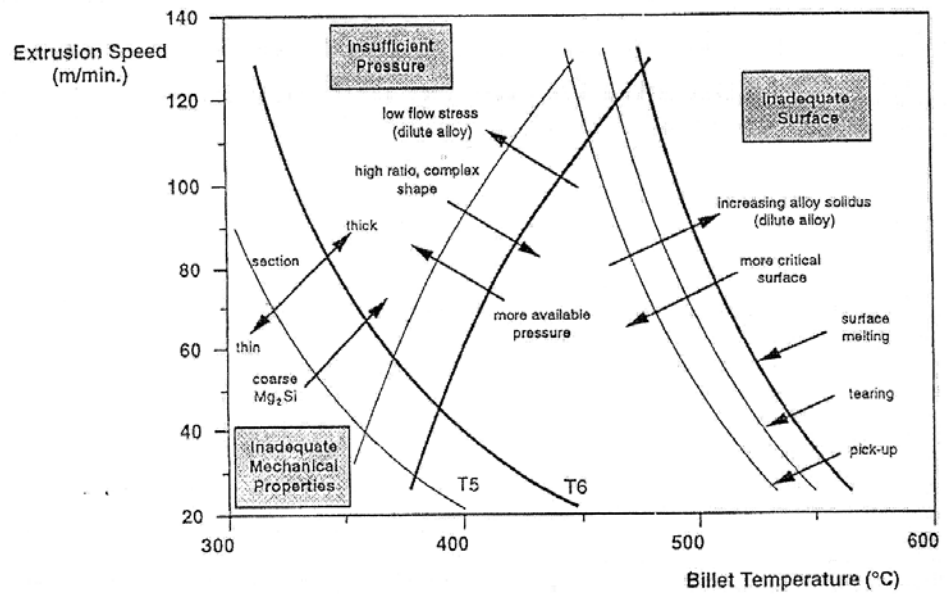

Figure 22 Possibilities of the limit diagram [24]

2.3 Theoretical modelling for extrusion pressure and exit temperature

As mentioned in the previous section hot extrusion is a process which involves temperature, speed and pressure, therefore it is quite important to understand the relationships between these parameters. Hot extrusion is carried out at temperatures where the flow stresses (σ) are controlled by composition, and strain rate. The strain rate could be explained at low stress levels and high stress levels [25]. At low stress levels the strain rate (ε) is;

$$\varepsilon = A_1 \sigma^n$$

At high stress levels the strain rate is;

$$\varepsilon = A_2 \exp(\beta\sigma)$$

These two equations could be combined as follows;

$$\varepsilon = A_3 (\sinh \alpha_1 \sigma)^n$$

where;

A_1, A_2, A_3, β, α_1 = Constants

Therefore by this equation the relationship for strain rate in terms of flow stress could be obtained. However these equations are only valid for a constant temperature. If flow stresses are needed at different strain rates and temperature an additional term called temperature compensated strain rate (Z) is necessary which is;

$$Z = \varepsilon \exp(\frac{\Delta H}{GT}) = A(\sinh \alpha_1 \sigma)^n$$

where;

ΔH = activation energy

G = universal gas constant

T = absolute temperature

Therefore the flow stress is;

$$\sigma = \frac{1}{\alpha} \ln \left\{ \left(\frac{Z}{A} \right)^{\frac{1}{n}} + \left[\left(\frac{Z}{A} \right)^{\frac{2}{n}} + 1 \right]^{\frac{1}{2}} \right\}$$

The flow stress found in above equation could be used to estimate the extrusion pressure. In the simplest estimations it considers a uniform deformation. Thus it calculates the minimum energy required to achieve deformation at steady state pressures. Therefore it represents a lower pressure than required.

Internal work done per unit volume is;

$$W_{in} = \sigma d\varepsilon$$

$$W_{in} = \sigma \int \frac{dL}{L} = \sigma \ln \frac{L_2}{L_1} = \sigma \ln \frac{A_1}{A_2} = \sigma \ln R$$

where;

R = extrusion ratio

External work done by the ram per unit volume is;

$$W_{ex} = \frac{pAL}{AL} = p$$

where;

A = cross section of billet

L = length of billet

Therefore extrusion pressure is;

$$p = \sigma R$$

As mentioned before, the above equation only accounts 60% of the pressure because friction, redundant deformation and peak pressure is ignored. However experimental data have refined the above equation to;

$$p = \sigma\left(a + b\ln R + cL\right)$$

where;

a, b, c = constants

The constant "a" is used for the contribution of the massive redundant work associated with deformation. While constant "c" is the friction co-efficient and constant "b" corresponds the deformation is not uniform. The extrusion pressure could be also modelled by bulk analysis, where it assumes the pressure within the container is the same at all points across any transverse plane. The only difference alteration to the above equation is that $c = \frac{4m}{D_B\sqrt{3}}$ where "m" is the friction co-efficient. The value for "m", closely yields to 1 [6].

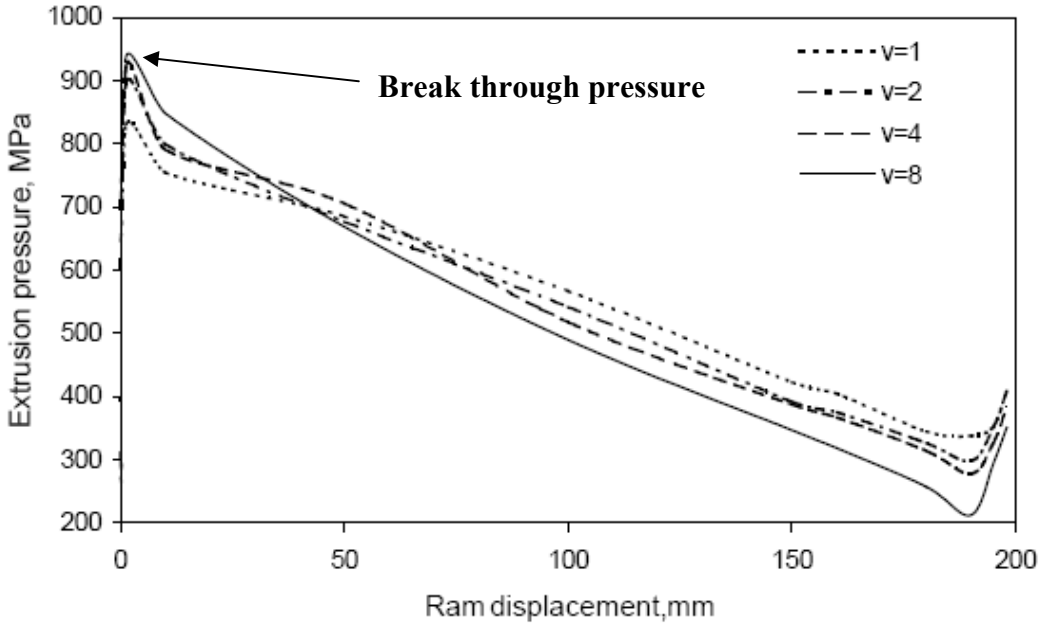

Figure 23 Extrusion pressure graph [26]

Figure 23 show a typical extrusion pressure for AA7075 as a function of ram displacement. There is a rapid increase of pressure at the initial stage and once the break through pressure is achieved, extrusion pressure decreases.

2.3.1 Heat generation during extrusion

Extrusion is a hot working process. All the work carried out during extrusion is converted to heat. Figure 24 shows a schematic of a typical heat loss and gain during extrusion.

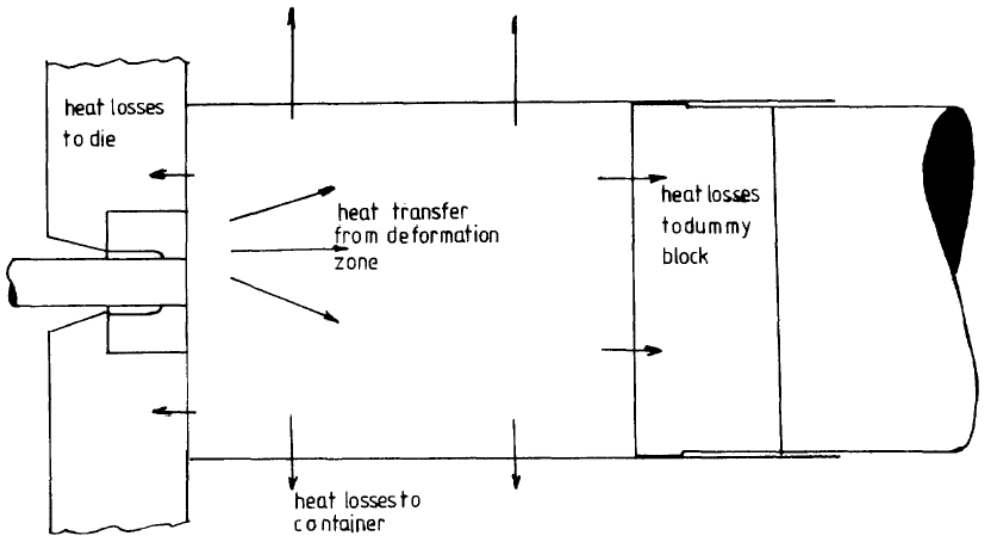

Figure 24 Heat flow during extrusion [25]

This heat loss and gain could be attributed to the following;

- Heat generated due to deformation at the die
- Heat generation due to friction between the billet and container
- Heat generation due to friction at the die
- Heat transfer due to the movement of the billet
- Heat conduction to the tooling such as container, ram and die
- Heat conduction to the billet
- Heat conduction to the extrudate

Consider one dimension heat flow. The exit temperature is governed by the heat loss from the deformation zone through the tooling and heat created by friction in the die. The temperature of the billet, container temperature, die temperature, physical properties of the billet, physical properties of the die and the extrusion speed dictate the heat flow from the shear zone and the deformation zone. Figure 25 shows the factors influencing the exit temperature.

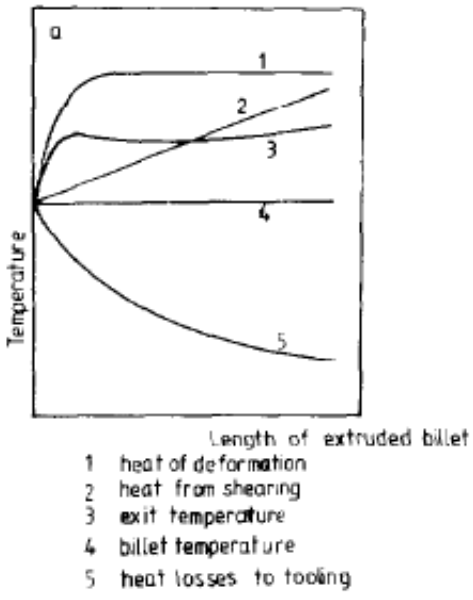

Figure 25 Factors influence on exit temperature [25]

At slower extrusion speeds the time available for heat conduction is higher than at higher extrusion speeds. Thus at higher extrusion speeds adiabatic thermal conditions could be achieved. At this condition the temperature rise in exit temperature is at the highest where the heat lost to the environment through the tooling is the lowest. At the beginning of the extrusion process when the ram pushes the billet the extrusion load increases when the deformation zones forms. At this point there is a positive

temperature rise. As ram speed increases, the deformation rate increases and hence the exit temperature also increases. Once the ram speed is stable the exit temperature could either increase or decrease depending on the amount heat loss or gain.

2.3.2 Temperature increase

There are several models which are available to estimate the exit temperature. The temperature increase which attributes to exit temperature is categorized into three components as follows;

A. Temperature increase due to deformation,

$$\Delta T_1 = \frac{\sigma \ln R}{\sqrt{3}(\rho C_p)}$$

where,

ρ = density

C_p = thermal conductivity

σ = shear stress

R = extrusion ratio

B. Temperature increase due to friction at billet and container wall,

$$\Delta T_2 = \frac{\sigma}{4\sqrt{3}(\rho C_p)}\sqrt{\frac{V_R L_B}{\alpha}}$$

where,

V_R = ram speed

L_B = billet length

α = thermal diffusivity

C. Temperature increase due to friction at the die,

$$\Delta T_3 = \frac{\sigma}{4\sqrt{3}(\rho C_p)}\sqrt{\frac{V_E L_D}{\alpha}}$$

where,

V_E = extrusion speed

L_D = die length

According to the above equations the ratio between the temperature increase due to friction at the die and the temperature increase due to friction at billet and container wall, equates to $\frac{\Delta T_3}{\Delta T_2} = \left(\frac{L_D}{V_R}\right)\left(\frac{V_E}{L_B}\right)$. This ratio equates approximately 10 – 20. Therefore the temperature increase due to friction from the container is quite negligible. The temperature increase during extrusion really depends on the deformation and friction at the die.

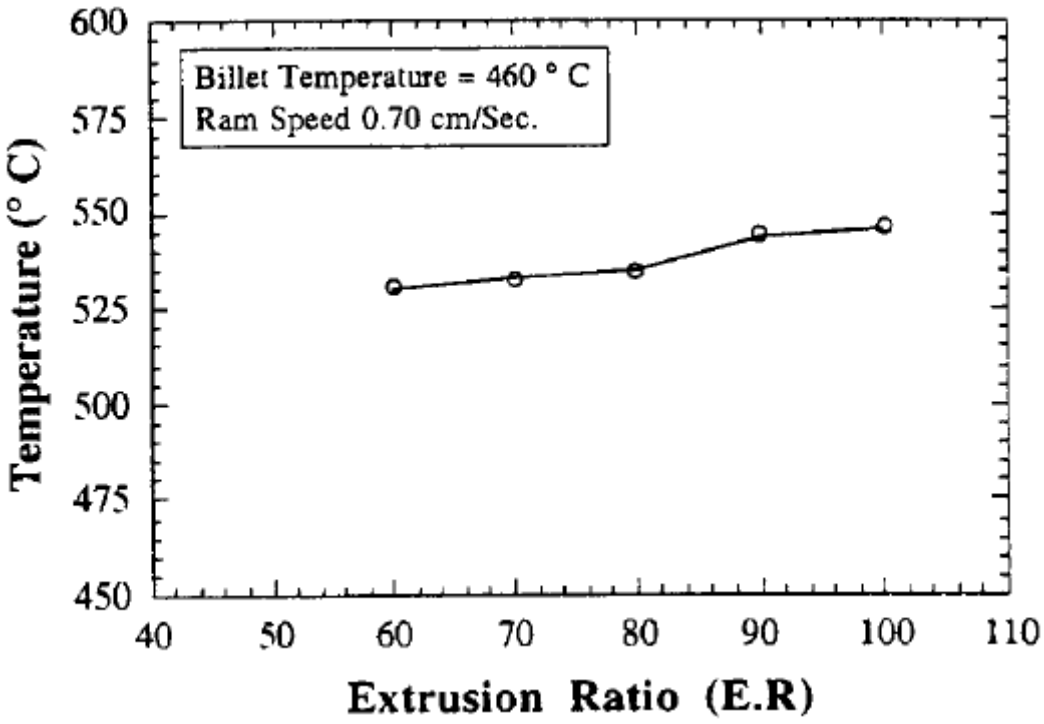

Figure 26 Influence of extrusion ratio on exit temperature [27]

Figure 26 shows the results of the influence of extrusion ratio for AA6063 alloy. The simulations were done for a pre-heat temperature of 460°C and ram speed of 0.7cm/s by varying the extrusion ratio. The temperature increase by deformation is governed by extrusion ratio. By increasing the extrusion ratio, the amount of deformation which the material undergoes increases. As expected the exit temperature increases as the extrusion ratio is increased. The extrusion ratio indirectly influences the exit temperature increase due to friction at the die. When the extrusion ratio is increased, extrusion speed also increases for a constant ram speed. Therefore the influence of extrusion ratio on exit temperature is caused by the rate of deformation and friction [27].

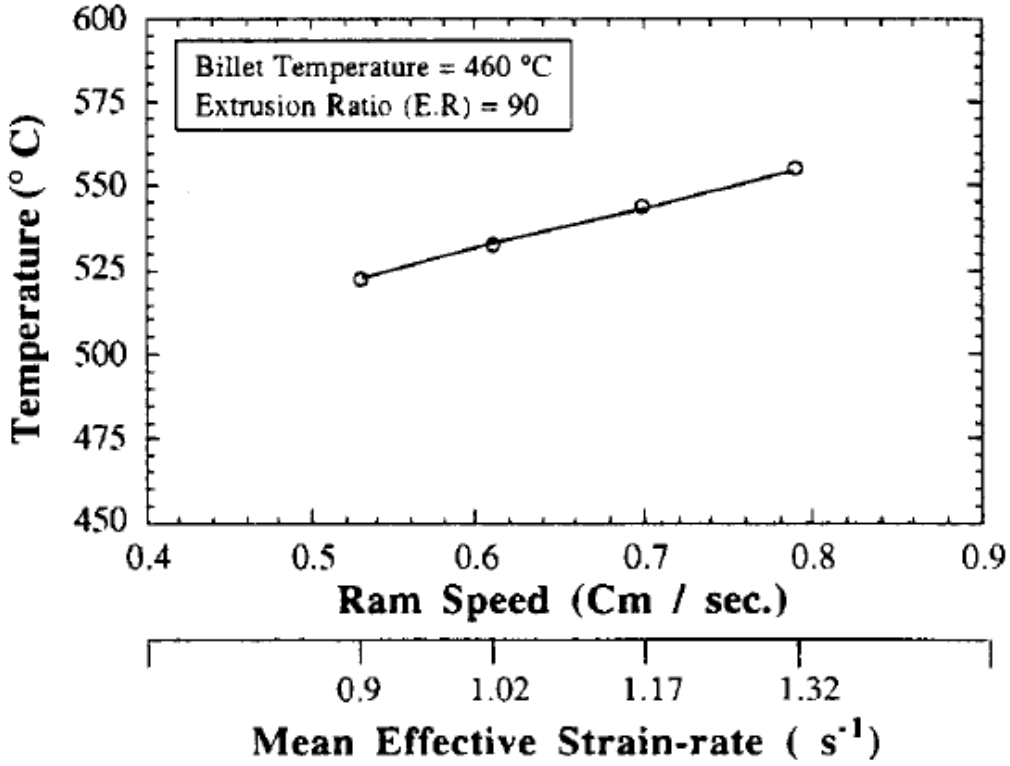

Figure 27 Influence of ram speed on exit temperature [27]

Figure 27 shows the influence of ram speed on the exit temperature for AA6063 alloy. In this case the extrusion ratio is fixed at 90 and the ram speed is varied. The ram speed directly governs the friction at the die bearing surface and also related to strain rate and extrusion speed (extrusion speed = extrusion ratio x ram speed). The flow stress is a function of strain rate. Therefore the temperature increase due to deformation could be related to ram speed. When the ram speed is increased, the exit temperature increases due to deformation and friction at the die [27].

2.4 Die pick-up

Die pick-up is a surface defect which has the appearance of scratch marks and is the main focus of this research. These defects have varying lengths between 3mm and 12mm [6, 10, 3]. The appearance of a die pick-up is shown in Figure 28. Die pick-up often starts with a deposit and ends with a narrowing tail [9, 28]. The causes of die pick-up could depend on many conditions and could be categorized as follows [6, 10, 3];

- alloy and homogenization condition
- tooling and equipment
- extrusion process parameters

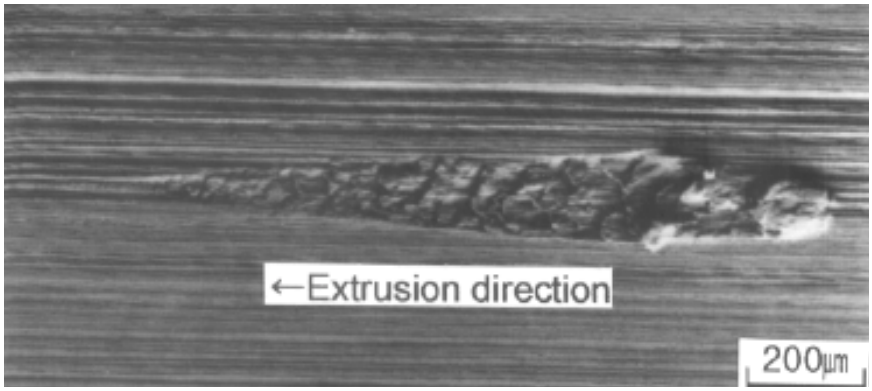

Figure 28 Top view of a die pick-up [28]

2.4.1 Interaction between die and extrudate

Before the billet is extruded, the surfaces of the billet and the die consist of oxides. During extrusion the metal undergoes shear deformation due to interaction between the container and dead metal zones. As a result of shear deformation the oxides are adhered to the die. Therefore the extrudate material is locally deformed and fragments may remove from the matrix and subsequently deposited on the harder die land surface. These deposits are further elongated in the extrusion direction. This event is a continuous process and occurs right throughout the extrusion cycle. This produces large areas of transferred material. This transferred material starts to build up at the rear portion of the die land and begin to spall. Subsequently a deposit is detached and embedded in the extrusion product [6, 3].

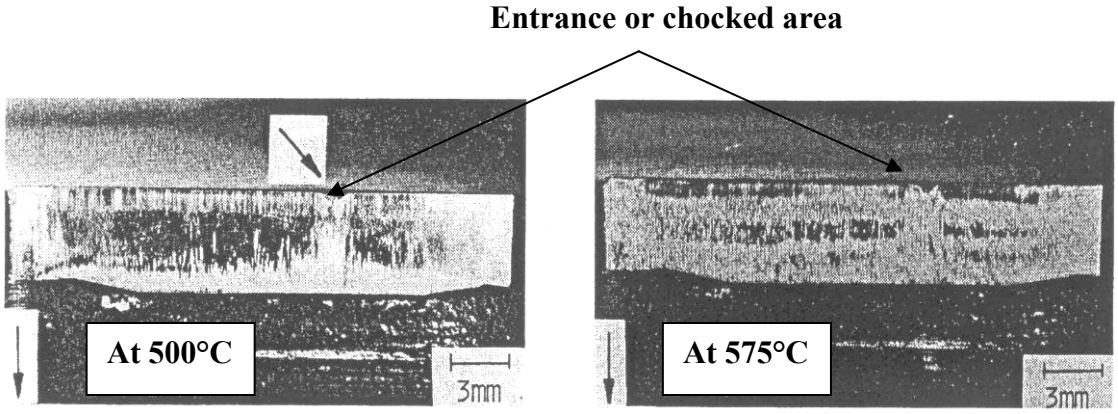

Figure 29 Die land areas [6]

Figure 29 shows the die bearing surfaces exposed at 500°C and 575°C. The profile of the extrudate is rectangular. At the entry of the die (chocked area) there could be seen a uniformly adhered aluminium layer. This layer is believed to be present right

throughout the extrusion cycle. Thus this aluminium layer is responsible for the developing of the extrudate surface. However it is not very clear whether this aluminium layer could influence the formation of die pick-up. After the chocked area this aluminium layer is exposed to atmospheric conditions. Therefore the aluminium layer consequently gets oxidized. It is in the wake of the chocked area that flakes of aluminium could be observed to be deposited in the mid section of the die land area. Most of these flakes of aluminium are carried forward by the emerging extrudate and get accumulated at the exit of the die land area. Figure 30 shows the aluminium build up at the exit of the die land area for 500°C and 575°C.

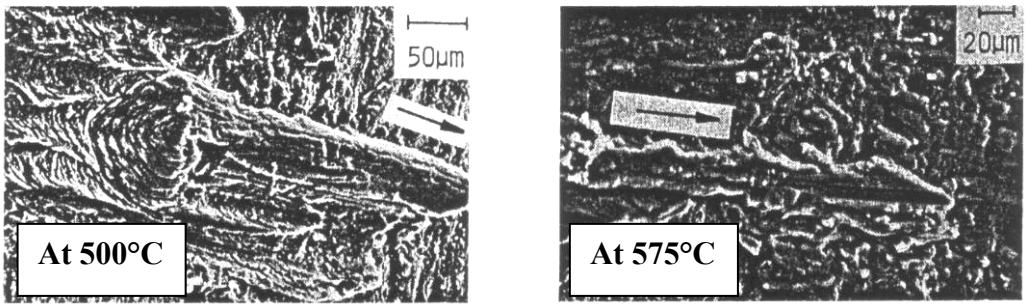

Figure 30 Aluminium build up [6]

At 500°C the aluminium layer looks to remain quite stable. Some of the flakes have been agglomerated and ironed as they progress through the die. This produces large pick-up deposits, smeared at the tail which will be removed from the die and becomes embedded on the extrusion product. This process is a continuous and isolated event which occurs during the extrusion process. At 575°C more ironing of aluminium particles have occurred. These particles have agglomerated in the direction of the extrusion due to the low flow stress in the material. There could be seen spalling occurring on either side of the elongated agglomerate. When the spalling is deposited on the exit side of the die land it gets harden due to lower temperature of the die. Die pick-up could occur due to dispersion of the material on either side of the elongated agglomerate. This will continue to scratch the extrudate. Generally the pickup damage is greater at 575°C than at 500°C. Hence the interaction between the extrudate and die could cause die pick-up. However the precise mechanism is not clear.

There could be two possibilities. As mentioned before pick-up could be formed due to the coated material on the die land area or a mechanism involving the extrusion material being partially sticking between the die and extrudate and the die is then responsible for

accumulating the extrusion material. The second theory could not be justified by single alloy extrusions are performed. AA5456 billet was extruded at 500°C and thus the initial deposit on to the die arrived from AA5456 billet. Next the same die was used to extrude AA6063 billet at 600°C and extrusion speed of 54m/min which resulted in pick-up and surface tearing. Samples of the AA6063 extrudate was analysed and contained high amounts of magnesium and manganese level which could be the AlFe(Mn)Si phase. This suggests that the origins of these deposits could have arrived from the AA5456 billet. It was also found the parent material had the same magnesium and manganese levels. After processing six more billet of AA6063, revealed that the pick-up later originated from the AA6063 billets. Therefore it could be suggested that a dual pick-up mechanism is present [6]. Figure 31 shows the possible stick and slipping regions could be found on a bearing surface. Therefore a transient stick-slip mechanism could be in operation.

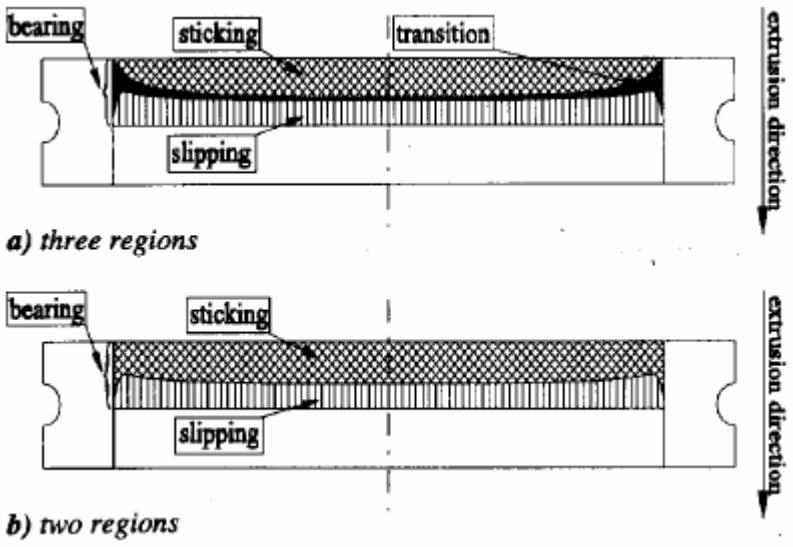

Figure 31 Stick and sliding mechanisms on bearing surface [29]

There is a rapid build up of aluminium at the exit of the die land area due to strong interaction between the die and extrudate and high frictional forces. As a result the aluminium coating agglomerates and elongates in the direction of the extrusion. Finally it starts to spall and then pick-up on the extrudate. Pick-up flakes are continuously transferred on the extrudate when the adhesion between the die and extrudate is approximately equal to the cohesive strength of the metal. This process is quite commonly observed when commissioning new dies.

2.4.1.1 Extrusion die conditions

The extrusion dies are very important for the extrusion process. The surface of the extrudate is generated in an unlubricated sliding contact between the die and aluminium. Extrusion dies are mainly manufactured from H13 hot work tool steel. This material characterizes high strength, high ductility and good tempering where 450 – 500 HV (48 – 50 R_c) is a hardness of a common tempered H13 for dies applications. The surface of the dies is surface treated by nitriding process where it could achieve a hardness of 1000 – 1200 HV. Generally nitriding of dies are done by diffusing nitrogen into the surface at the temperatures of 450°C – 580°C.

Due to severe operating conditions in the extrusion process there could be severe wear on the die bearing surface. Usually there could be craters up to 20µm - 100µm in depth. Figure 32 shows a typical die bearing surface condition.

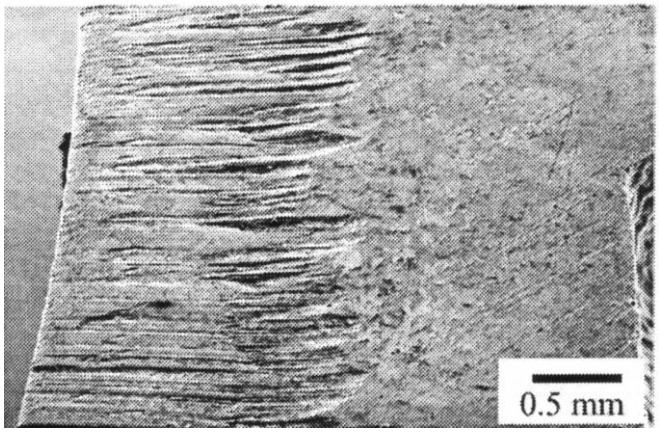

Figure 32 Die wear at entrance [30]

At severe worn regions the bearing surface is typically becomes coarsely ridged. Beyond this area the bearing surface had suffered mid wear, where the compound layer was partly removed and partly chemically transformed [30]. Figure 33 shows this chemical transformation. This figure also shows that these chemically formed layers have poor bonding and may have caused cracking between the layers. The chemical composition reveals that these layers are consists of magnesium, oxygen and iron. It is quite interesting to note that nitrogen was detected in the substrate of the material and not in the layers. It was also found a thin aluminium layer was present.

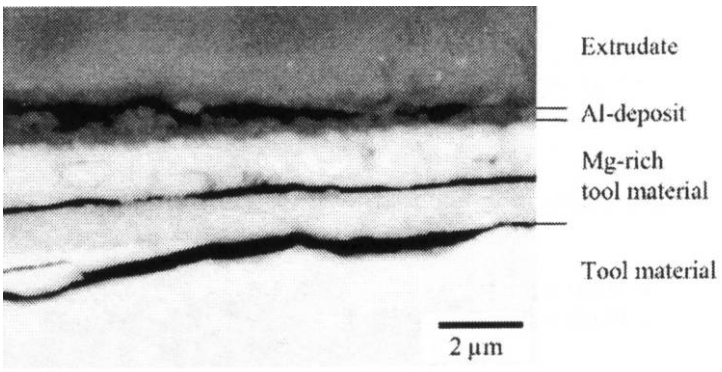

Figure 33 Sub surface cracking between layers [30]

Figure 34 shows a schematic of a typical worn die bearing surface. As shown most of the wear is concentrated at the entry or chocked area of the die.

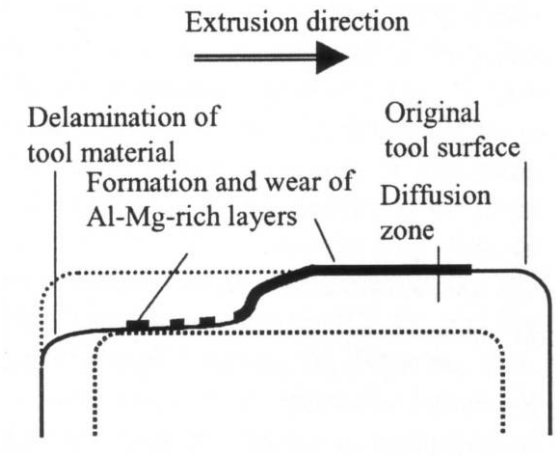

Figure 34 Schematic of wear in a nitrided die [30]

The amount being adhered to the bearing surface is probably the good indication how much the die bearing surface has undergone wearing. The chemically formed material could be found before and after cleaning the dies with NaOH solution. It could be concluded that these interfacial reactions occur during the extrusion process. This types of interfacial reactions are also found in high pressure die casting [31] and friction stir welding tools [32]. The intermettalic layer grows uniformly across the die bearing surface since the temperature and chemical condition may not vary along the die bearing surface. It really depends on the amount the extrudate touches the surface. Generally intermettalic particles are hard and brittle. This could lead to flaking on the die bearing surface and creates the surface to be uneven. Therefore there could be some influencing factors where these intermettalic particles could contribute to assist to form die pick-up.

2.4.2 Influence due to eutectic reactions on die pick-up

Mg_2Si and β-AlFeSi particles form during the casting process. These constituent particles undergo eutectic reactions and influence incipient melting. The β-AlFeSi particles (monoclinic structure) are transformed into α-AlFeSi particles (hexagonal structure) during the homogenization process. Figure 35 shows the morphology of α-AlFeSi and β-AlFeSi particles. The homogenization process is also used to dissolve Mg_2Si particles as much as possible. The amount being transformed depends on the homogenization temperature and duration. To increase the α-AlFeSi formation, high homogenization temperature and longer hours are used.

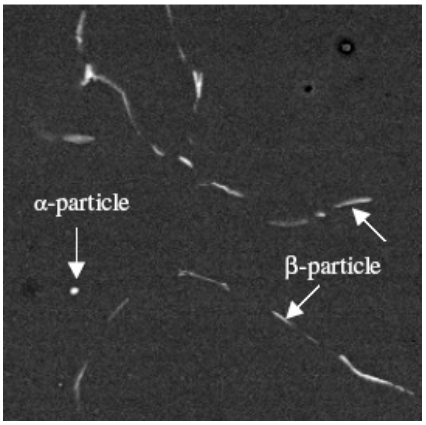

Figure 35 α-AlFeSi and β- AlFeSi for an unhomogenized state [33]

Figure 36 shows the microstructure for the samples homogenized at 580°C for 48 hours. It also shows most of the β-AlFeSi particles have transformed into α-AlFeSi particles when compared with Figure 35. However due to current production schedules the duration for homogenization is reduced to about 2 – 3 hours. Therefore most of the β-AlFeSi particles may not have transformed into α-AlFeSi particles [34].

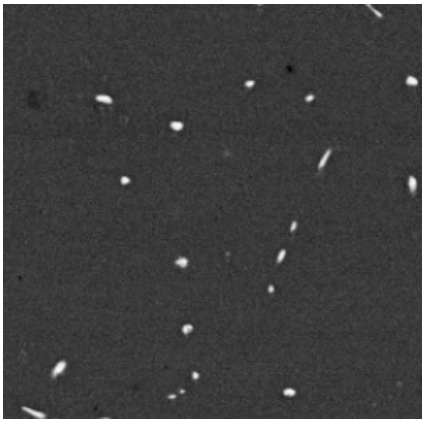

Figure 36 Homogenized structures showing α-AlFeSi at 580°C for 48 hours [33]

When homogenizing at 570°C for 4 hours, 20 hours and 100 hours the β-AlFeSi into α-AlFeSi transformation increases by 5%, 40% and 95% respectively [28]. It was also conclusive when the transformation percentage is increased the amount of die pick-up decreases. It has also been found that when iron content is increased, the amount of β-AlFeSi into α-AlFeSi transformation also increases and hence the die pick-up formation could be reduced [28].

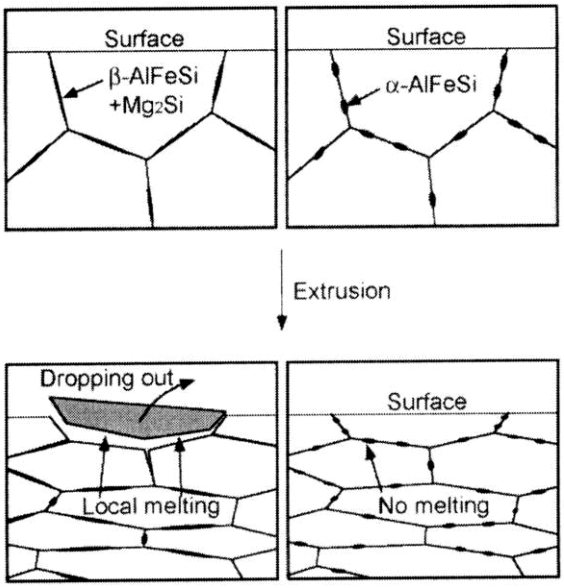

Figure 37 Schematic diagram showing a possible pick-up formation [28]

Figure 37 shows a schematic of a possible die pick-up formation mechanism. As mentioned in section 2.1.1, eutectic reactions form when the exit temperature increases. At 555°C, Mg_2Si particles cause the first eutectic reaction and hence local melting. At 576°C the second eutectic reaction form due to β-AlFeSi particles and hence local melting occur. If the homogenization process is properly achieved the amount of β-AlFeSi particles could be reduced. However as mentioned in section 2.1 it almost take 6 – 7 days to fully dissolve Mg_2Si particles and therefore the eutectic reaction occurring at 555°C may not be avoided [4].

2.4.3 Quantification of die pick-up

Die pick-up creates a bad cosmetic appearance on the extrudate surface. Therefore it is important to quantify and identify the limits where the extrusion process could be operated in safe conditions. Normally the number of die pick-up formed on a unit area is quite often used to quantify. However a theoretical approach could also be adopted. The severity of die pick-up increases with temperature and strain rate which also

coincides with the amount of aluminium build up on the die land area. Unacceptable die pick-up could be related to the temperature compensated strain rate (Z). The flow stress of the material is also a function of ln(Z).

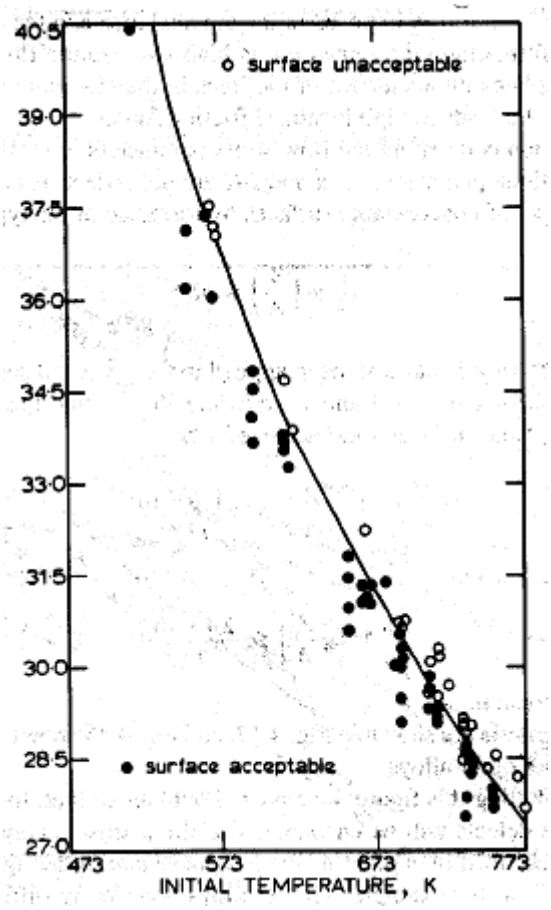

Figure 38 Prediction of excess pick-up [35]

Figure 38 shows a graph where ln(Z) is plotted against the initial billet temperature. The dots on the graph are the points where the surface is acceptable or not. The boundary of these two regimes is governed by an inequality as shown below;

$$\ln Z \leq aT^{-b}$$

where;
a, b = constants

The constants a and b are unique to a particular alloy, cast condition, homogenization condition, tooling design and tooling temperature. This tool is quite important for extruders where they use feed back loop to control the extrusion process.

2.5 Summary

Current literature identifies the importance of extrusion speed, exit temperature and die bearing surface. The extrusion speed and exit temperature are related to each other. These conditions could be related to die pick-up. The pre-heat temperature seems to be considered as a process parameter, but there is not much influence other than reducing the plasticity of the material. If the pre-heat temperature is low, a higher extrusion speed could be achieved, but a greater extrusion pressure is needed. The pre-heat temperature does not significantly influence the microstructure of the billet; therefore there is no correlation with die pick-up due to the shorter industrial practices which is approximately 20 – 30 minutes. Literatures have suggested that die pick-up is closely related to the eutectic melting. However the temperature measurements have not been done to justify this claim. There is also some contradicting evidence suggesting Mg_2Si particles may or may not dissolved during the short pre-heating practices. Therefore it is not clear whether Mg_2Si particles actually involved in the die pick-ups. The die bearing surface has some influence on die pick-up. There are suggestions there is a stick-slip mechanism operating at the bearing surface. Due to this stick-slip condition die pick-up could be formed.

The research objectives of this study are:

- To quantify the occurrence of die pick-up
- To relate the die pick-up in terms of extrusion speed, exit temperature and die condition
- To suggest the likely possibilities for the formation mechanism of die pick-up

3 Methodology

The previous chapter highlighted the possible causes for extrusion surface defects described in available literatures. Based on this current knowledge, trials at Fletcher Aluminium and AUT University were planned and conducted. This chapter details the equipment, trials procedure and sample preparation. Experiments were done to quantify the die pick-up relationship with extrusion speed and exit temperature and to quantify the maximum exit temperature that AA6060 alloy could be extruded. Maximum exit temperature relates to the incipient melting temperature.

3.1 Extrusion conditions

Trials were conducted on AA6060 alloy which has an Mg concentration of 0.40% as mentioned in Table 2. These trials were conducted to monitor and correlate die pick-up with extrusion parameters such as extrusion speed and exit temperature. Die profile 610103 as shown in Figure 39 was selected for these trials since it is one of the most extruded profile at Fletcher Aluminium.

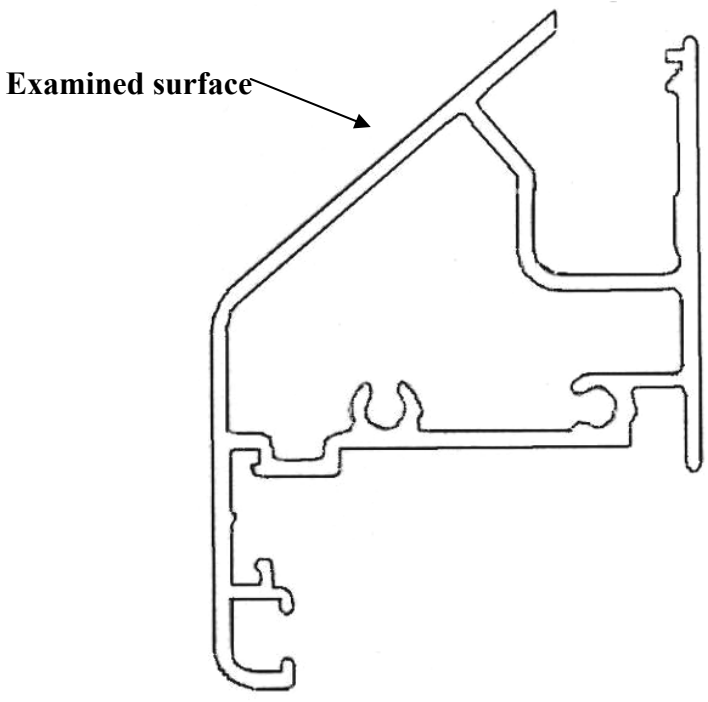

Figure 39 Cross section of profile 610103

Table 2 AA6060 specification [36]

Component	Wt %
Aluminium (Al)	Max 97.8
Chromium (Cr)	Max 0.05
Copper (Cu)	Max 0.1
Iron (Fe)	0.1 – 0.3
Magnesium (Mg)	0.35 – 0.6
Manganese (Mn)	Max 0.1
Silicon (Si)	0.3 – 0.6
Titanium (Ti)	Max 0.1
Zinc (Zn)	Max 0.15
Other each	Max 0.05
Other total	Max 0.15

3.1.1 Conditions for trials

As mentioned in the previous chapters extrusion parameters for this trials are homogenization condition, pre-heat temperature, extrusion speed and exit temperature. All the logs used in this study were homogenized at 575°C for 2 hours. Billet samples were also collected for pre-heat temperatures at 430°C, 450°C and 470°C to compare microstructure for the given trials.

The pre-heat furnace was set to the desired pre-heat temperature, 15 minutes before the trial could commence. Before the billet comes out from the pre-heat furnace the temperature of the billet was checked automatically by the thermocouple probes installed in the furnace. This was done to make sure that the billet is at the correct pre-heat temperature. For every trial the billet length was set at 610mm, this roughly equates to a 45m long extrudate. Once the die was installed into the extrusion press the first 10 billets were used to heat up the die to its stable temperature range. This stable temperature range is unknown. However it was assumed that the die reached the stable temperature range within the first 10 billets. The trial commenced on the 11^{th} billet, which was the starting point of data gathering. 11^{th} billet to 15^{th} billet were extruded at 25m/min and the next 5 billets were extruded at 30m/min or higher extrusion speeds.

This procedure was followed for each trial listed in Table 3. Extrusion speed 25m/min was used as a basis to compare the performance of the extrudate when the speed was increased. A preliminary investigation was done to verify whether the extrusion speed was operating at the set extrusion speed.

Table 3 Trial conditions

Trial	Pre-heat temperature	11^{th} – 15^{th} Billet Extrusion speed	16^{th} – 20^{th} Billet Extrusion speed
1	430°C	25m/min	30m/min
2	450°C	25m/min	30m/min
3	450°C	25m/min	35m/min
4	450°C	25m/min	40m/min
5	450°C	25m/min	45m/min
6	470°C	25m/min	30m/min

3.1.2 Ram speed and ram pressure determination

When a billet is extruded the control panel of the extrusion press produces a ram speed and ram pressure curves. This control panel was recently installed and the performance of the control panel is unknown, therefore it was essential and was part of this work to gather the ram speed and ram pressure to verify whether extrusion press is operating at the set extrusion speed. However these data could not be stored due to the instrumental limitations. Therefore a snap shot of the control panel, as shown in Figure 40, was taken by a digital camera for every billet being extruded during the experiments and used to carry out the preliminary investigation.

Figure 40 Control panel ram speed and pressure plots of the extrusion press

3.1.3 Exit temperature curves determination

The exit temperature data was only displayed on the control panel and presently could not be recorded. Therefore to record the exit temperature data, a digital video camera was used for every billet being extruded. The exit temperature of the extrusion was measured by using infra red camera at a location approximately 1m away from the exit of the die and therefore calibration of the infra red camera was done to estimate the drop in exit temperature from the die cavity.

Figure 41 Exit temperature display for the extrusion press

The temperature data was manually retrieved and was used to plot the exit temperature. This was a very time consuming activity, but have to be done. The digital video camera was recording 8 slides per second. Generally the length of a trial was about 20 – 26 minutes for a total of 10 billets for each trial depending on the extrusion speed. Therefore 9600 (20x60x8) – 12480 (26x60x8) data points were manually retrieved to construct the exit temperature curves.

3.1.3.1 Accuracy of infra red cameras

The infra red cameras measure the exit temperature of the extrusion approximately 1m from the exit of the die cavity. Therefore the exit temperature measured values are not the true values and probably few degrees below the actual exit temperatures. A high sensitive K type thermocouple probe was used to measure the exit temperature drop. The thermocouple probe was placed on the surface of the extrudate for roughly about 2 seconds while it was being extruded at 5m/min. A lower extrusion speed was selected for safety purposes. As shown in Table 4 the infra red cameras have 2°C – 3°C error.

Table 5 lists the exit temperature drop with distance. This data could be used to estimate the temperature at exiting the die cavity. Figure 42 shows the exit temperature drop along with the distance from the die cavity. This graph was produced based on the data listed in Table 5. According to the graph, the exit temperature at the die cavity is approximately 4°C higher than the temperature measured by the infra red camera. Therefore the total temperature error is approximately 7°C.

Table 4 Calibration data of infra red camera

Infra red camera reading	Thermocouple probe reading
522°C	525°C
522°C	524°C
522°C	524°C

Table 5 Temperature drop

Infra red camera	Corrected	Position	Thermocouple	Temperature drop
522°C	525°C	1m	520°C	5°C
527°C	530°C	2m	520°C	9°C
528°C	531°C	3m	508°C	22°C

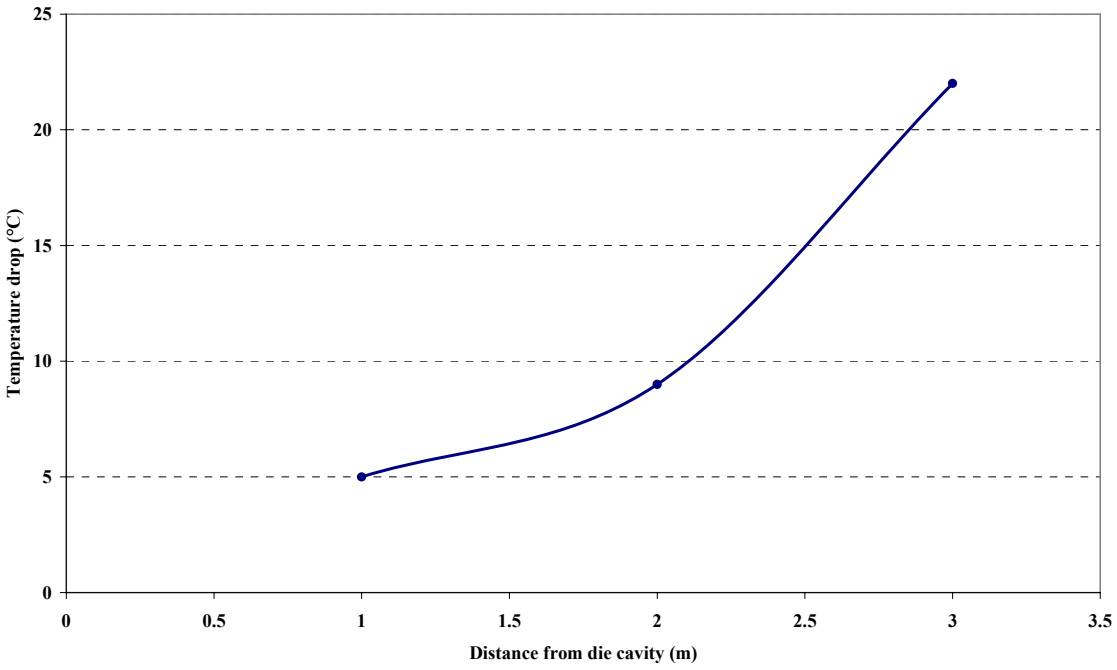

Figure 42 Exit temperature drop with distance

3.1.4 Sampling for microstructure and surface analysis

Samples from the extrusion logs were taken to analyse the microstructure and this could determine how well the homogenization process has affected the structure of the logs. Samples were also taken after pre-heating for temperatures of 430°C, 450°C and 470°C to check whether the microstructure has changed during the pre-heating process.

After extruding the 10 trial extrudates, they were sent for stretching and cutting. At the cutting operation samples of a length of 0.75m was collected for every trial extrudate. The sample was taken at the location where the extrusion process achieved the steady state condition. The steady state location was determined when the extrusion process operates at the highest exit temperature and at a constant extrusion speed. This usually occurs beyond the half way point of the extrusion process. Therefore these collected samples correspond to the stable exit temperature and the set extrusion speed. Samples of the extrudates were collected for pre-heat temperature of 450°C. Extrudate samples were not collected for pre-heat temperature at 430°C and 470°C since there was no correlations to link die pick-up with pre-heat temperature.

3.1.5 Analysis of extrusion samples

The samples collected after cutting were used to analyse the surface defects. The extrudate surface indicated in Figure 39 was used to count the number of die pick-up. On this surface an area length of 10cm and width of 5cm was selected (which was the worst affected) and was scanned at 2400 dots per inch. This image was then enlarged 3 times to fit an A4 paper and was printed. The printed image was used to count the amount of die pick-up and the length of each die pick-up. This was used to determine whether the number of die pick-up had increased when the extrusion speed was increased.

Samples contained surface defects such as die pick-up were gathered for microstructural analysis. These samples were cross sectioned and were viewed using scanning electron microscope and optical microscope.

3.1.6 Analysis of die samples

Figure 43 shows a typical die bearing surface. This die sample was used to examine the cross section, where it could reveal the condition of the bearing surface in terms of

microstructure and roughness. It is very important to observe the die bearing surface since it could have some influence on die pick-up.

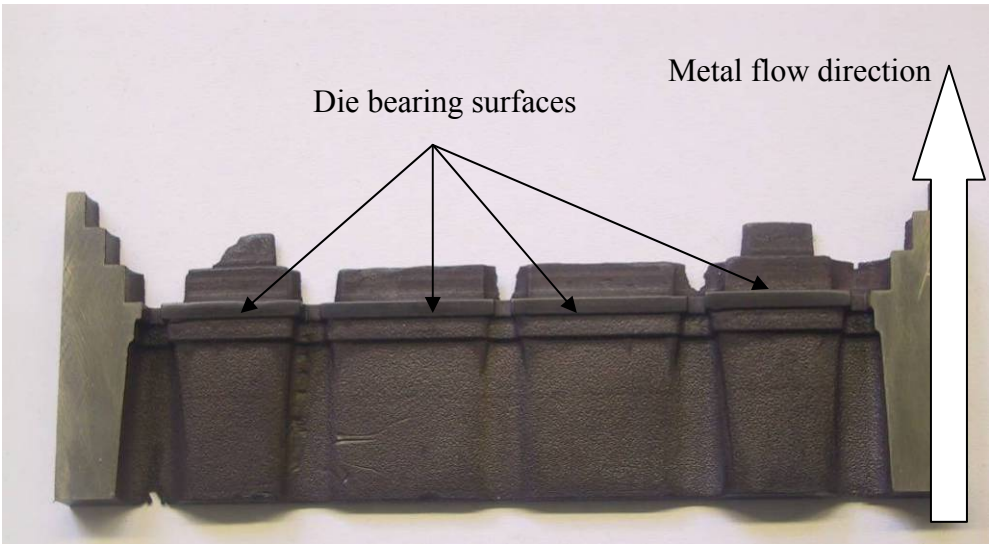

Figure 43 Top view of bearing surfaces of a die

The die of which the shown sample was taken had done nearly 20runs which roughly equates to 10 – 15 tons. When the die is removed from an extrusion cycle, the die cavity is filled with solid aluminium and therefore to collect a sample of the die, the die was immersed in NaOH solution at elevated temperature to remove the aluminium. The NaOH solution attacks only the aluminium and any aluminium based intermetallics. Therefore if there are any irregularities on the surface it could be that the surface was damaged during extrusion or the cavities generated due to any intermetallics which was decayed due to NaOH solution.

3.2 Trials for determination of incipient melting temperature

3.2.1 Calibration of the furnace

The trials at AUT University were conducted to determine the incipient melting temperature for AA6060. As mentioned in sections 1.2 and 1.3.3 incipient melting may cause die pick-up and this temperature determines the maximum temperature that AA6060 alloy could be extruded. The eutectic melting reactions and their melting temperatures are well established. However depending on the alloy composition and kinetics of dissolution, some of the eutectic melting reactions may not occur. Therefore it is important to determine the incipient melting temperature for AA6060 alloy.

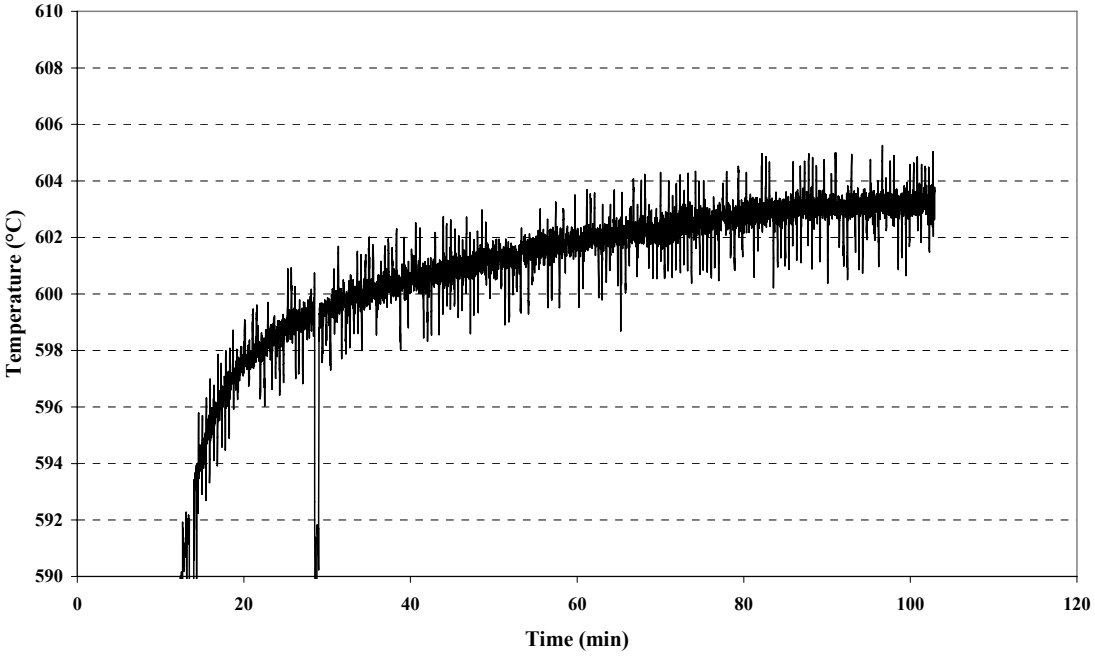

Figure 44 Temperature measurement for the furnace at AUT University

The furnace at AUT University was used for these trials. Before the trials could commence the furnace was checked to confirm whether it could operate accurately at the set temperature. The furnace was set at 605°C and the temperature was measured at the centre of the furnace with the aid of a thermocouple. The thermocouple was inserted into an AA6060 aluminium sample which had the dimensions of 20mmx10mmx20mm. This was done to measure the temperature at the centre of the aluminium sample. Figure 44 shows the temperature of the aluminium sample when the furnace was set at 605°C. However the furnace did not remain at 605°C but fluctuated between 602°C and 605°C and almost took 2 hours to reach 605°C. Therefore the error of the furnace was -3°C and during the trials this error was considered when setting the furnace temperature.

3.2.2 Trial procedure

The trial procedure is listed below.

- Set the furnace temperature (for example 577°C) and leave it for 2 hours to heat up
- Put the AA6060 aluminium sample in the middle of the furnace and leave it for 1 hour
- Take the aluminium sample and dip it into water for water quenching
- Repeat the above for temperatures of 577°C, 587°C, 597°C, 602°C, 612°C, 622°C and 632°C

Water quenching was done to capture the instantaneous microstructure of the AA6060 alloy for each temperature.

3.2.3 Sample preparation for microstructure examination

Samples collected from extrusions (section 3.1.5), die (section 3.1.6) and heat treated aluminium alloy (section 3.2.2) were used to examine the microstructure with the optical microscope and a scanning electron microscope. To examine the microstructure, the sample has to be prepared according to procedure below.

- Mount sections in a polymer resin mixture and allow 24 hours to harden
- Grind the surface of the section from 120 grit through to 2400 grit and water was used as lubrication
- Clean thoroughly with alcohol and dry
- Polish surface using material polishing disk with 6μm and 1μm diamond paste
- Chemically etch sections by immersing in 0.5%HF for 15 seconds
- Clean thoroughly with alcohol and dry

3.3 Microscopy analysis

Nikon optical microscope and the Phillips scanning electron microscope (SEM) were used in this study.

3.3.1 Optical microscopy

The Nikon optical microscope was used to view the microstructure of the samples. It has objective lenses of 5 times to 100 times and images were taken accordingly. The optical microscope was mainly used to identify important aspects of the microstructure and then later to be further analysed by SEM.

3.3.2 Scanning electron microscopy

The scanning electron microscope was most desired equipment used to view the microstructure of the samples. Energy dispersive X-ray spectroscopy (EDS) was used identify the types of elements present in the samples and is attached to the SEM. The SEM machine was located at University of Auckland, Department of Chemical and Material Engineering.

4 Results and Discussion

This chapter presents the results obtained by the trials explained in the previous chapter and discussed in order to analyse the results. Results and discussion chapter is structured into three components, which are the analysis on the highest exit temperature for AA6060 alloy, analysis on types of die pick-up and suggestions on how the types of die pick-up formed.

4.1 Incipient melting

As mentioned in section 3.2.3, these experiments were done to determine the incipient melting temperature of AA6060 alloy. This temperature determines the maximum temperature that the extrusions could be extruded for AA6060 alloy. At the incipient melting temperatures, the grain boundary starts to melt (section 2.1.1). Figure 45 to Figure 51 show the microstructure of samples heated at 575°C, 585°C, 595°C, 600°C, 610°C, 620°C and 630°C respectively. These samples were heated for 1 hour followed by water quench.

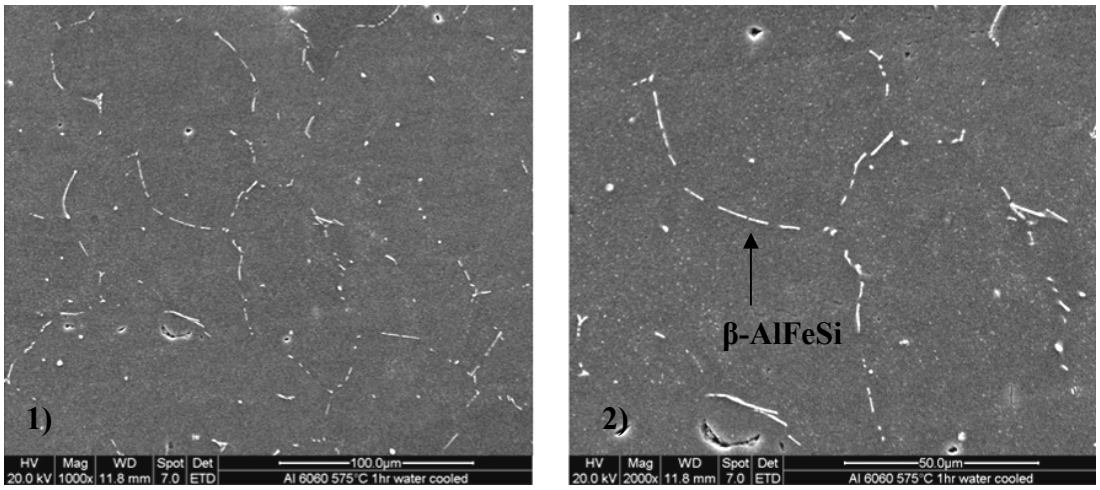

Figure 45 Microstructure of AA6060 heated at 575°C for 1 hour and water quenched, 1)Magnification of 1000x 2)Magnification of 2000x

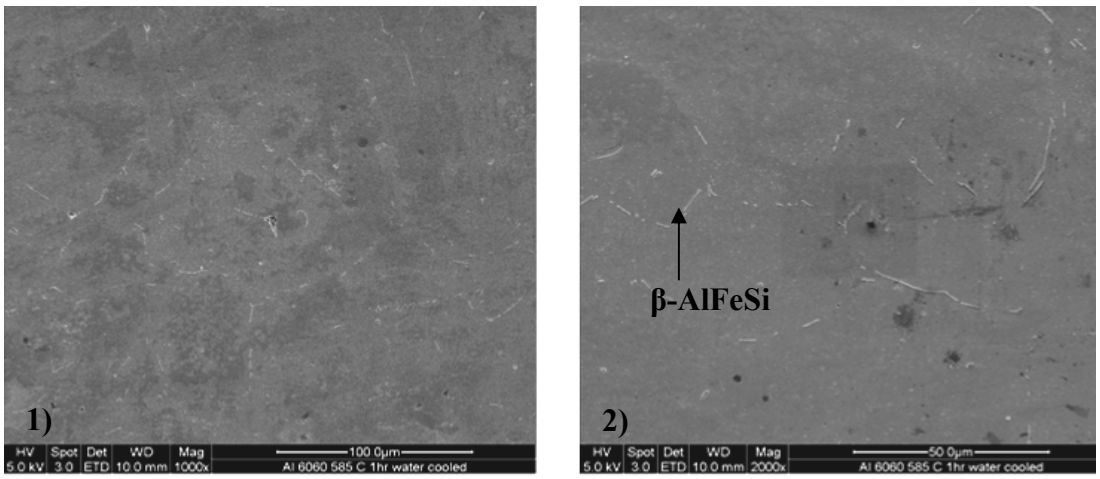

Figure 46 Microstructure of AA6060 heated at 585°C for 1 hour and water quenched, 1)Magnification of 1000x 2)Magnification of 2000x

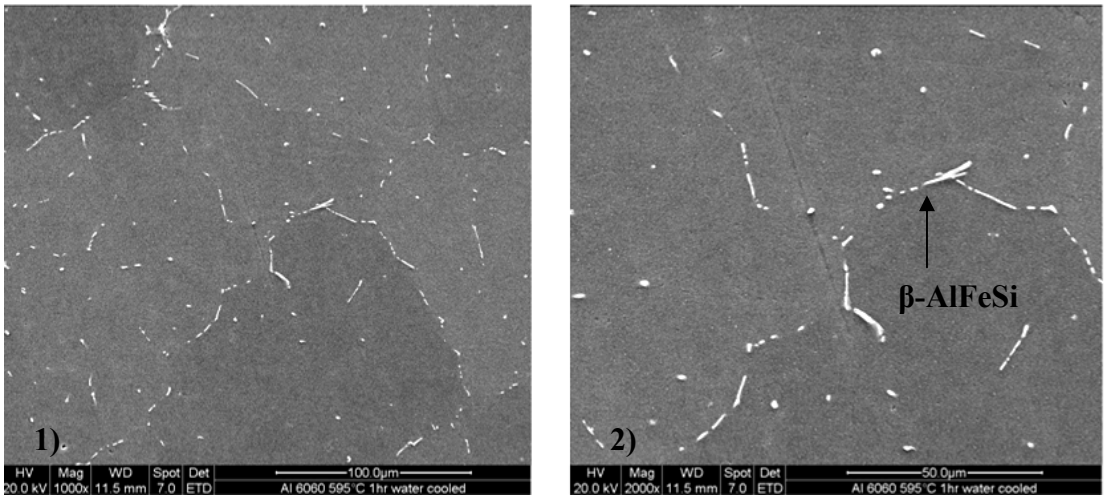

Figure 47 Microstructure of AA6060 heated at 595°C for 1 hour and water quenched, 1)Magnification of 1000x 2)Magnification of 2000x

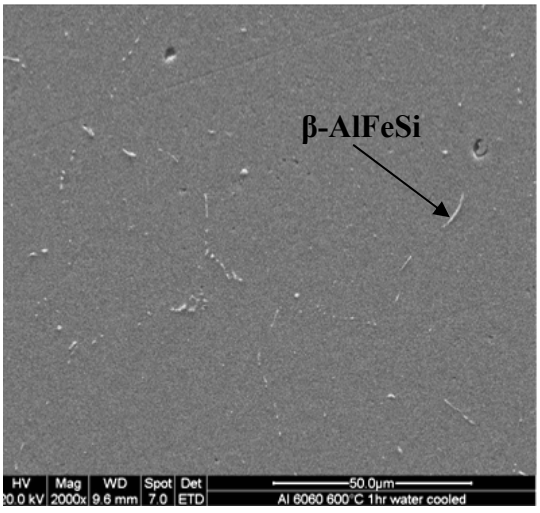

Figure 48 Microstructure of AA6060 heated at 600°C for 1 hour and water quenched, magnification of 2000x

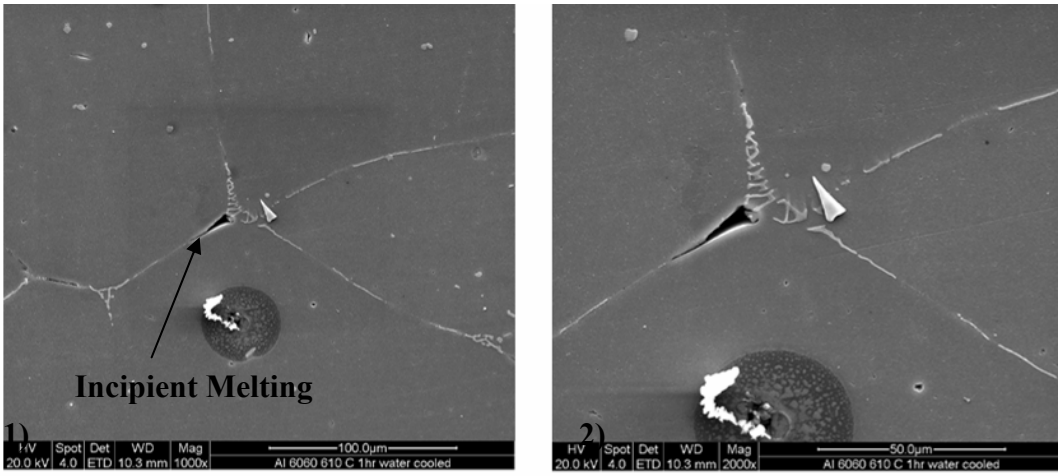

Figure 49 Microstructure of AA6060 heated at 610°C for 1 hour and water quenched, 1)Magnification of 1000x 2)Magnification of 2000x

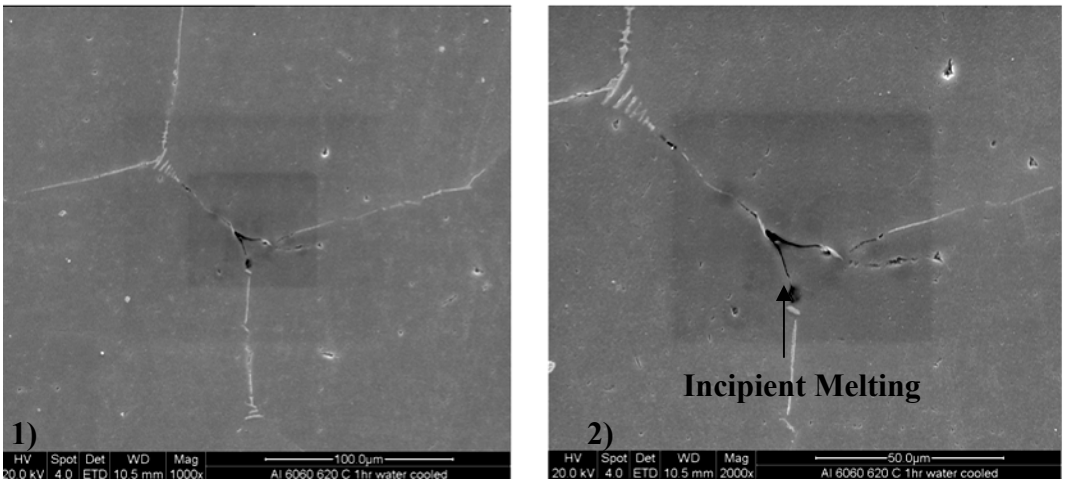

Figure 50 Microstructure of AA6060 heated at 620°C for 1 hour and water quenched, 1)Magnification of 1000x 2)Magnification of 2000x

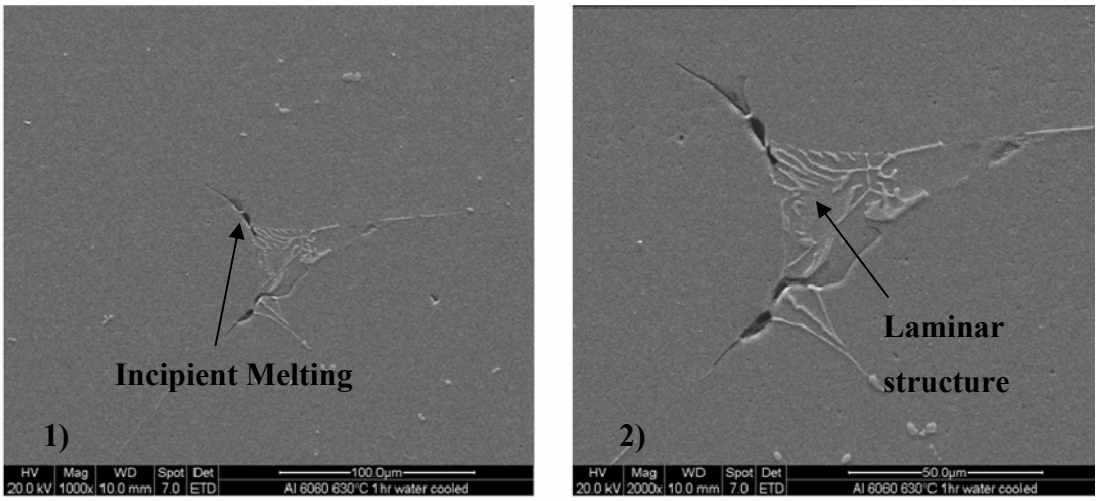

Figure 51 Microstructure of AA6060 heated at 630°C for 1 hour and water quenched, 1)Magnification of 1000x 2)Magnification of 2000x

The microstructure for 575°C, 585°C, 595°C and 600°C had not changed in terms of incipient melting. However the microstructure had changed at 610°C, 620°C and 630°C. This suggests that a phase transformation had occurred at 610°C. At 610°C and beyond there were pores on the grain boundary and laminar structure had developed.

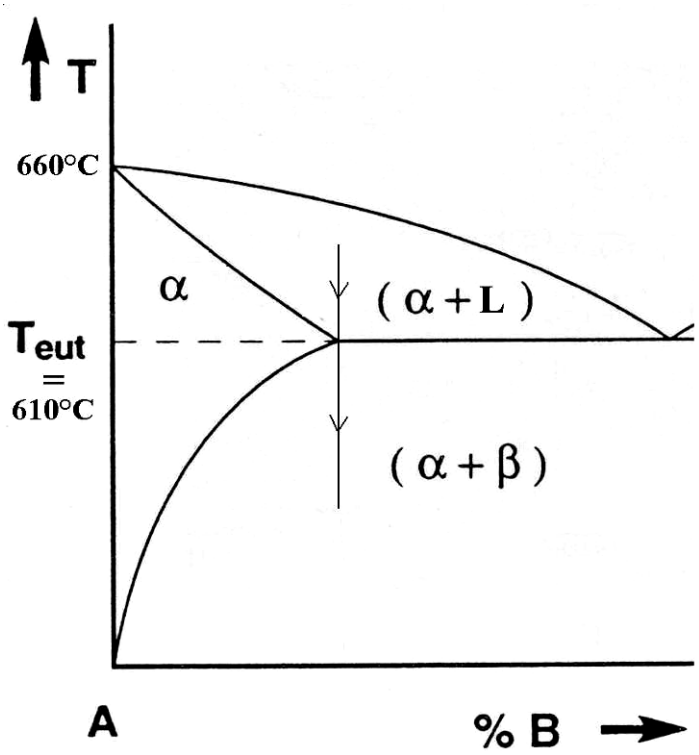

Figure 52 Possible eutectic binary phase diagram for AA6060

Figure 52 shows a suggested eutectic phase diagram for AA6060 alloy. Eutectic temperature is the lowest melting temperature for an alloy. Below the eutectic temperature the alloy represents as (α + β) phase or α phase. Above the eutectic temperature the alloy represents as (α + liquid) phase. The grain boundary contain second phase particles, in the case of AA6060 alloy, Mg_2Si and β-AlFeSi are present.. It is also not clear whether the Mg_2Si have fully dissolved into the solid solution. If sufficient Mg_2Si were present in the alloy system the grain boundary would have started to melt at 555°C [4, 7, 16, 17, 21]. Since eutectic melting was not detected above 555°C, therefore the β phase for AA6060 alloy is most likely to be β-AlFeSi.

Above 610°C and below the liquidus temperature, the β-AlFeSi combines with α phase and produces liquid. When the material is cooled down below 610°C, the liquid phase starts to solidify. There is also a volume difference between liquid and solid state, and

therefore when the liquid is solidifying, pores could form due to shrinkage. Pores found in Figure 49 to Figure 51 are evidence that liquid has formed at 610°C to 630°C. Therefore this confirms that the lowest melting point or eutectic temperature for AA6060 alloy is 610°C and hence the highest exit temperature that AA6060 extrudate could be exposed to is 610°C.

4.2 Preliminary investigation on extrusion conditions

4.2.1 Microstructure of billet before pre-heating

Before the trials were commenced, samples were taken from the extrusion logs. The logs were in the as-homogenized conditions. The extrusion logs were AA6060 Comalco super flow alloy, which has a low magnesium composition.

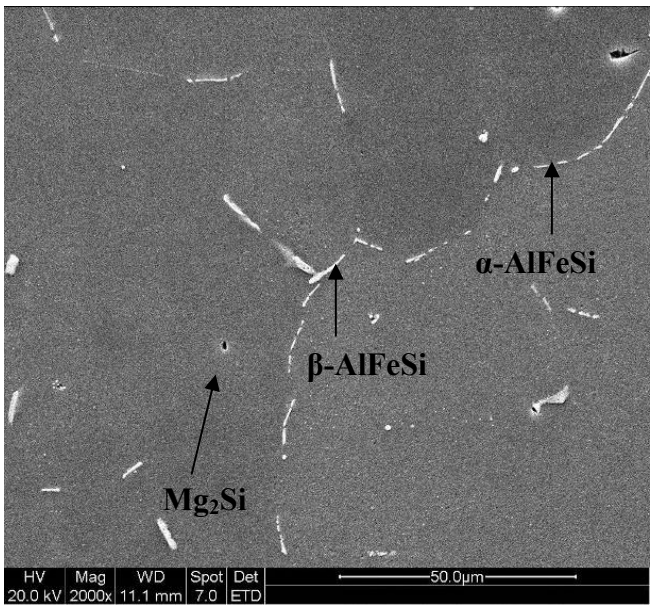

Figure 53 Microstructure before pre-heating at magnification of 2000x

Figure 53 shows the microstructure of the samples from the extrusion logs after homogenization. The extrusion logs were homogenized at 575°C for 2 hours. The second phase particles which appear in white are quite fragmented with few large in size. The chemical composition of the second phase particle was obtained at location AA as shown in Figure 54. EDS analysis of these particles is given in Figure 55.

Figure 54 Second phase particle before pre-heating

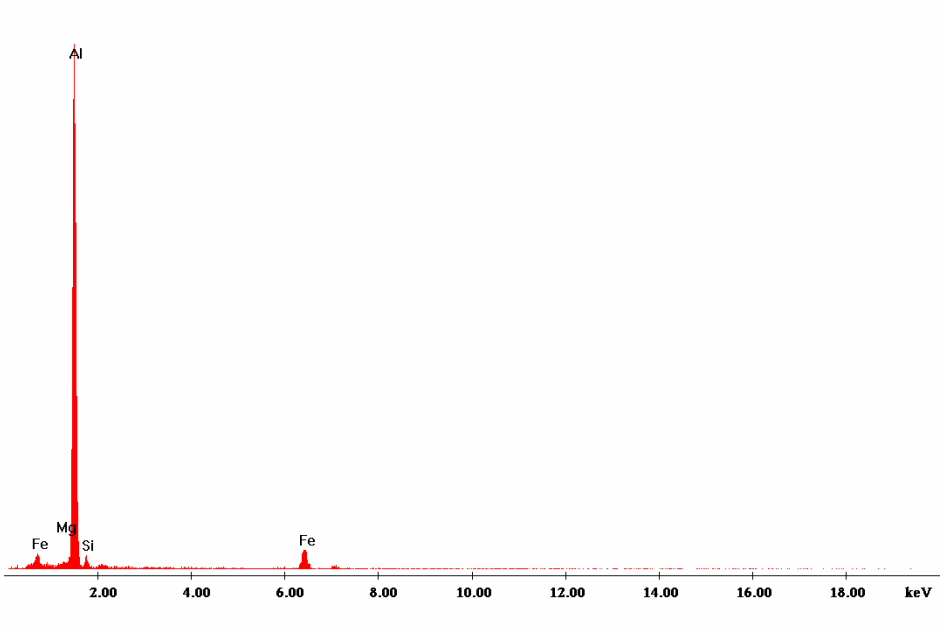

Figure 55 EDS spectrum of second phase particle

The EDS spectrum shown in Figure 55 confirms that these particles are β-AlFeSi. The compositions of the black spots were too small to obtain but however according to the literature these particles may be Mg_2Si [20, 21]. Since the Mg_2Si particles are too small it was unable to obtain the composition.

4.2.2 Microstructure of billet after pre-heating

Figure 56 to Figure 58 show the microstructure of the samples pre-heated at 430°C, 450°C and 470°C just before extruding. The samples were water quenched to obtain the

instantaneous microstructure. Figure 58 was taken by the optical microscope, due to the time limitations for using the SEM. The microstructure of billets just before extruding (after pre-heating) appears to be very similar to the microstructure of the extrusion logs after homogenization with some fragmented AlFeSi particles.

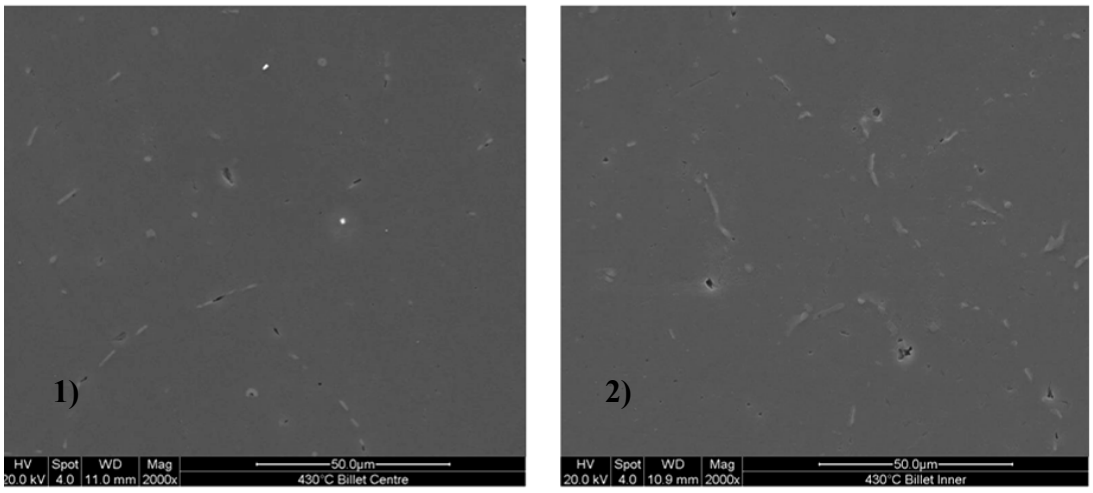

Figure 56 Microstructure for 430°C pre-heat temperature 1) centre of the billet 2) closer to the edge of the billet

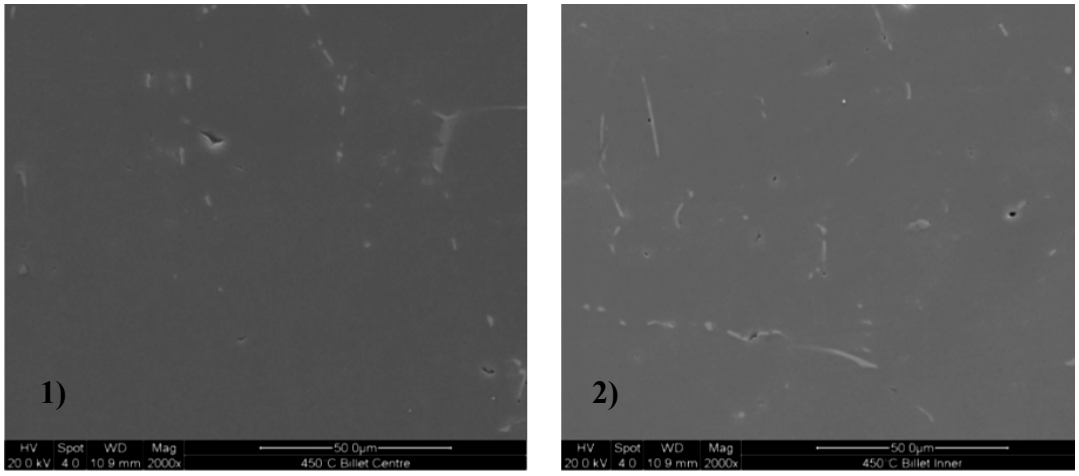

Figure 57 Microstructure for 450°C pre-heat temperature 1) centre of the billet 2) closer to the edge of the billet

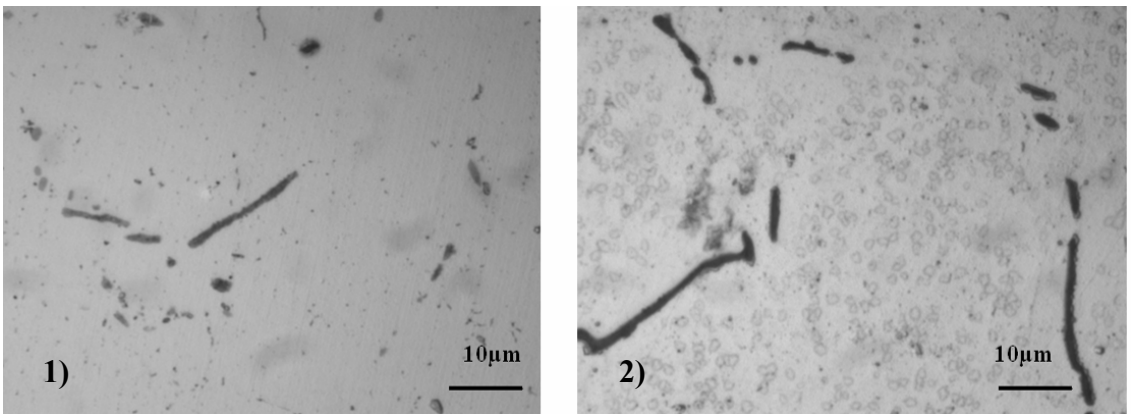

Figure 58 Microstructure for 470°C pre-heat temperature 1) centre of the billet 2) closer to the edge of the billet

4.2.3 Estimation of extrusion speed using ram speed curves

Ram speed and ram pressure curves were captured with a digital camera as described in section 3.1.2. In these curves the yellow line denotes the ram pressure and the red line denotes the ram speed as shown in Figure 59. There were 60 ram speed and ram pressure curves captured.

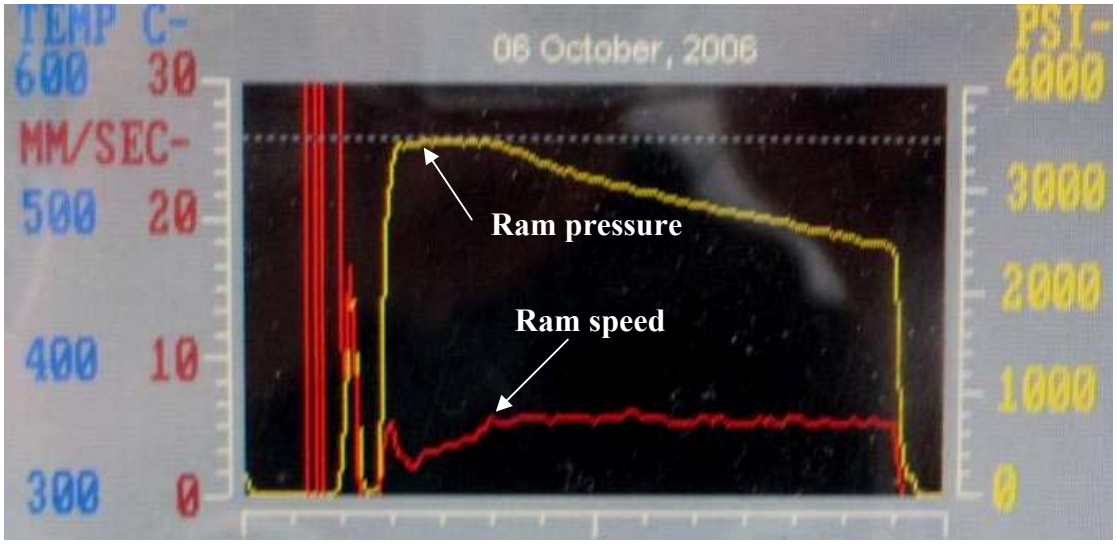

Figure 59 Ram speed and ram pressure curves

The ram speed and ram pressure curves could be further simplified as shown in Figure 60. This simplified version was used to identify the important data on the ram speed and ram pressure curves.

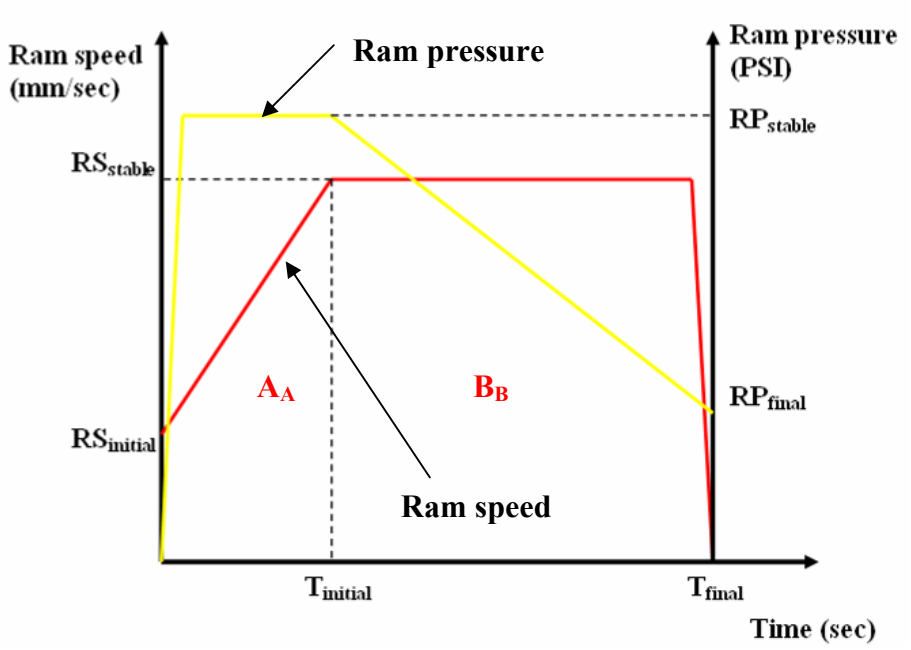

Figure 60 Simplified ram speed curve and ram pressure curve

The full list of ram speeds and ram pressure data could be seen in the appendix. The simplified graph (but accurate) shown in Figure 60 and the data could be used to estimate the exact and actual extrusion speed.

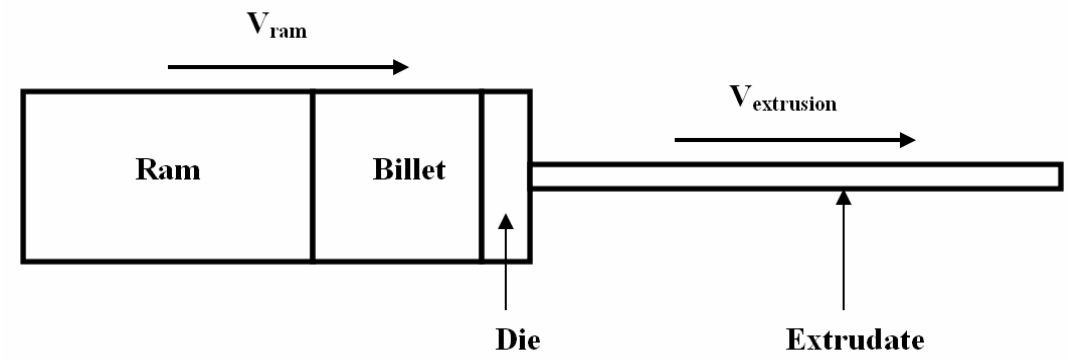

Figure 61 Schematic diagram for extrusion process

Figure 61 shows a schematic of the extrusion process and the derivation is given below; From mass balance, weight reduced per unit time of the billet is equal to the weight of the extrudate per unit time. Therefore;

$$\mathrm{Vol}_{\mathrm{extrudate}} = \mathrm{Vol}_{\mathrm{billet}}$$

where $Vol_{extrudate}$ is defined as the volume of material already exited the die per time unit and Vol_{billet} is defined as the volume of material being used from the billet to produce the exited extrudate per time unit.

The above equation could be further expanded as follows, where $V_{extrusion}$ is defined as the extrusion speed, $A_{extrusion}$ is defined as the cross sectional area of the extrudate, A_{billet} is defined as the cross sectional area of the billet and V_{ram} is defined as the ram speed.

$$V_{extrusion} \times A_{extrusion} = A_{billet} \times V_{ram}$$

The above equation is further simplified as follows.

$$V_{extrusion} = \frac{A_{billet} \times V_{ram}}{A_{extrusion}}$$

$$A_{billet} = \frac{\pi D^2}{4} = \frac{\pi \times (0.202)^2}{4} = 32.047 \times 10^{-3} m^2$$

$$A_{extrusion} = 476.4 \times 10^{-6} mm^2 \text{ (given by Fletcher Aluminium)}$$

By substituting the values for A_{billet} and $A_{extrusion}$, the value for $V_{extrusion}$ could be found in terms of V_{ram}.

$$V_{extrusion} = \left(\frac{32.047 \times 10^{-3} \times 60 \times V_{ram}}{476.4 \times 10^{-6} \times 1000} \right) \frac{m}{min} = \left(4.036 \times V_{ram} \right) \frac{m}{min}$$

V_{ram} could be further considered as $V_{ram\text{-}stable}$ and $V_{ram\text{-}average}$. $V_{ram\text{-}stable}$ is defined as the speed of the ram when it is stable and $V_{ram\text{-}average}$ is the average of the ram speed. Therefore the following equations could be used to calculate $V_{ram\text{-}stable}$ and $V_{ram\text{-}average}$.

$$V_{ram-stable} = RS_{stable}$$

$$V_{ram-average} = \frac{A_A + A_B}{T_{final}} = \frac{\left(\frac{(RS_{initial} + RS_{stable}) \times T_{initial}}{2}\right) + ((T_{final} - T_{initial}) \times RS_{stable})}{T_{final}}$$

By substituting V_{ram} in terms of $V_{ram\text{-}stable}$ and $V_{ram\text{-}average}$, the corresponding $V_{extrusion\text{-}stable}$ and $V_{extrusion\text{-}average}$ could be calculated. $V_{extrusion\text{-}stable}$ is defined as the stable extrusion speed and $V_{extrusion\text{-}average}$ is defined as the average extrusion speed. $V_{extrusion\text{-}stable}$ and $V_{extrusion\text{-}average}$ are calculated as follows.

$$V_{extrusion-exact} = (4.036 \times RS_{stable}) \frac{m}{min}$$

$$V_{extrusion-average} = \left(4.036 \times \frac{\left(\frac{(RS_{initial} + RS_{stable}) \times T_{initial}}{2}\right) + ((T_{final} - T_{initial}) \times RS_{stable})}{T_{final}}\right) \frac{m}{min}$$

From the above equations the $V_{extrusion\text{-}stable}$ and $V_{extrusion\text{-}average}$ could be estimated and are listed in Table 6. According to the data in Table 6, the estimated stable extrusion speeds and the estimated average extrusion speeds do not match closely with the set extrusion speeds. The error percentages of the stable extrusion speed were more than 30%. It seems to be that the values on the axes of the ram speed curves are not accurate or the ram speed measuring device is not calibrated. Therefore the ram speed data obtained from the control panel is not accurate to suggest or indicate whether the extrusion press is operating at the set extrusion speed.

Table 6 Estimated exact extrusion speed and average extrusion speed from ram speed data

Trial 1 set speed (m/min)	25	25	25	25	25	30	30	30	30	30
Stable extrusion speed (m/min)	17	17	17.5	17	17	19	19	19	19	19
Average extrusion speed (m/min)	15.5	15	14.5	14	14.2	15.7	14.8	15.3	16	15.7
Error(%)	**32.2**	**32.2**	**30.6**	**32.2**	**32.2**	**36.8**	**36.8**	**36.8**	**36.8**	**36.8**
Trial 2 set speed (m/min)	25	25	25	25	25	30	30	30	30	30
Exact extrusion speed (m/min)	17	16.5	16.5	16.5	17	21.4	21.4	21.4	21.4	22.2
Average extrusion speed (m/min)	14.9	14.9	15.4	15.7	16	19.5	20	17.7	18.7	20.5
Error (%)	**32.2**	**33.9**	**33.9**	**33.9**	**32.2**	**28.7**	**28.7**	**28.7**	**28.7**	**26**
Trial 3 set speed (m/min)	25	25	25	25	25	35	35	35	35	35
Exact extrusion speed (m/min)	17	17	17	17	17	22.2	24.2	23	23	21.8

Average extrusion speed (m/min)	15.7	16	15.8	15.3	15.8	20.5	22.3	21.6	21.6	20.8
Error (%)	**32.2**	**32.2**	**32.2**	**32.2**	**32.2**	**36.6**	**30.9**	**34.3**	**34.3**	**37.8**
Trial 4 set speed (m/min)	25	25	25	25	25	40	40	40	40	40
Exact extrusion speed (m/min)	15	17	15.8	16.5	17.4	25	27	28.3	27.5	28.3
Average extrusion speed (m/min)	14.1	16	15	15.3	16.6	21.2	23.2	24.8	25	26.1
Error (%)	**40.3**	**32.2**	**37.1**	**33.9**	**30.6**	**37.5**	**32.4**	**29.4**	**31.4**	**29.4**
Trial 5 set speed (m/min)	25	25	25	25	25	45	45	45	45	45
Exact extrusion speed (m/min)	15	16.2	16.2	15	17	28.3	30.3	31.5	27	29
Average extrusion speed (m/min)	13.7	15	14.7	14	16	24.2	27.7	29	23.8	25.4
Error (%)	**40.3**	**35.5**	**35.4**	**40.3**	**32.2**	**37.3**	**32.8**	**30.1**	**40**	**35.5**
Trial 6 set speed (m/min)	25	25	25	25	25	30	30	30		
Exact extrusion speed (m/min)	16.6	16.6	14.5	17.8	16.6	18.2	18.6	19.4		
Average extrusion speed (m/min)	15.5	15.8	14	17	15.9	17.6	17.7	18.3		
Error (%)	**33.9**	**33.9**	**41.9**	**29**	**33.9**	**39.5**	**38.2**	**35.5**		

The ram pressure curve shown (which is very similar to the rest of the ram pressure curves) in Figure 59 indicate that the extrusion press has a maximum pressure output of 3500psi and therefore the press almost takes 25% of the time during a cycle to achieve the set extrusion speed. Therefore during the initial period of the cycle the press did not operate at the set extrusion speed. When the pressure starts to decrease from the maximum ram pressure the extrusion press achieves its set extrusion speed. This relates in the ram speed graph when the ram speed continues to remain almost constant.

4.2.4 Estimation of extrusion speed by using exit temperature curves

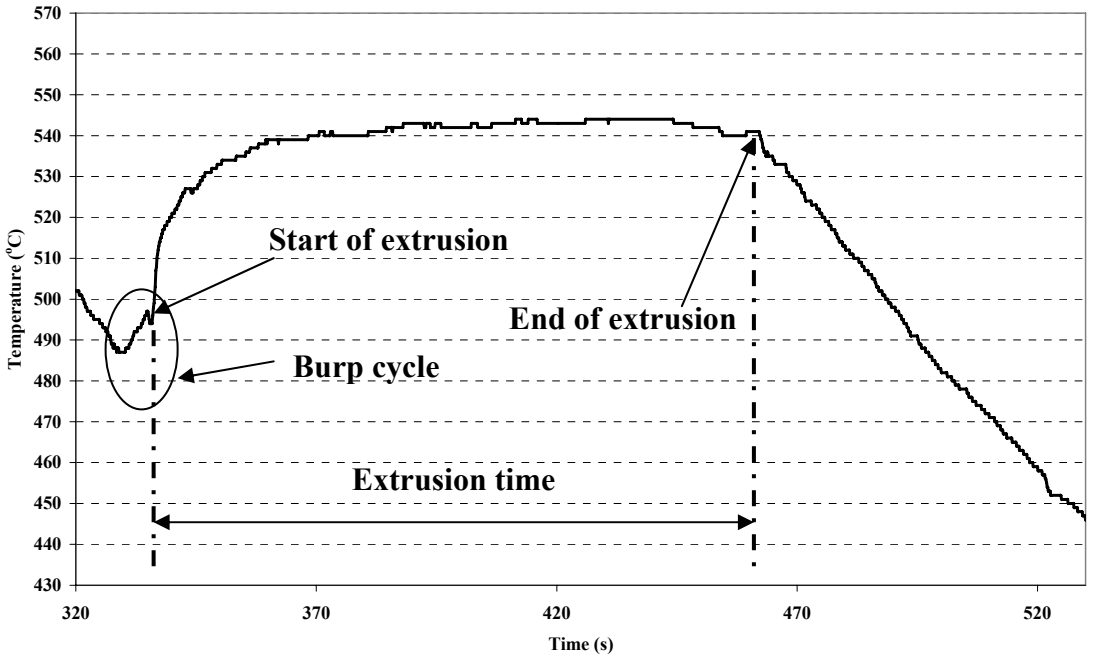

Figure 62 Typical exit temperature graph

Figure 62 shows a typical exit temperature curve for a 45m long extrudate. When the billet is loaded on to the extrusion press, the billet is pushed for few seconds and released. This process is called as the burp cycle, which is done to remove the air trapped between the new billet and die, by compressing the air and suddenly releasing it. During the process the material flows through the die and the exit temperature increases slightly and suddenly drops when the billet stops moving. After the burp cycle the extrusion process begins, where the exit temperature gradually increases and stabilizes when the extrusion speed reaches the set extrusion speed. When the extrusion is completed the extrudate stops moving and hence the exit temperature starts to decrease gradually. From the exit temperature curve, the extrusion time could be found, which is the time taken just after the burp cycle to when the exit temperature starts to drop as shown in Figure 62. When the extrudate length and extrusion time is known, the average extrusion speed could be calculated.

$$V_{extrusion-average} = \frac{\text{Length of extrusion}}{\text{Extrusion time}} \left(\frac{\text{m}}{\text{min}} \right)$$

Table 7 shows the calculated average extrusion speed by using the exit temperature curves. Generally the average extrusion speed is lower than the set extrusion speed,

since the extrusion press is unable to achieve the set extrusion speed for a period after the start of the extrusion cycle. Therefore, the average extrusion speed was lower than the set extrusion speed.

Table 7 Average extrusion speed calculated from exit temperature data

Trial 1 set speed (m/min)	25	25	25	25	25	30	30	30	30	30
Average extrusion speed (m/min)	21.2	18.2	21	20	21.7	23	22.7	23.5	25.2	25.9
Error (%)	**15.5**	**27.4**	**16.3**	**20**	**13.43**	**23.5**	**24.5**	**21.8**	**16.3**	**13.8**
Trial 2 set speed (m/min)	25	25	25	25	25	30	30	30	30	30
Average extrusion speed (m/min)	20.8	21.1	22.1	21.9	21.2	24.8	25.6	21.9	23	23
Error (%)	**17.1**	**15.8**	**11.9**	**12.4**	**15.5**	**17.5**	**14.8**	**27.4**	**23.5**	**23.2**
Trial 3 set speed (m/min)	25	25	25	25	25	35	35	35	35	35
Average extrusion speed (m/min)	21.1	21.4	21.4	21.6	21	29.8	29.2	27.9	29.6	28.1
Error (%)	**15.8**	**14.7**	**14.8**	**13.8**	**16.3**	**15.2**	**16.8**	**20.4**	**15.6**	**19.9**
Trial 4 set speed (m/min)	25	25	25	25	25	40	40	40	40	40
Average extrusion speed (m/min)	24.3	24.3	23.1	23.6	22.5	27.4	35.8	37.9	37.3	36.6
Error (%)	**3.2**	**3.2**	**7.7**	**5.7**	**10.2**	**31.7**	**10.6**	**5.3**	**6.9**	**8.7**
Trial 5 set speed (m/min)	25	25	25	25	25	45	45	45	45	45
Average extrusion speed (m/min)	24.8	24.6	23.2	23.5	23.5	35.3	40.4	41	39.8	41
Error (%)	**1**	**1.9**	**7.5**	**6.3**	**6.1**	**21.6**	**10.5**	**9.1**	**11.8**	**9.1**
Trial 6 set speed (m/min)	25	25	25	25	25	30	30	30		
Average extrusion speed (m/min)	20.6	20.2	21.7	21.7	21.9	21.5	20.9	21.4		
Error (%)	**17.8**	**19.5**	**13.4**	**13.6**	**12.6**	**28.4**	**30.5**	**29**		

The error percentage calculated for average extrusion speed by exit temperature data (Table 7) is less than the error percentage for average extrusion speed by ram speed data (Table 6). This confirms that the ram speed curves displayed on the control panel of the extrusion press is not accurate.

4.3 Exit temperature variation with extrusion speed

The construction of the exit temperature curves was done as explained in section 3.1.3. Figure 63 to Figure 68 show the exit temperature curves for trial 1 to trial 6.

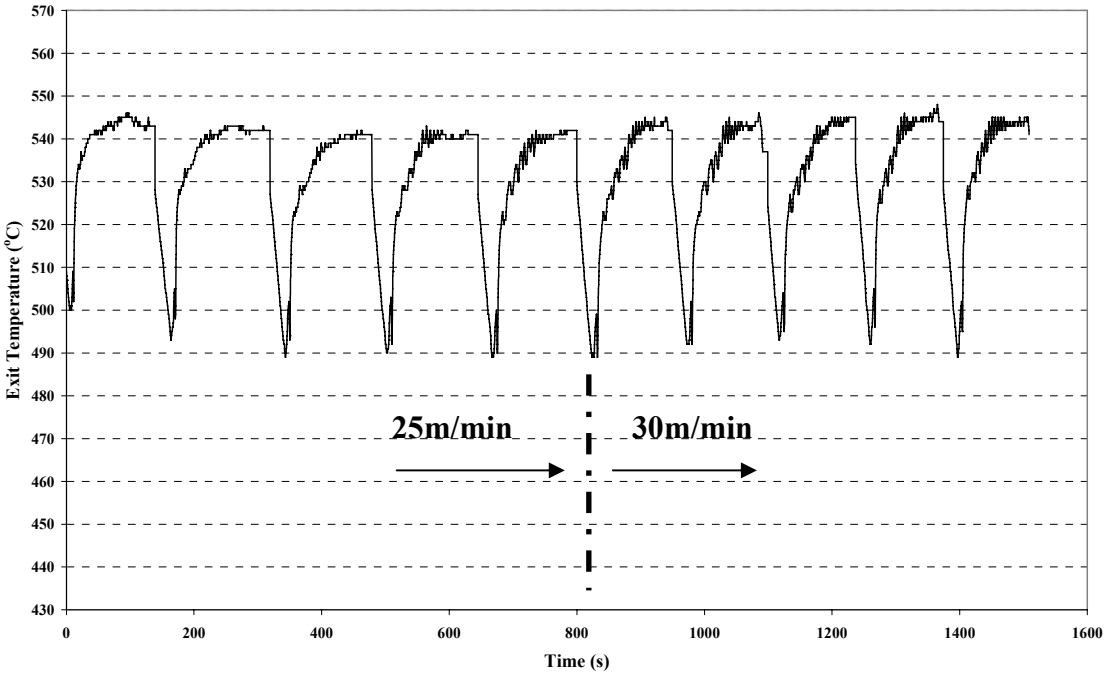

Figure 63 Exit temperature for extrudates of billets pre-heated at 430°C and extruded at 25m/min (billet 1-5) and increased to 30m/min (billet 6-10) - Trial 1

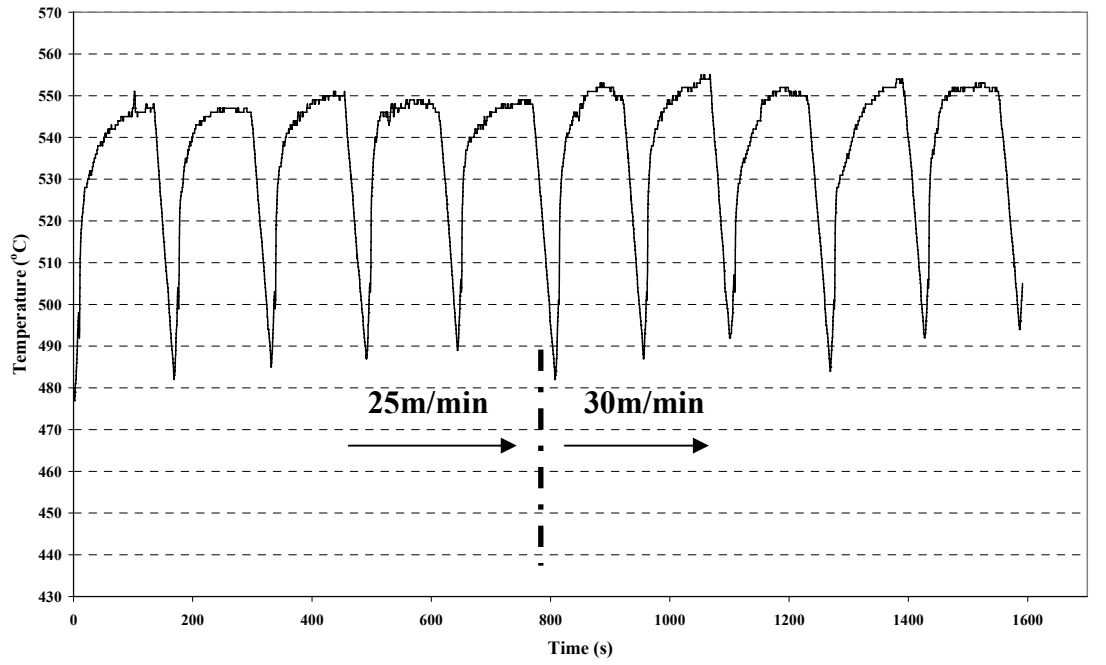

Figure 64 Exit temperature for extrudates of billets pre-heated at 450°C and extruded at 25m/min (billet 1-5) and increased to 30m/min (billet 6-10) – Trial 2

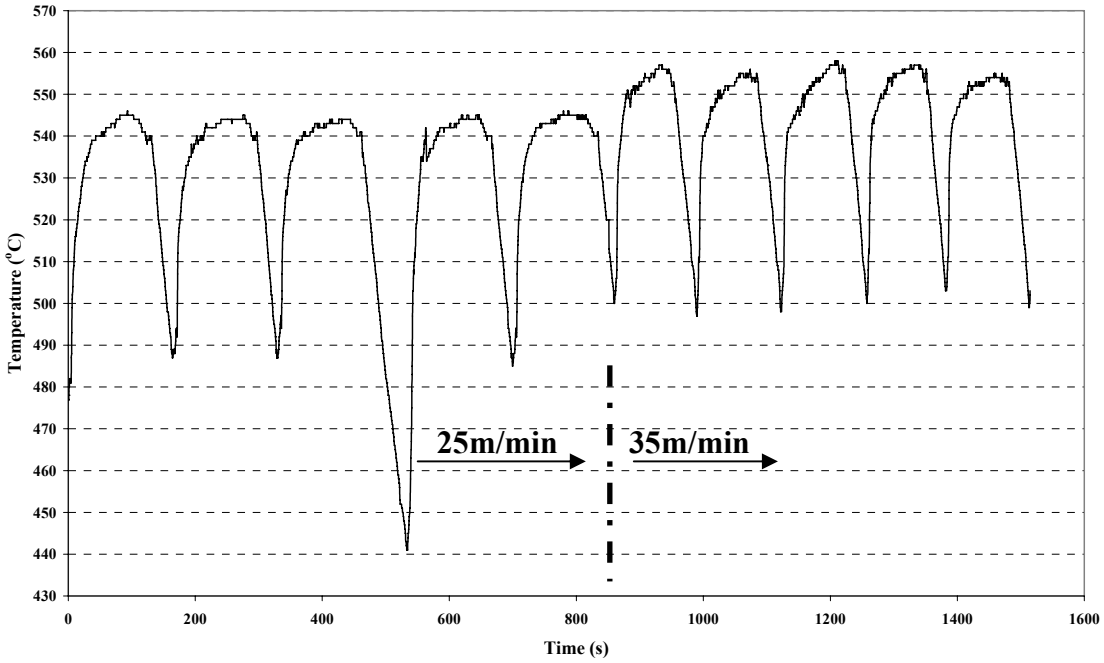

Figure 65 Exit temperature for extrudates of billets pre-heated at 450°C and extruded at 25m/min (billet 1-5) and increased to 35m/min (billet 6-10) – Trial 3

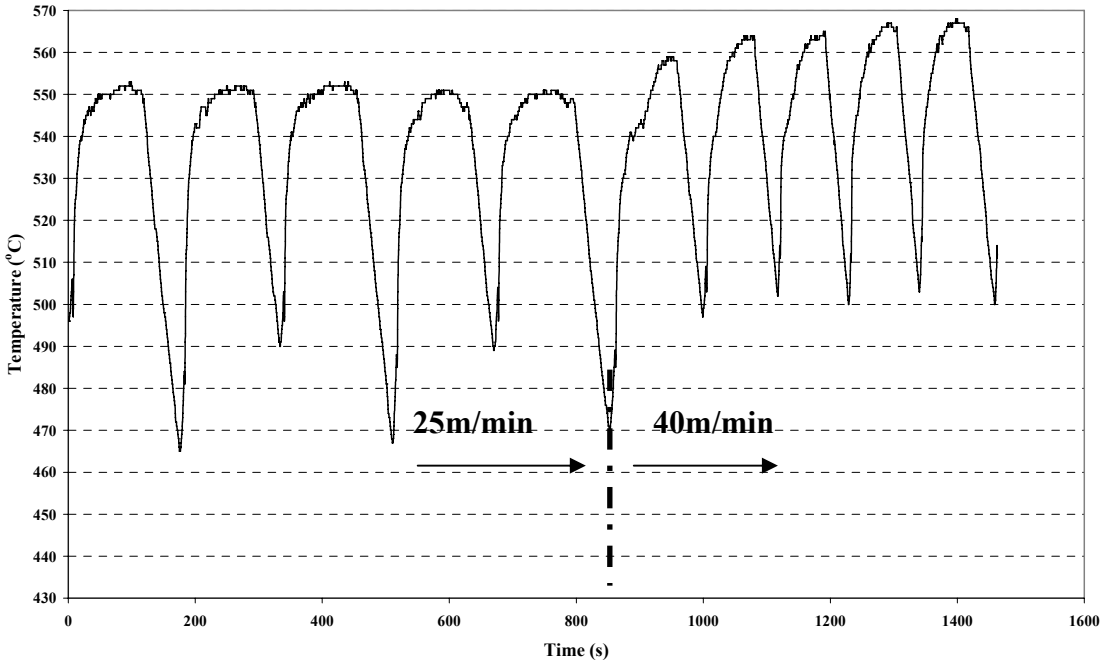

Figure 66 Exit temperature for extrudates of billets pre-heated at 450°C and extruded at 25m/min (billet 1-5) and increased to 40m/min (billet 6-10) – Trial 4

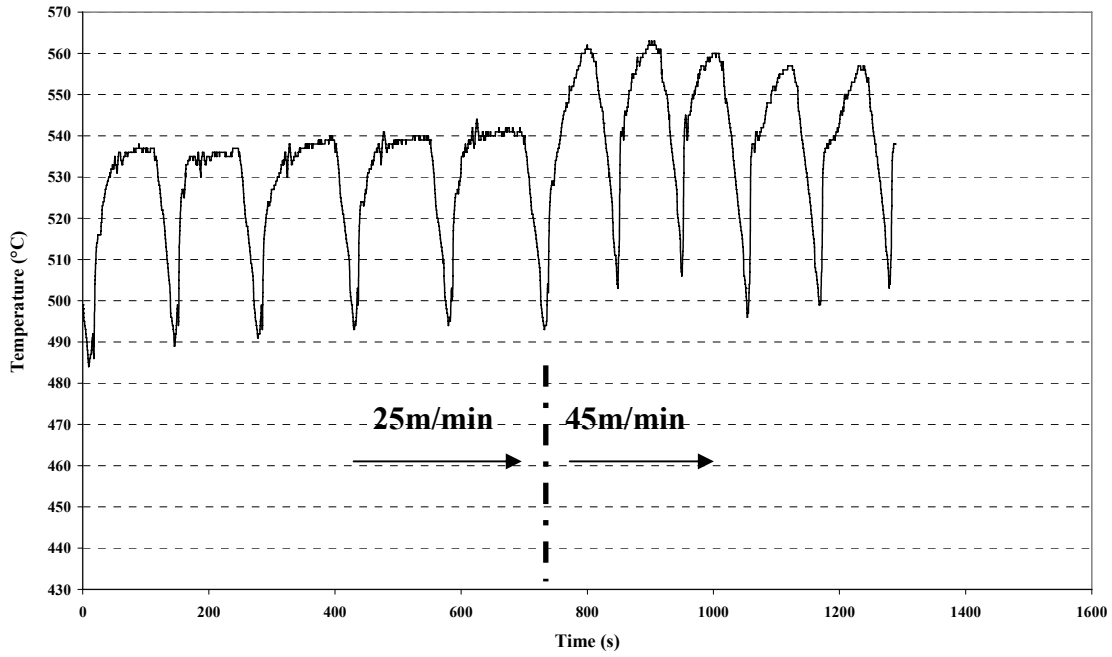

Figure 67 Exit temperature for extrudates of billets pre-heated at 450°C and extruded at 25m/min (billet 1-5) and increased to 45m/min (billet 6-10) – Trial 5

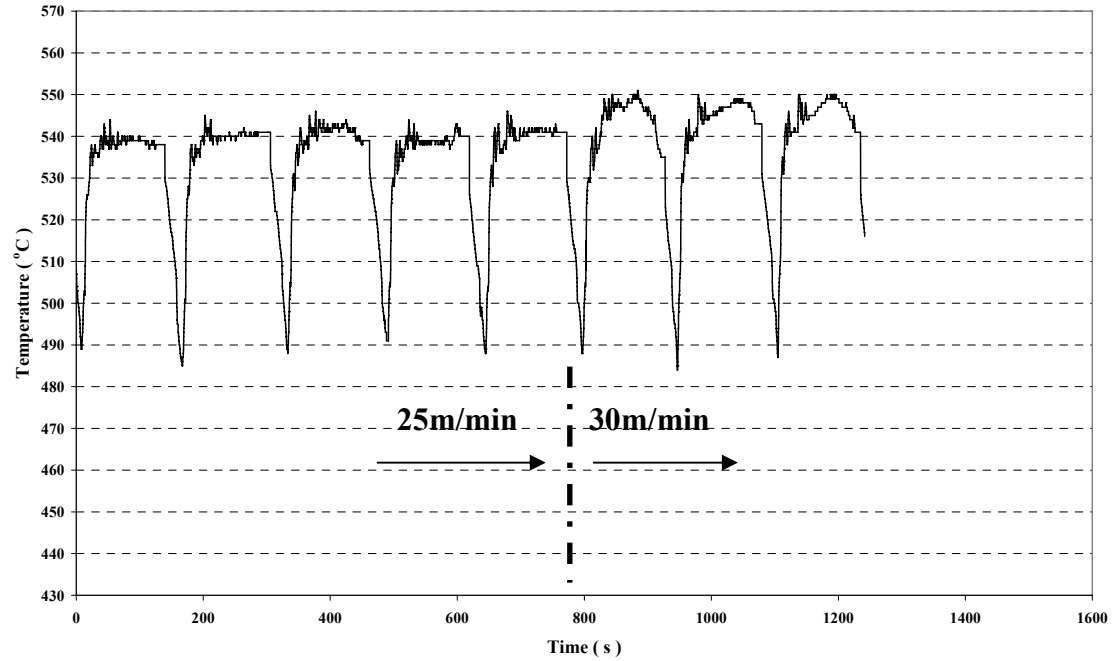

Figure 68 Exit temperature for extrudates of billets pre-heated at 470°C and extruded at 25m/min (billet 1-5) and increased to 30m/min (billet 6-8) – Trial 6

The maximum exit temperature for trial 1 increased from 542°C to 545°C when the extrusion speed is increased from 25m/min to 30m/min. Similarly for trial 6 the maximum exit temperature increases from 542°C to 549°C. In trial 2 the maximum exit temperature increases from 547°C to 552°C. When considering the exit temperature

measurements for trial 1, trial 2 and trial 6 the pre-heat temperature difference did not significantly influence the exit temperature. This suggests that when the extrusion process achieves a stable state, the pre-heat temperature has little influence on the exit temperature.

For trial 3 the maximum exit temperature changed from 547°C to 557°C, then for trial 4 the maximum exit temperature changed from 552°C to 567°C and for trial 5 the maximum exit temperature changed from 542°C to 562°C. Therefore an extrusion speed increase of 5m/min, 10m/min, 15m/min and 20m/min increased the exit temperature approximately by 5°C, 10°C, 15°C and 20°C respectively.

4.4 Die pick-up

Samples were collected from trial 2 – trial 5 as described in Table 3. Mainly die pick-ups were identified from these collected samples. There were three types of pick-up identified which are named as ***normal pick-up***, ***die line pick-up*** and ***lump pick-up***. In the sixty samples collected there was only one lump pick-up found.

4.4.1 Normal pick-up

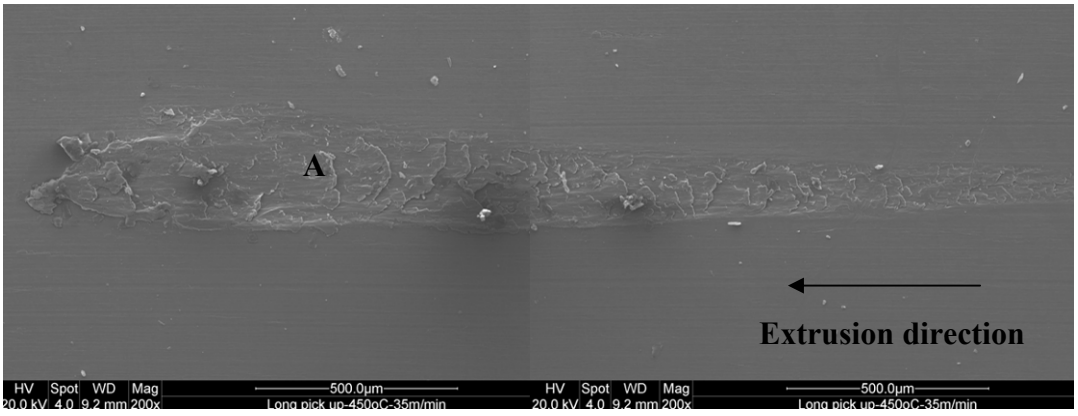

Figure 69 SEM macrograph showing pick-up at 200x

Figure 69 shows a typical (of many hundreds measured normal pick-up) which was found on the observed surface which was extruded at a speed of 35m/min. This pick-up is approximately 2.5mm in length and the width has a tapered feature which has a maximum width of about 330µm.

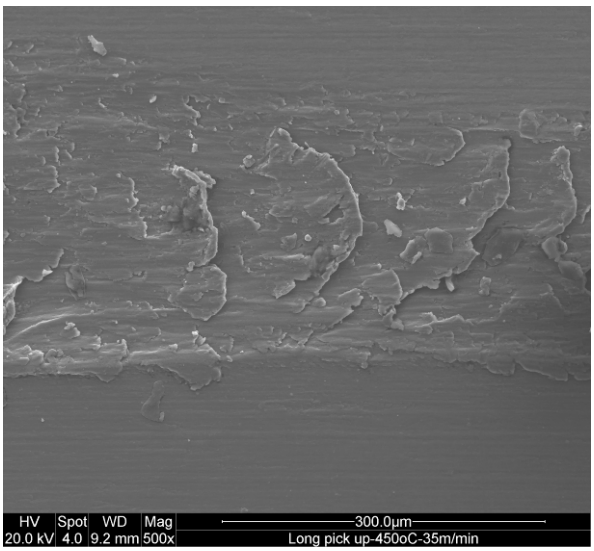

Figure 70 SEM macrograph showing a relative high magnification of area A in Figure 69

Figure 70 shows the pick-up surface at magnification of 500x at location A in Figure 69. The main feature observed at the surface of this pick-up was wave-like surface appearance.

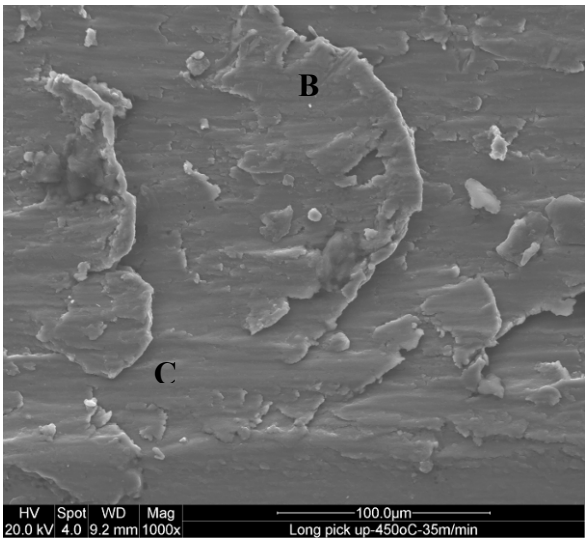

Figure 71 Pick-up surface at 1000x

Figure 71 shows the pick-up surface at magnification of 1000x. The EDS spectrum of location B and C are shown in Figure 72 and Figure 73 respectively. It revealed that the composition of these two locations are almost identical and contain almost only aluminium and some magnesium.

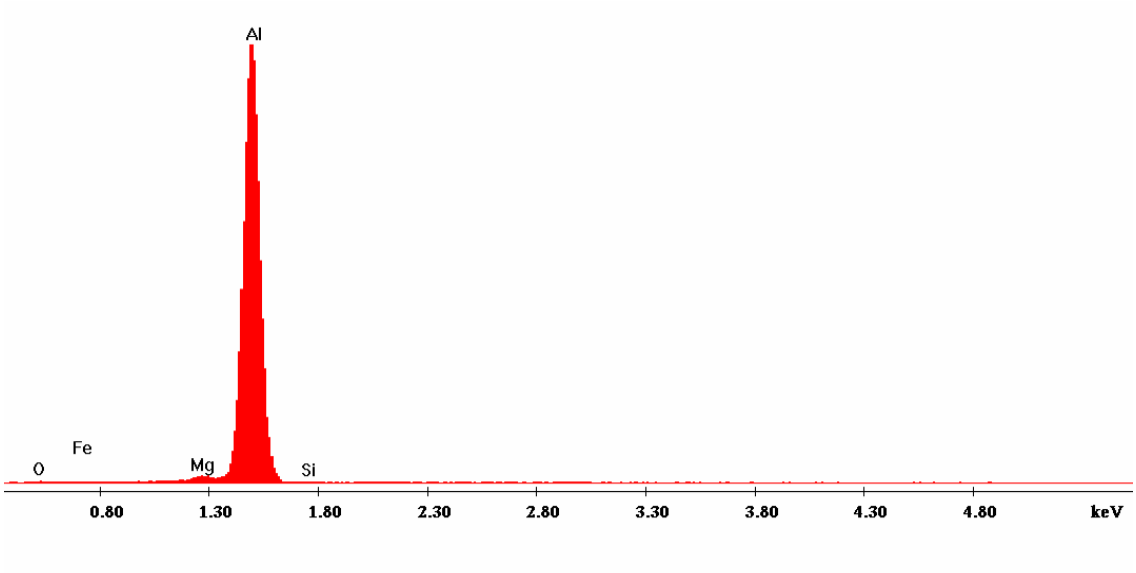

Figure 72 EDS spectrum at location B in Figure 71

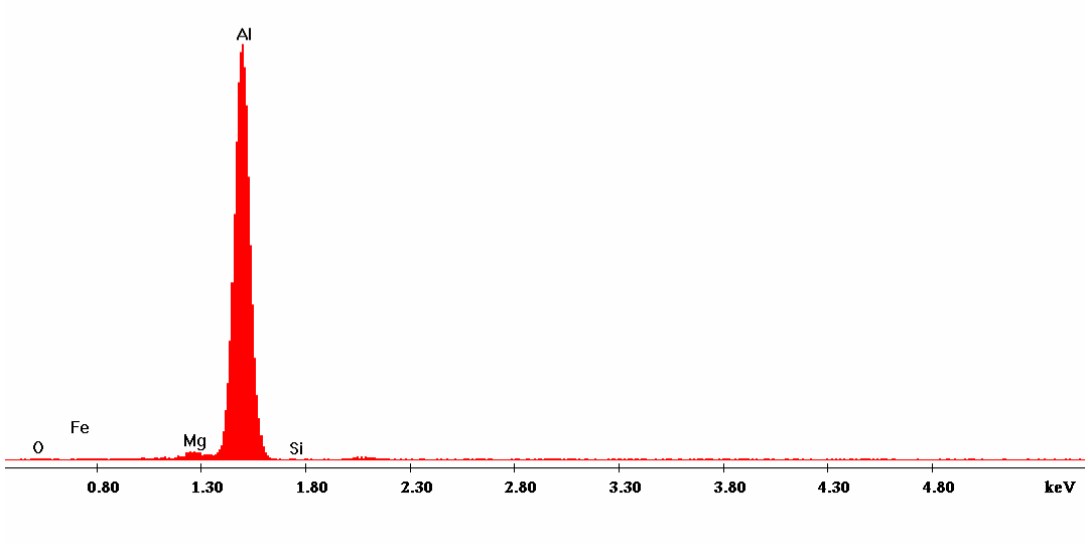

Figure 73 EDS spectrum at location C in Figure 71

Figure 75 shows the microstructure of a cross section of a normal pick-up. A normal pick-up shown in Figure 74 was cross sectioned in the middle and in the direction of the extrusion speed. As in the top view of the normal pick-up, the cross section shows waved like appearance. There is also no evidence of any micro cracks.

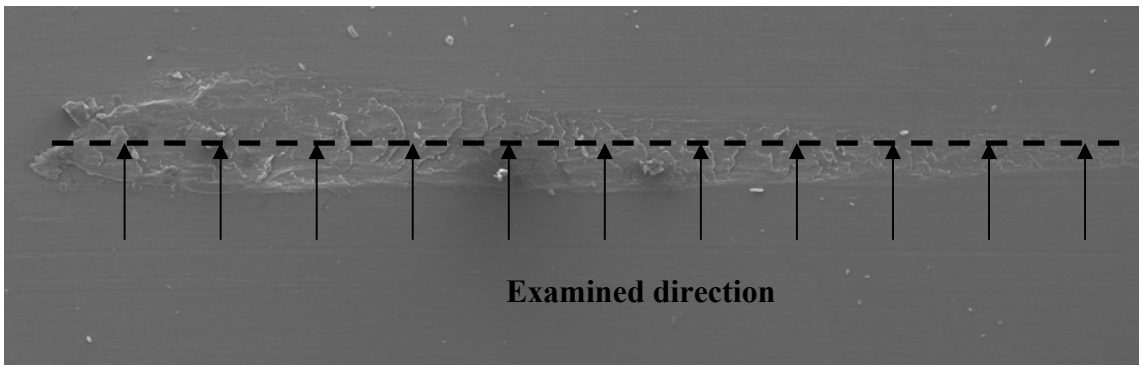

Figure 74 Cross sectioning location of normal pick-up

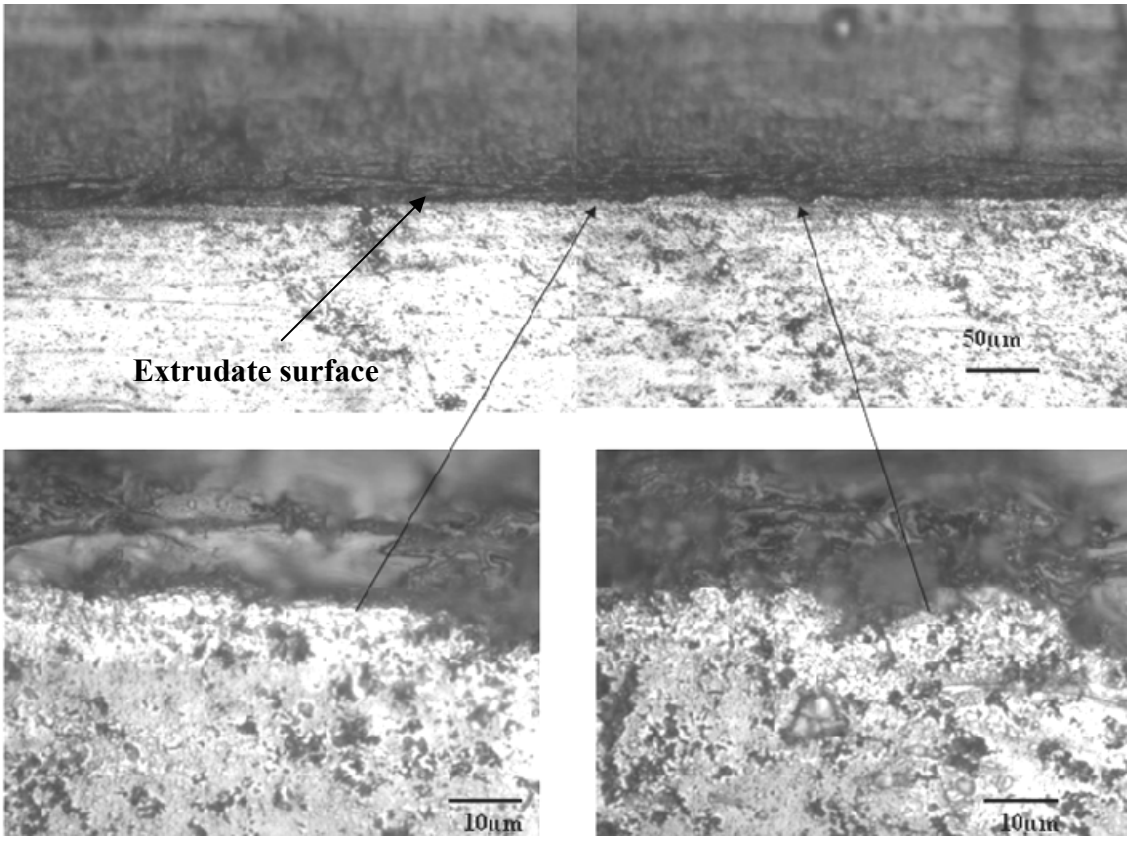

Figure 75 Cross section of normal pick-up

4.4.2 Effect of extrusion speed on normal pick-up

The number of normal pick-up per sample extrudate was done as explained in section 3.1.5. This data were useful to analyse whether the amount of die pick-up increases or decreases significantly when the extrusion speed is increased. The length of the die pick-up varies between 0.3mm and 4mm. However only die pick-up larger than 0.5mm were considered. According to Fletcher Aluminium, pick-up less than 0.5mm in length does not affect the visual appearance of an extrudate. Figure 76 to Figure 83 show the amount of die pick-up found for different die pick-up lengths in trial 2 to trial 5.

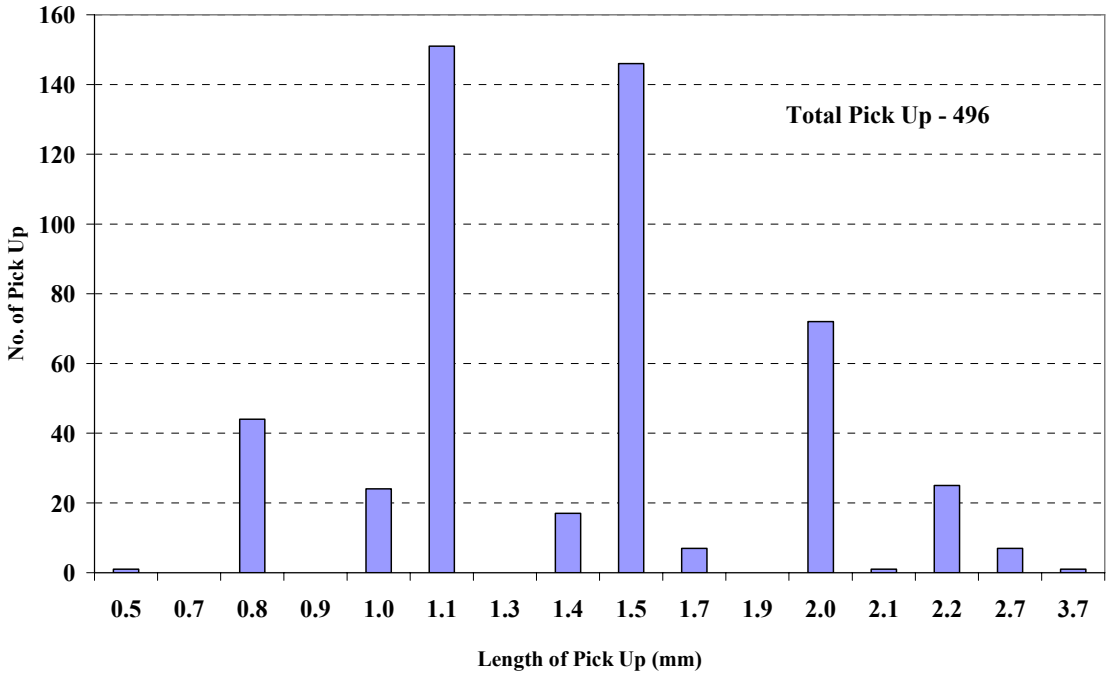

Figure 76 Pick-up distribution for pre-heat temperature 450°C, extrusion speed 25m/min – trial 2

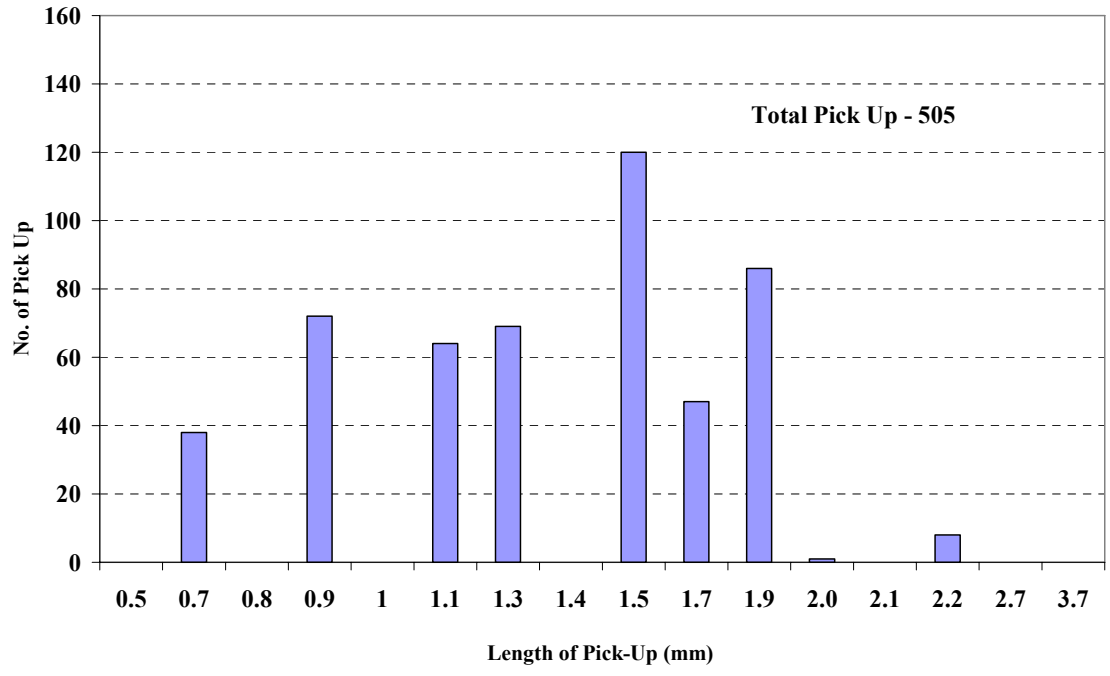

Figure 77 Pick-up distribution for pre-heat temperature 450°C, extrusion speed 30m/min – trial 2

Figure 76 and Figure 77 shows the distribution of normal pick-up at 25m/min and 30m/min for pre-heat temperature of 450°C. The exit temperature increased from 547°C to 552°C when the extrusion speed was increased. There is a slight increase in normal pick-up by 9 and this increase is not significant. Most of the normal pick-up length

varied between 1mm to 2mm. The number of normal pick-up did not increase when the extrusion speed was increased by 5m/min.

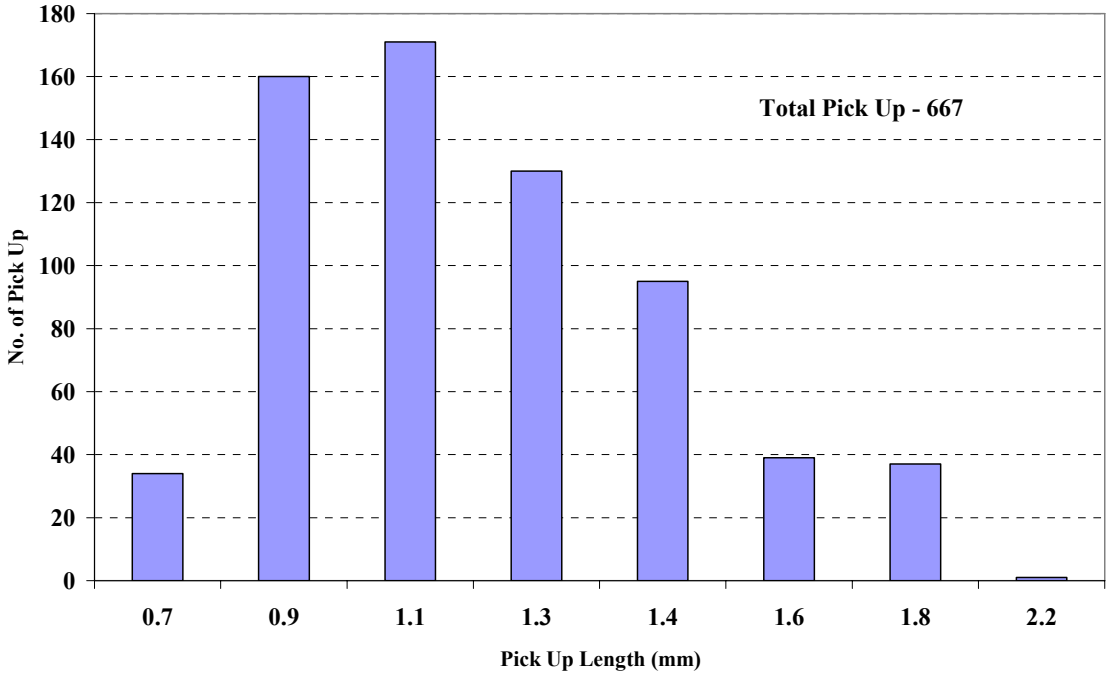

Figure 78 Pick-up distribution for pre-heat temperature 450°C, extrusion speed 25m/min – trial 3

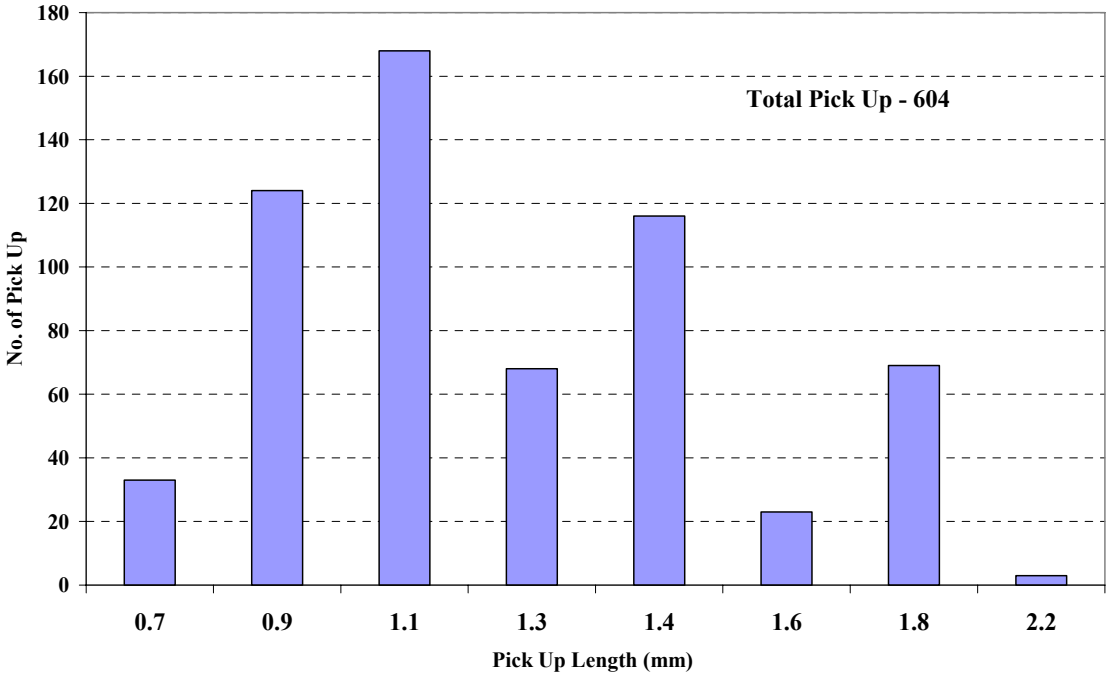

Figure 79 Pick-up distribution for pre-heat temperature 450°C, extrusion speed 35m/min – trial 3

Figure 78 and Figure 79 shows the distribution of normal pick-up at 25m/min and 35m/min for pre-heat temperature of 450°C. The exit temperature changed from 547°C to 557°C when the extrusion speed was increased. There is a noticeable decrease in

normal pick-up. Most of the normal pick-up length varied between 0.9mm to 1.8mm. The number of normal pick-up did not increase when the extrusion speed was increased by 10m/min.

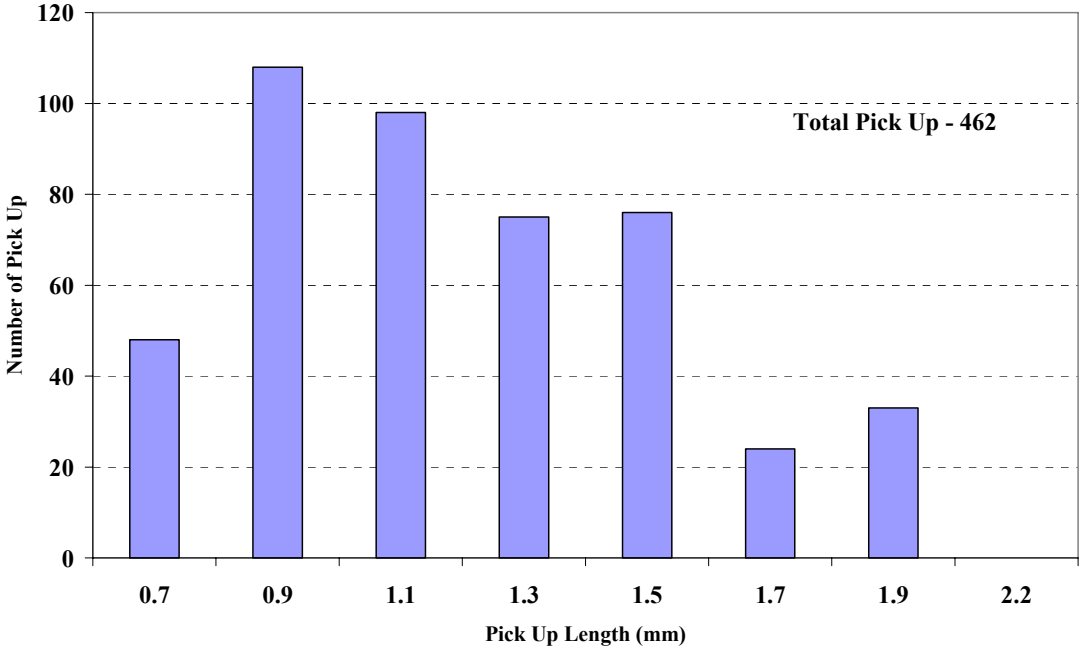

Figure 80 Pick-up distribution for pre-heat temperature 450°C, extrusion speed 25m/min – trial 4

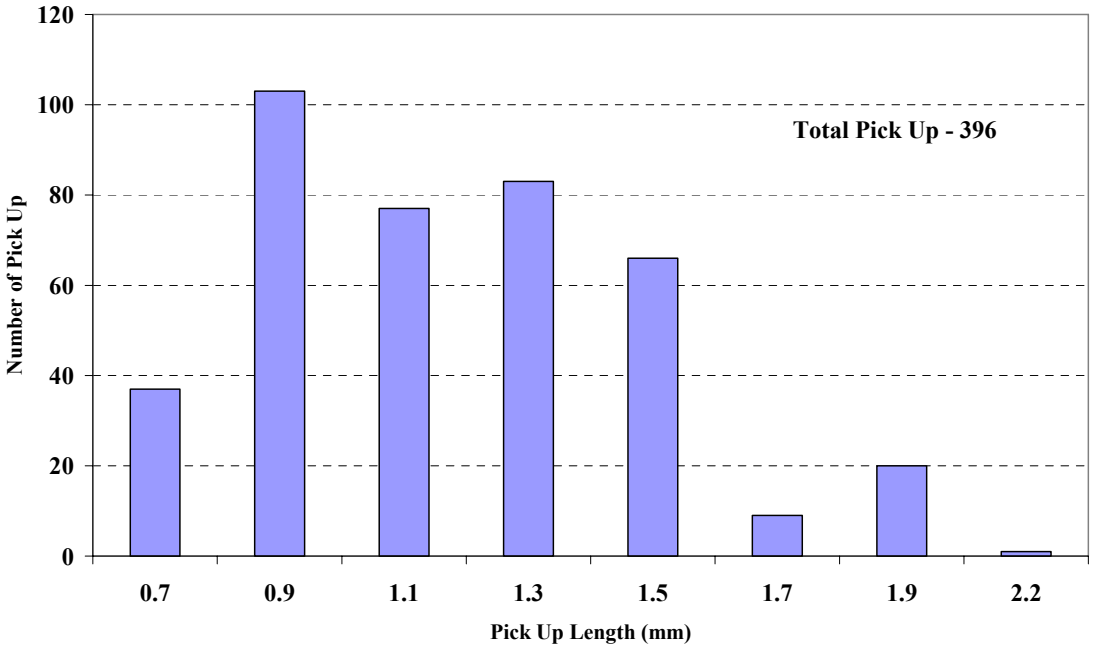

Figure 81 Pick-up distribution for pre-heat temperature 450°C, extrusion speed 40m/min – trial 4

Figure 80 and Figure 81 shows the distribution of normal pick-up at 25m/min and 40m/min for pre-heat temperature of 450°C. The exit temperature changed from 552°C to 567°C when the extrusion speed was increased. There is a decrease in normal pick-

up. Most of the normal pick-up length varied between 0.9mm to 1.9mm. The number of normal pick-up did not increase when the extrusion speed was increased by 15m/min.

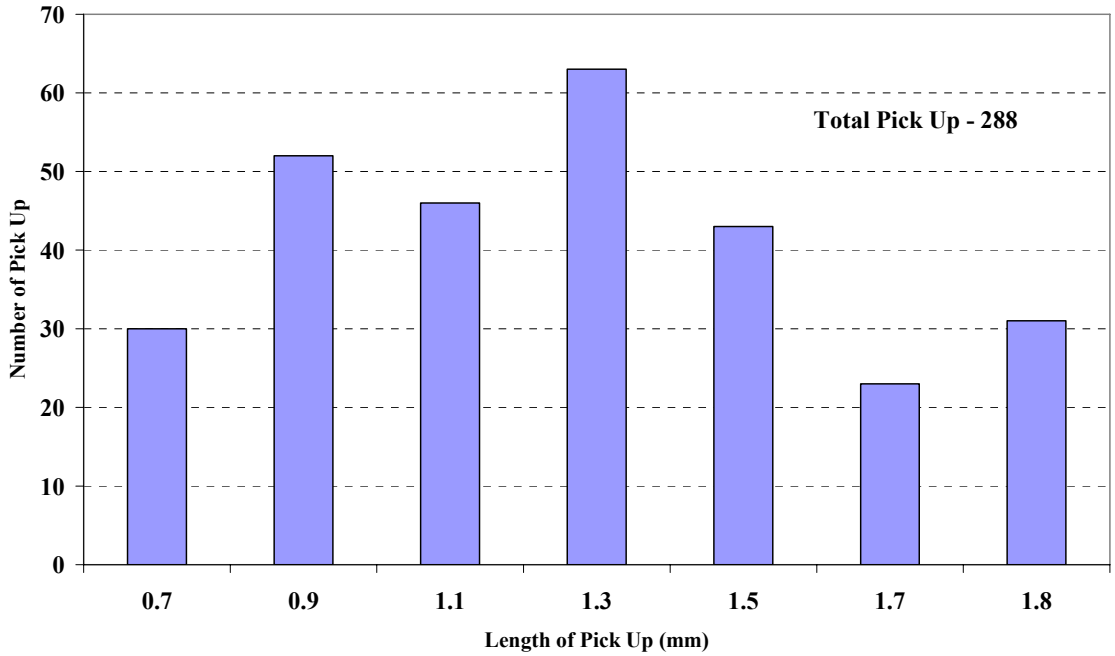

Figure 82 Pick-up distribution for pre-heat temperature 450°C, extrusion speed 25m/min – trial 5

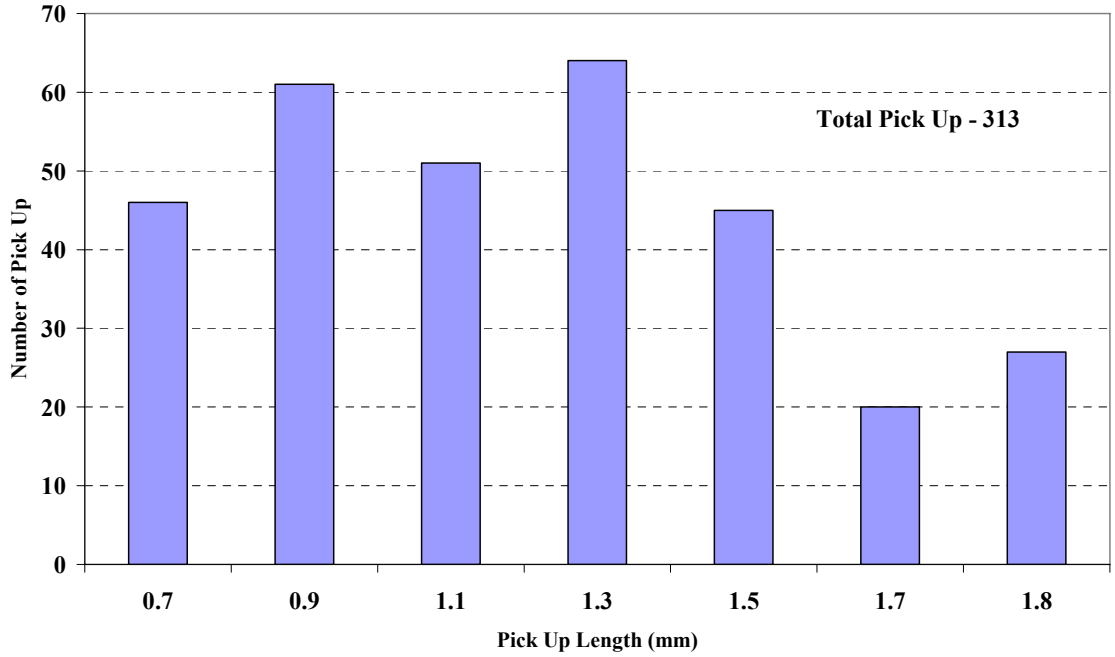

Figure 83 Pick-up distribution for pre-heat temperature 450°C, extrusion speed 45m/min – trial 5

Figure 82 and Figure 83 shows the distribution of normal pick-up at 25m/min and 45m/min for pre-heat temperature of 450°C. The exit temperature changed from 542°C

to 562°C when the extrusion speed was increased. There is an increase in normal pick-up but not significant. Most of the normal pick-up length varied between 0.7mm to 1.8mm. The number of normal pick-up did not increase significantly when the extrusion speed was increased by 20m/min.

There was a variation in the number of normal pick-up identified for every trial. Each trial was done on a different day and therefore the same die may not have been used. Therefore the die condition was changed in every trial. For each trial (trial 2 to trial 5) when the extrusion speed is increased from 25m/min to a higher extrusion speed (the exit temperature also increases), the amount and the length of normal pick-up did not change significantly. This suggests that the extrusion speed and exit temperature have little influence on the normal pick-up within this extrusion speed and exit temperature range. This finding has cast doubt on the exiting suggestion of eutectic melting of the β-phase relating to formation of pick-up and will be discussed in a later section.

4.4.3 Lump pick-up

Only one lump pick-up was found in the 60 samples observed. The extrusion parameters were 450°C pre-heat temperature and 45m/min extrusion speed.

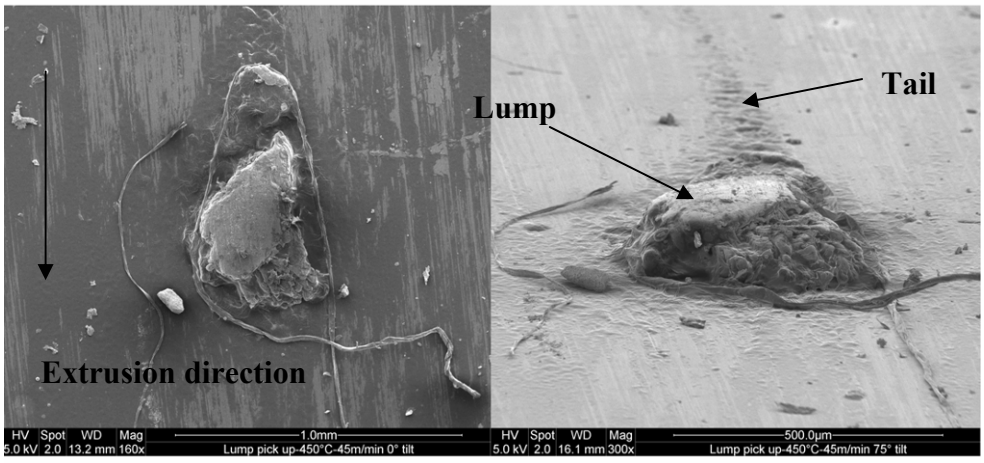

Figure 84 SEM macrograph showing lump pick-up

Figure 84 shows the top view and side view of a lump pick-up. The lump pick-up consists of two parts which are the lump and the tail. The chemical composition was done on the lump and on the tail of the pick-up.

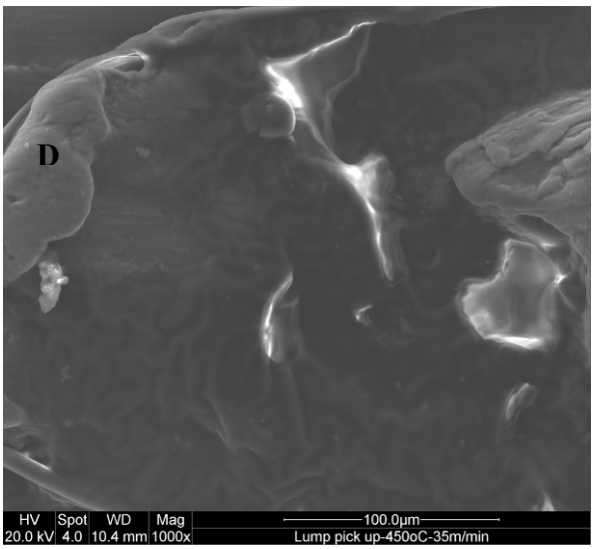

Figure 85 SEM micrograph showing a location on the lump

Figure 85 shows the surface at magnification of 1000x of the lump and the chemical composition were obtained at location D.

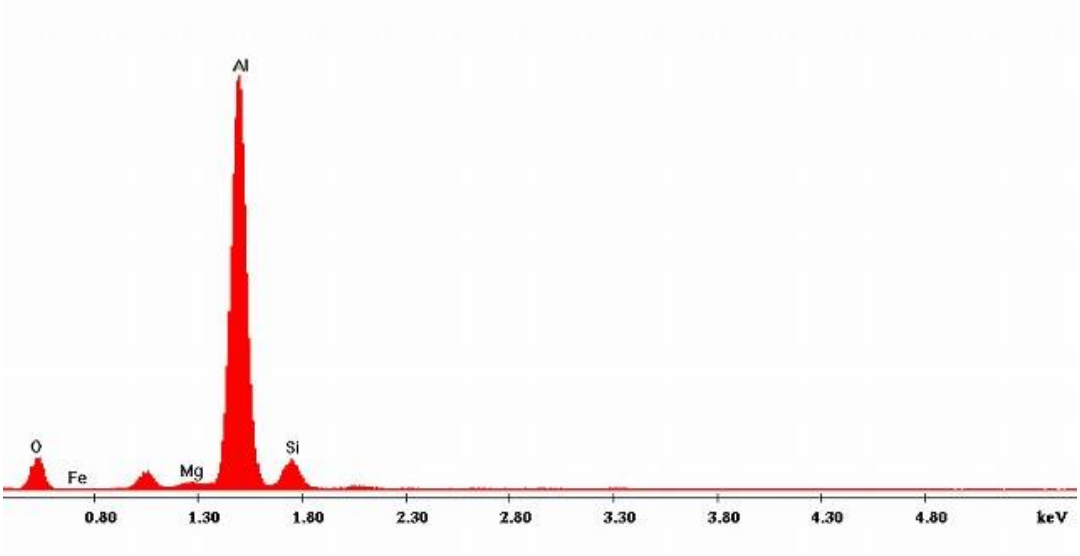

Figure 86 EDS spectrum at location D as indicated in Figure 85

Figure 86 shows the composition at location D. The main elements found were aluminium, silicon, magnesium and oxygen. Most likely the lump consists a collection of oxides and possibly of Mg_2Si particles.

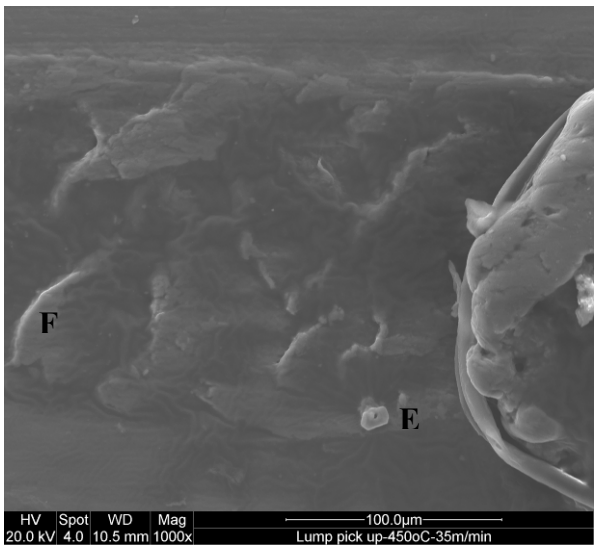

Figure 87 SEM micrograph showing the tail of the lump pick-up

Figure 87 shows the surface of the tail of the lump pick-up. The EDS spectra of location E and location F are given in Figure 88 and Figure 89 respectively.

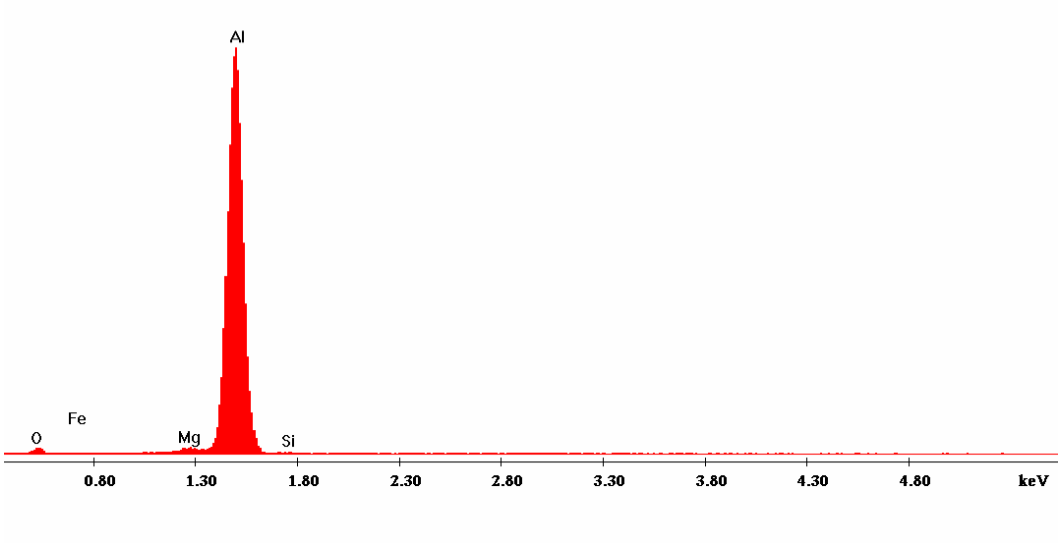

Figure 88 EDS spectrum at location E as indicated in Figure 87

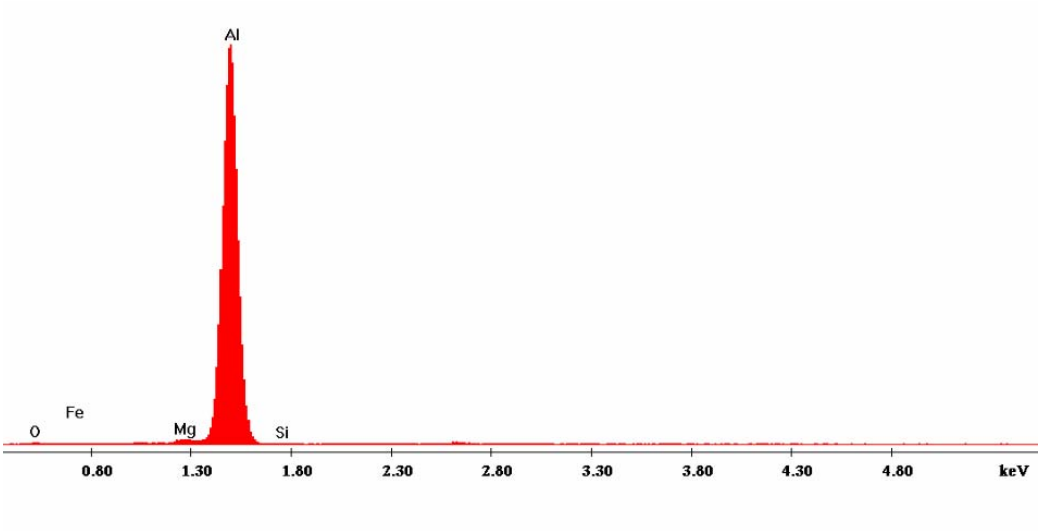

Figure 89 EDS spectrum at location F as indicated in Figure 87

Figure 88 and Figure 89 show the composition of location E and location F. Location E contains some oxygen apart from aluminium when compared with location F. This suggests that there may be some aluminium oxide present on location E. When compared the composition of the tail of the lump pick-up and the normal pick-up it could be suggested that they have similar characteristics.

4.4.4 Die line pick-up

Die line pick-up was only observed when the extrusion speed was at 45m/min and was located at the edge of the surface shown in Figure 90.

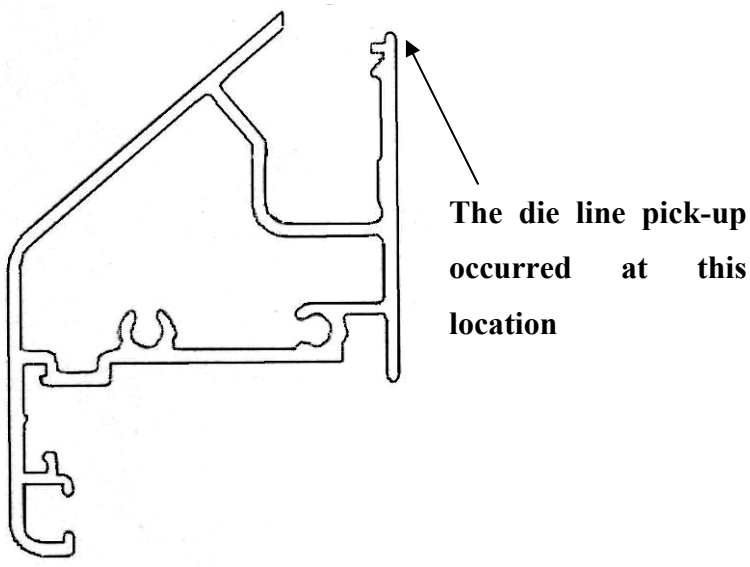

Figure 90 Cross section of the 610103 extrudate. Location of die line pick-up (arrowed)

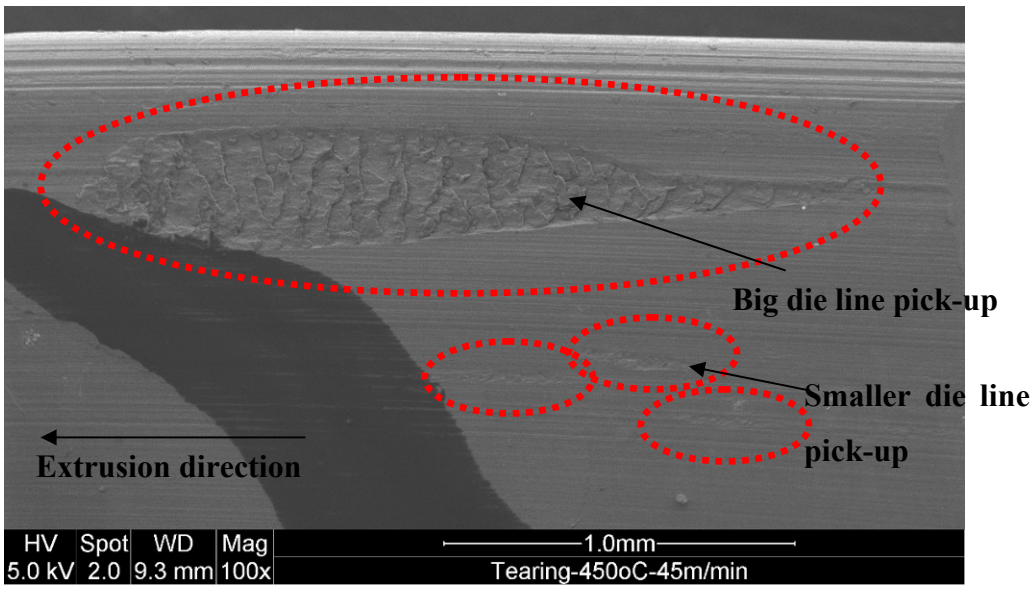

Figure 91 SEM macrograph showing die line pick-up

Figure 91 shows a typical die line pick-up found on the samples in trial 5. It has similar surface appearance when compared with the normal pick-up (see Figure 69 to Figure 71), however the wave-like appearance are closely packed and more regular than the ones found in the normal pick-ups. The width and length of the die line pick-up are greater than a normal pick-up. Figure 92 shows the die line pick-up at magnification of 1000x. The compositions of location G, location H and location I were obtained and are presented in Figure 93 and Figure 95.

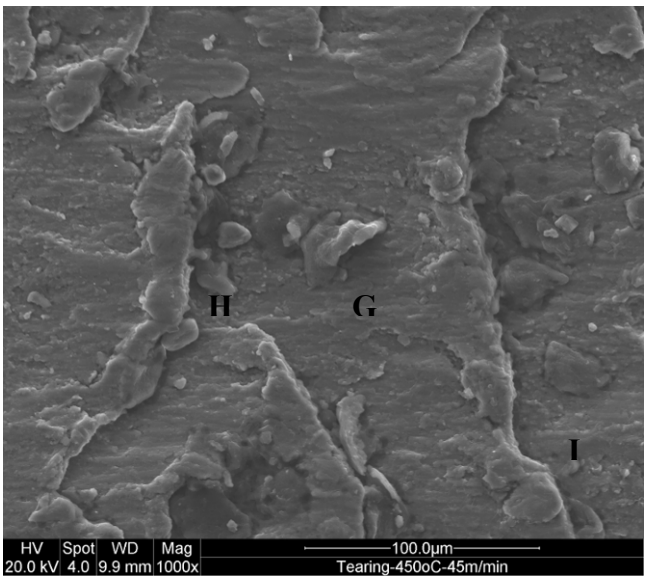

Figure 92 SEM micrograph showing surface tearing at magnification of 1000x

Figure 93, Figure 94 and Figure 95 shows the EDS spectrum of location G, location H and location I respectively on the tearing surface.

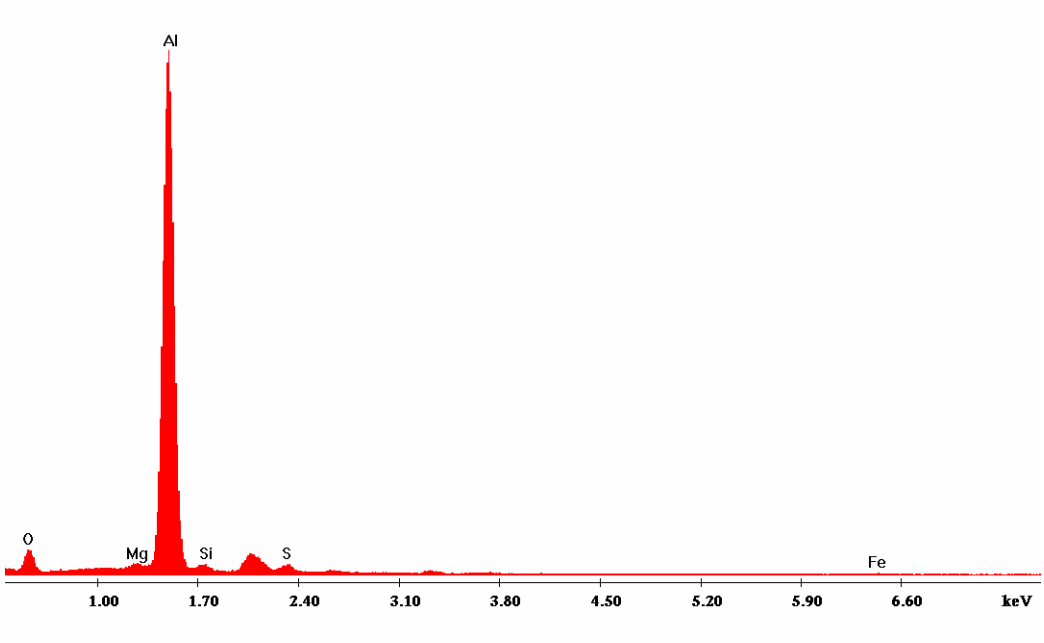

Figure 93 EDS spectrum at location G as indicated in Figure 92

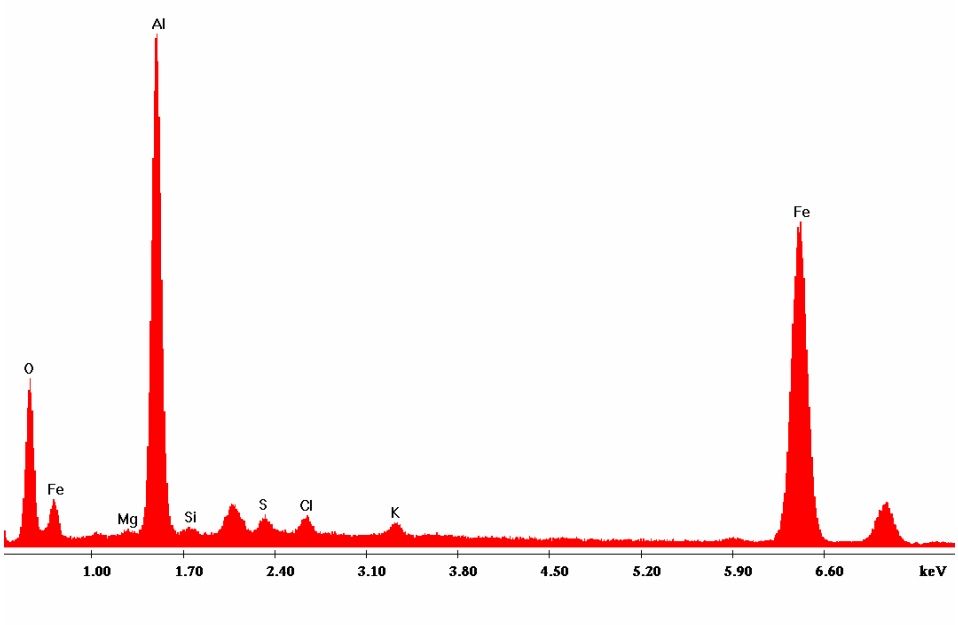

Figure 94 EDS spectrum at location H as indicated in Figure 92

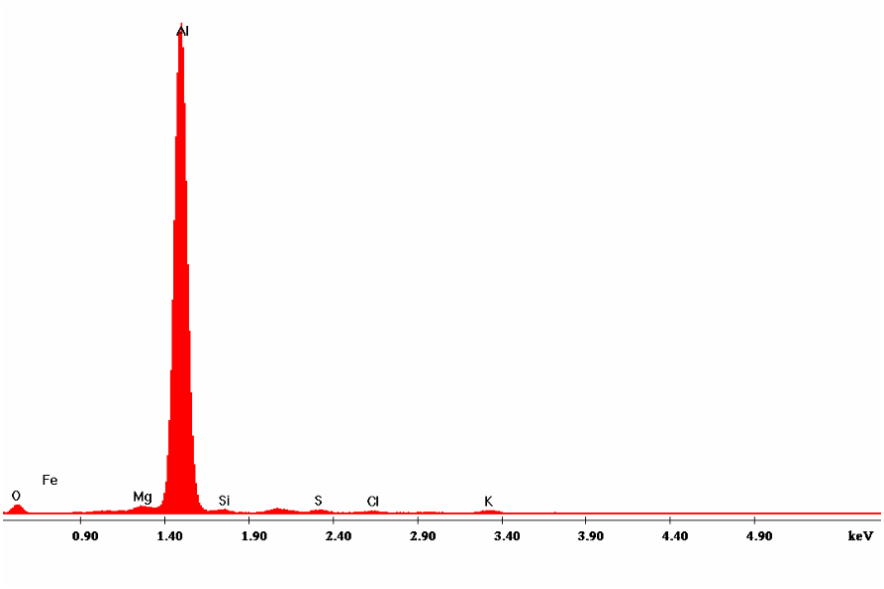

Figure 95 EDS spectrum at location I as indicated in Figure 92

The composition of the die line pick-up is quite different than the composition on the normal pick-ups, since iron was found on the surface. The appearance of tearing and normal pick-up looks similar but the cause and formation may be different to each other.

Figure 97 shows the cross section of a die line pick-up and was cross section in the direction as shown in Figure 96. As in the top view of the die line pick-up, the cross section shows the wave look alike structure. There is also no evidence of any micro cracking the surface however there was a crack initiated locally.

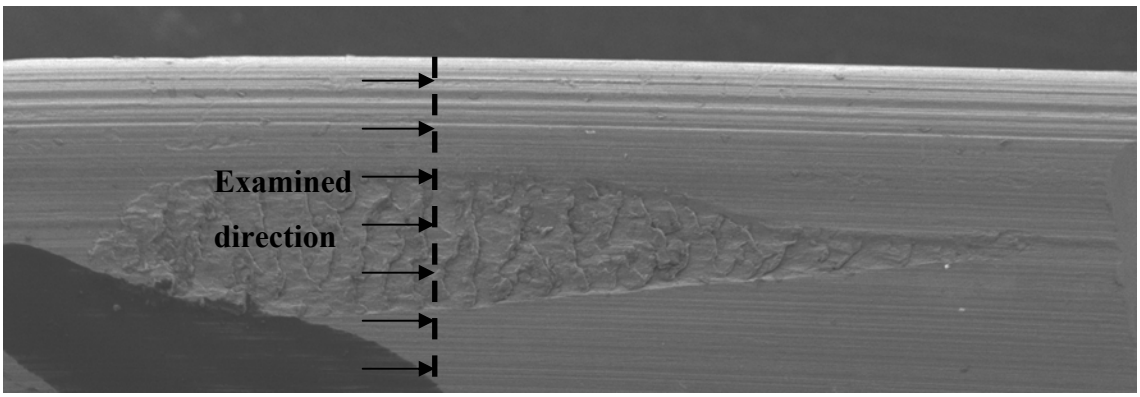

Figure 96 Cross sectioning location on the die line pick-up for examication

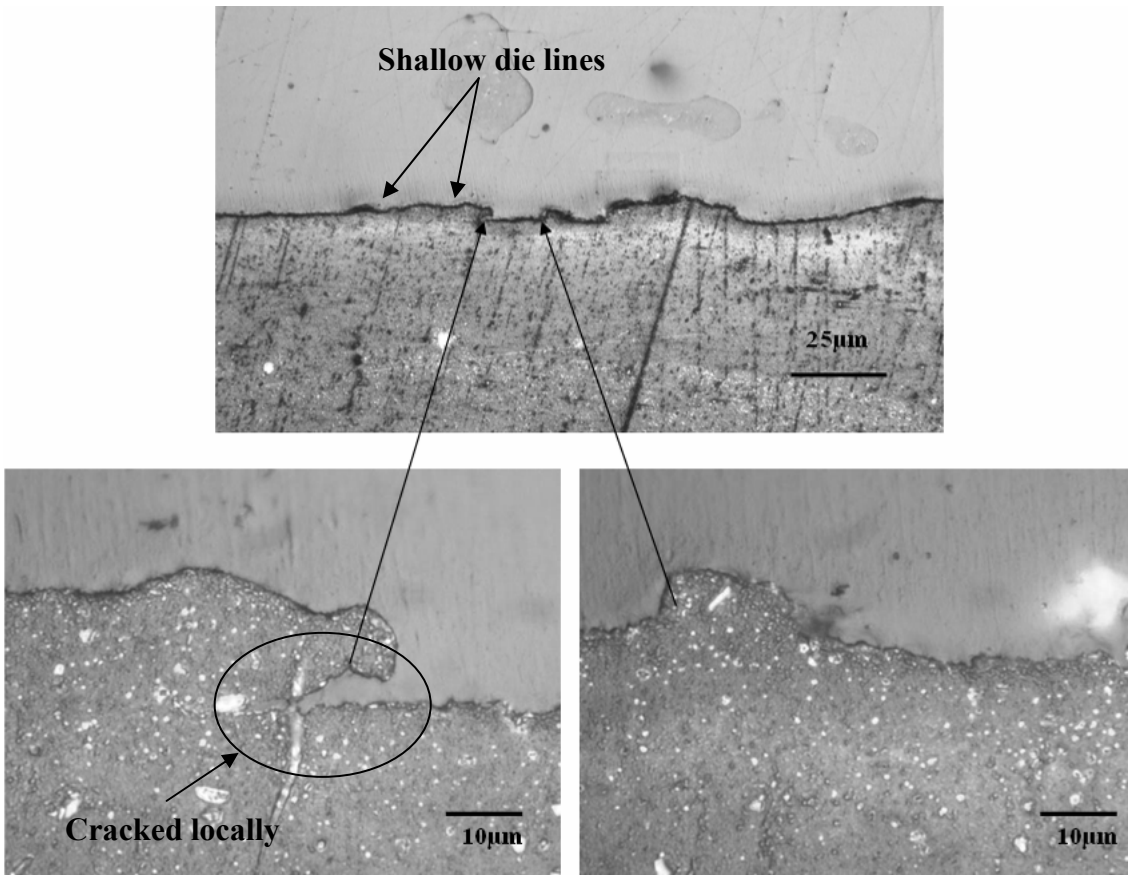

Figure 97 Optical micrographs of cross section from a die line pick-up showing ridges and cracks

4.5 Die bearing surface condition

During extrusion, plasticized metal flow through the die cavity on the die bearing surface and hence the flowing material has a direct interaction with the die bearing surface. Therefore it is vital to investigate the die bearing surface condition since it may influence the formation of die pick-up on extrusion surfaces. Figure 98 shows the cross sectional view of the die bearing surfaces described in section 3.1.6.

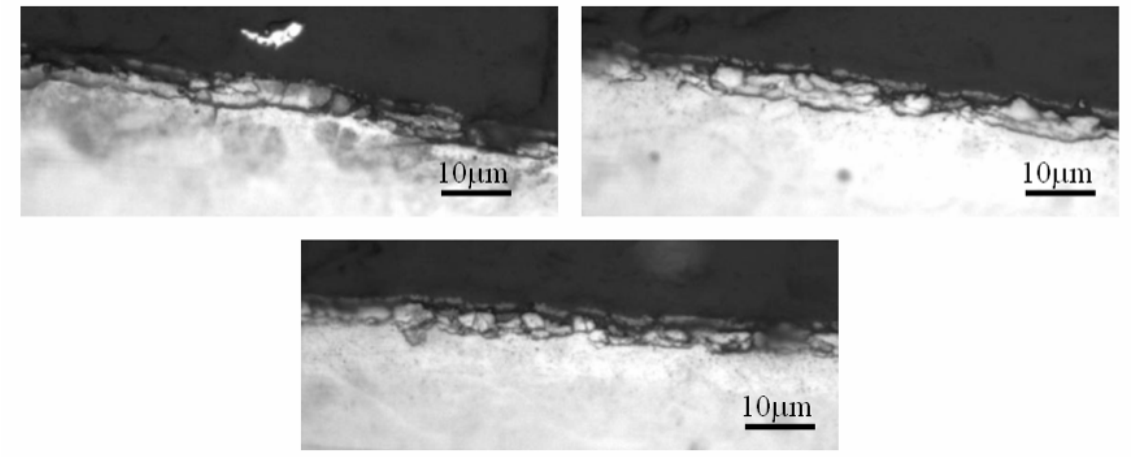

Figure 98 Optical micrographs showing die bearing surface at the entrance of the die cavity

As seen in Figure 98 the bearing surface looks irregular and scattered into many pieces. These scattered broken pieces could be a broken die bearing surface or intermettalic particles. Therefore EDX was performed on the area to identify what elements were present. Figure 99 shows the location at which the EDX were obtained on the cross section of the die bearing surface.

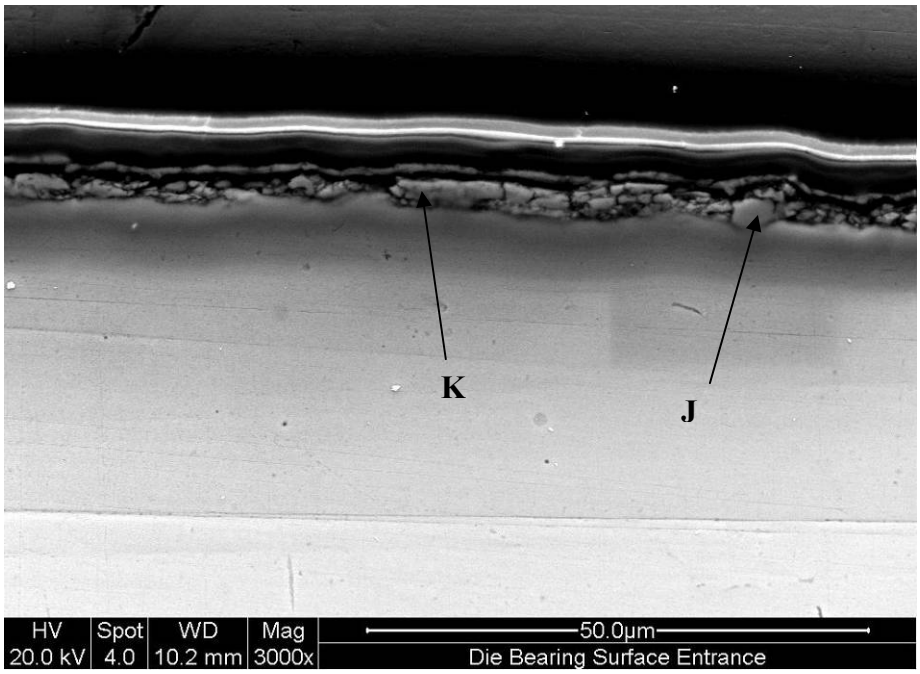

Figure 99 SEM micrograph of die bearing surface at entrance showing fragmented particles

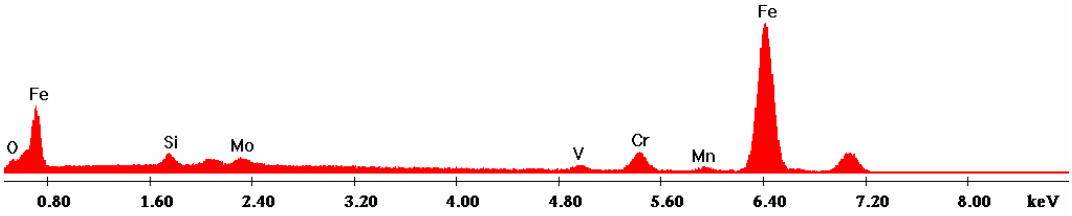

Figure 100 EDS spectrum at location J as indicated in Figure 99

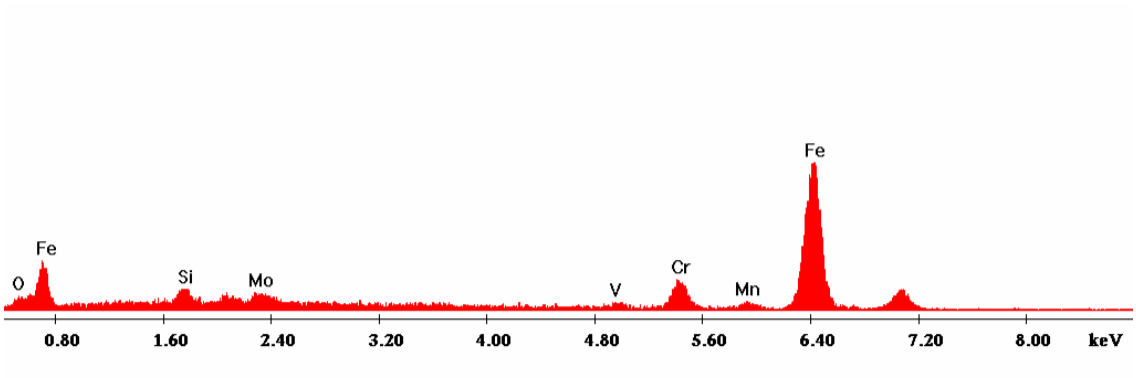

Figure 101 EDS spectrum at location K as indicated in Figure 99

The EDS spectrum of location J and location K suggests that the shattered particles on the bearing surface are H13 material since there is no trace of aluminium. However as mentioned in section 3.1.6 the die was etched with NaOH which attacks any aluminium compound. The gaps found between the H13 material could have being filled with aluminium compounds. Regardless of the composition the die bearing surface looks very irregular and uneven.

4.6 Formation mechanism of die pick-up

4.6.1 Formation mechanism of normal pick-up

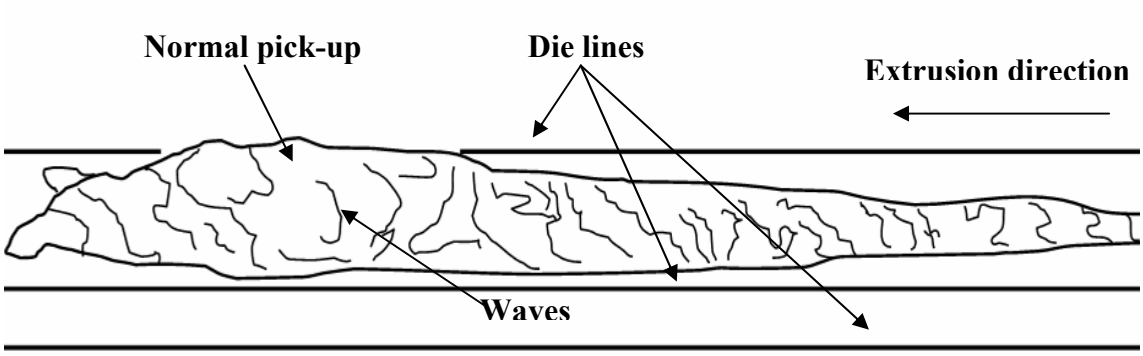

Figure 102 Schematic diagram of normal pick-up with respect to extrusion direction and die lines

Figure 102 shows a schematic of the top view of a normal pick-up. The normal pick-up is surrounded by die lines and occurred regardless of the extrusion speed and exit temperature. The extrusion speed varied between 25m/min and 45m/min, the exit temperature varied between 542°C and 567°C. Within these extrusion speeds and exit temperatures the amount of normal pick-up did not increase or decrease. At 555°C, Mg_2Si particles react with aluminium and excess silicon to form liquid [4, 23, 28]. There are suggestions that die pick-up are related to eutectic reactions provided the

temperature and excess silicon are available [28]. However in this case of AA6060 alloy, magnesium and silicon content was 0.4% and 0.5% respectively, which creates 0.23% excess silicon, therefore localized liquid could form. As described in section 4.1 eutectic melting occurred above 610°C and exit temperature was also well below 610°C. However regardless of the exit temperature normal die pick-up did occur and the intensity of normal pick-up did not increase even when the extrusion speed was increased. Therefore the occurrence of normal pick-up does not relate to the eutectic reactions.

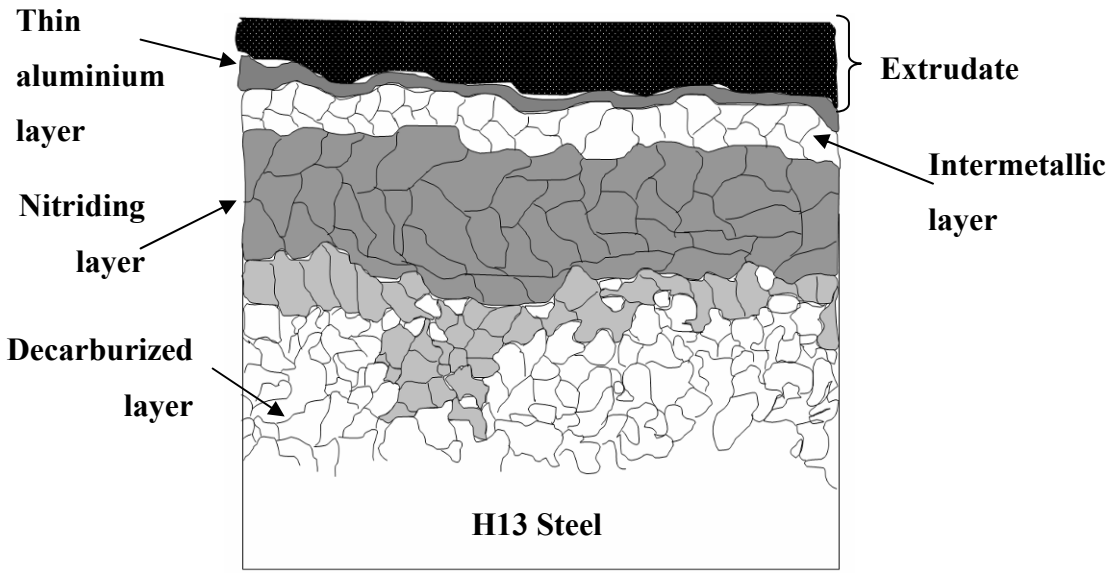

Figure 103 Schematic diagram of cross section of die and extrudate while being extruded when normal pick-up is formed

Figure 103 shows the schematic of the cross section of the die and extrudate while being extruded. The die is made out of H13 steel and heat treated to increase the toughness. Due to the heat treatment operation, decarburized layer in introduced because of the diffusion of carbon out of the die material. Once the heat treatment is completed the die is nitrided. Nitriding is a process which is done to increase the hardness of the die and is a process where nitrogen is diffused into the die material. The nitriding layer is not a stable compound, where the nitrogen could diffuse out of the die material. When the nitrogen diffuses out of the die material, H13 steel is exposed. Therefore during the extrusion process the nitriding layer could be destroyed. The newly formed H13 material reacts with aluminium and form intermetallic particles. Intermetallic particles are found in processes such as friction stir welding [32] and high pressure die casting [31]. These intermetallic particles could form within few cycles of operation in high pressure die casting and friction stir welding. However, Intermetallic particles were not

found on the die bearing surface due to the NaOH solution etching process. These intermetallic particles increase the coefficient of friction on the bearing surface. This could cause a sticking condition on the bearing surface.

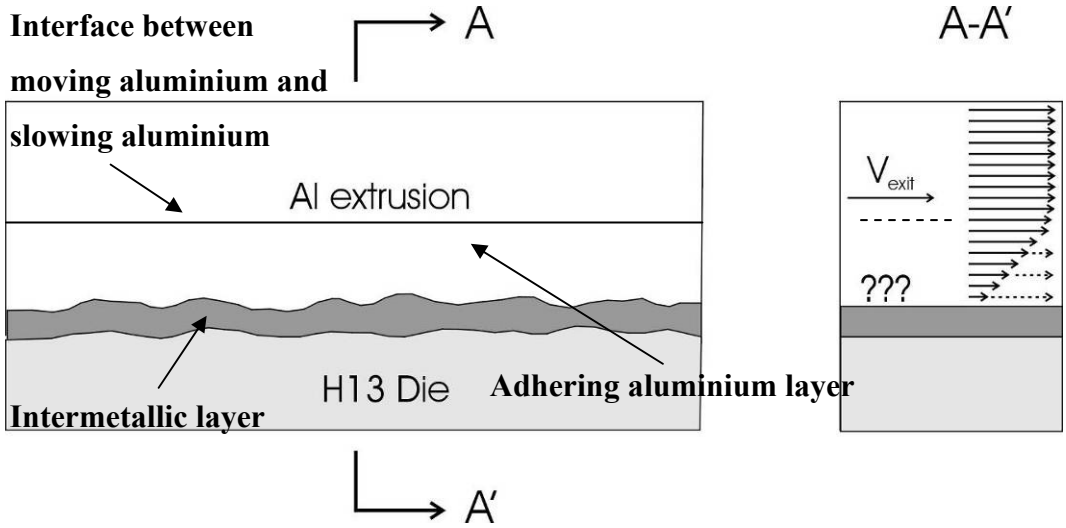

Figure 104 Schematic diagram showing sticking condition on the die bearing surface

Figure 104 shows the possible velocity profile of an extrudate. Due to the high friction coefficient which is close to 0.8 (very high friction co-efficient) [3, 6, 35] generated by the intermetallic particle layer, the velocity of the extrudate close to the layer could be reduced or in fact could be stationary. Therefore a thin aluminium layer which the velocity is lower than the extrusion speed is generated, but however the thickness of this layer was not established during this study. Due to this velocity difference, a pulling effect or shearing effect is generated by the faster moving aluminium on to the slower moving aluminium. The material during extrusion exposes to high temperature (close to solidus temperature), high pressure, high strain and high strain rate. These factors reduce the strength of the aluminium and hence the cohesive strength of the aluminium matrix reduces. However the cohesive strength of the extrudate did not decrease, up to the extrusion speed of 45m/min where complete surface tearing could occur. The cohesive strength may have decreased locally at isolated points where small tearing and chipping could occur. Therefore it could be suggested that normal pick-up occur at the interface of the adhering aluminium layer and moving aluminium due to the localized sticking condition.

4.6.2 Formation mechanism of die line pick-up

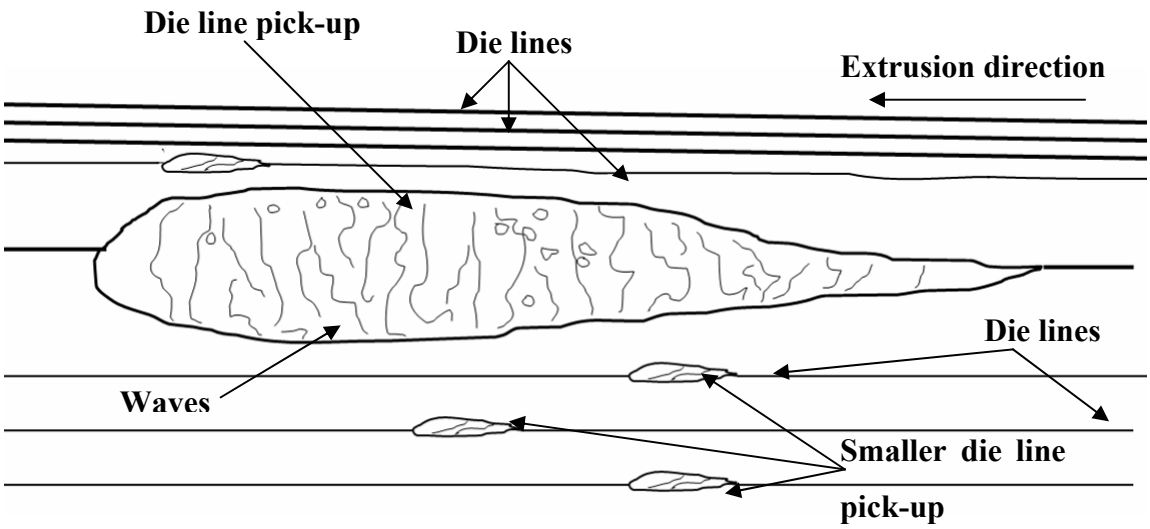

Figure 105 Schematic of die line pick-up with respect to extrusion direction and die lines

Figure 105 shows the schematic of a die line pick-up. This type of die pick-up occurs on a die line. A bigger die line pick-up was surrounded by smaller die line pick-up. As shown in Figure 97, the bigger die line pick-up corresponds to a deeper die line and the smaller die line pick-up corresponds to a shallower die line. This suggests that the size of the die line pick-up depends on the depths of the die line.

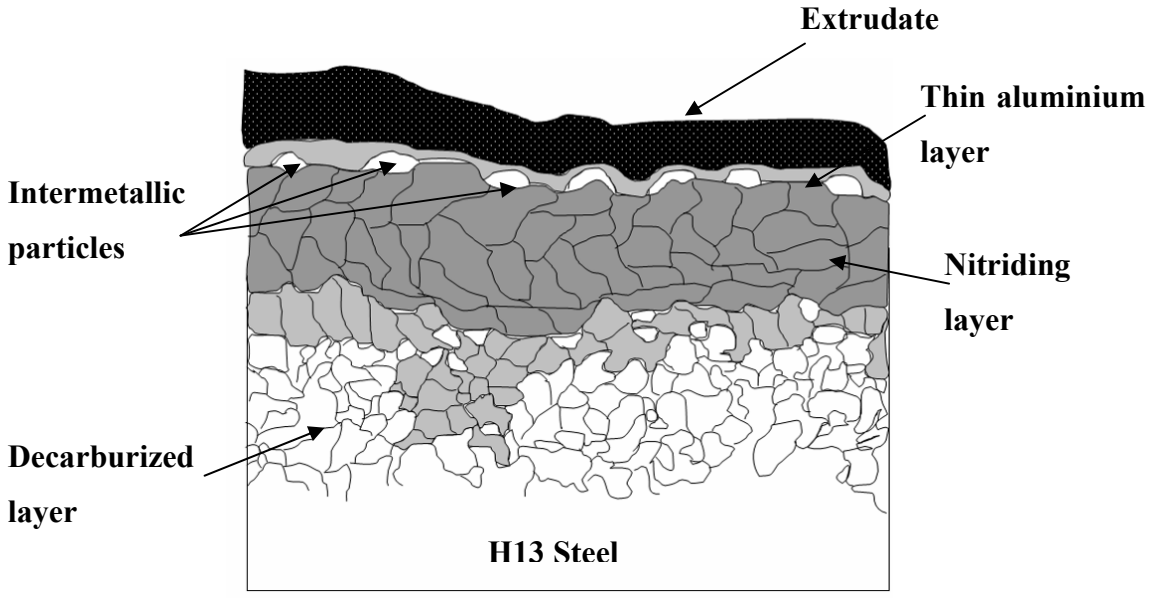

Figure 106 Schematic diagram of cross section of die and extrudate while being extruded when die line pick-up is formed

Figure 106 shows the possible cross section when a die line pick-up is formed. In this case it is not clear whether the intermetallic particles form as a layer as in normal pick-

up or at isolated locations. There is a greater possibility that the intermetallic particles formed in this area of the die was not uniform and were located as clusters. The velocity profile of the thin aluminium layer is expected to be similar as the thin aluminium layer as seen at a normal pick-up. Therefore a sticking condition is possible. The die line pick-up only occurred at 45m/min and therefore the extrusion speed had an effect. The EDS spectrum of the die line pick-up revealed traces of iron. This suggests that the iron could have been from the die. There were many iron containing particles found on the die line pick-up. The formation of the die line pick-up is quite similar to a normal pick-up, but the die line pick-up occurred when the intermetallic particles starts to collapse and as a consequence local tearing and chipping occurred.

5 Conclusions and Recommendations

Based on the results discussed in the previous chapter the following conclusions and recommendation could be made.

- Incipient melting for AA6060 alloy was identified to be around 610°C. Therefore the lowest melting temperature or eutectic temperature for AA6060 alloy is 610°C. Hence for AA6060 alloy the maximum extrusion exit temperature could be reached up to 610°C.

- It was found that the extrusion speed could be increased considerably from 25m/min to 40m/min without increasing the amount of surface defects for extrudate profile of 610103.

- Three types of die pick-up was identified which were named as normal pick-up, die line pick-up and lump pick-up. The latter occurred very rarely.

- The size and number of normal pick-up were not affected by extrusion speed and exit temperature, for the experimented extrusion speeds and exit temperature ranges. The number of normal pick-up did not increase when the extrusion speed and exit temperature were increased.

- Die line pick-up occurred at 45m/min and was only on die lines. Therefore die lines have a strong influence on die line pick-up. Die line pick-up was longer and wider than normal pick-up, and affected the surface appearance significantly.

- The results indicate that normal pick-up and die line pick-up was probably caused by a mechanical process rather than a metallurgical process. Therefore eutectic reactions have no influence on normal pick-up and die line pick-up, since pick-up occurred below and above the eutectic melting temperatures.

- It could be suggested that pick-up is formed at the interface between the thin aluminium layer (attached to the die bearing surface due to the friction at the intermetallic layer) and the moving extrudate. Due to the localized extrusion

speed variation, the surface of the extrudate is locally scratched and torn. Therefore there is nothing to pick up from the die to form die pick-up.

- It is recommended to do further investigation on die pick-up for different homogenization conditions. The type and size of the second phase particles depend on the homogenization conditions and therefore it could be used to further establish the influence on incipient melting on die pick-up.

- It is also recommended to further investigate on die pick-up for different die bearing surface conditions. The bearing surface condition determines the friction co-efficient between the die bearing surface and extrudate. Therefore it could establish the influence by coefficient of friction on die pick-up.

6 Reference

1. The International Aluminium Institute, "Aluminium Applications and Society - Construction", 2000 [cited; Available from: http://www.world-aluminium.org/iai/publications/lifecycle_construction.html

2. European Aluminium Association, "Aluminium and Aluminium Alloys - Extrusion", 2000 [cited; Available from: http://www.azom.com/details.asp?ArticleID=1554

3. Sheppard T., Clode M. P., "The origin of surface defects during extrusion of AA6063 alloy", 4th International aluminium extrusion technology seminar, 1988:329 - 341.

4. Usta M., "The influence of thermal treatment on the cast structure of 6xxx aluminium alloys", PhD Thesis, Rensselaer Polytechnic Institute, 2001.

5. Degarmo E.P., Black J. T., Kohser R.A., "Materials and processes in manufacturing", 1997.

6. Sheppard T., "Extrusion of aluminium alloys"; 1999, Kluwar publications.

7. Couto K.B.S., Clave S. R.,Van Geertruyden W.H., Misiolek W.Z., Goncales M., "Effects of homogenization treatment on microstructure and hot ductility of aluminium alloy 6063", Materials Science and Technology. 2005, 21:263-268.

8. Kuijpers N.C.W., "Kinetics of the β-AlFeSi to α-Al(FeMn)Si transformation in Al-Mg-Si alloys", PhD thesis, Delft University of Technology, 2004.

9. Matienzo L.J., Holub K.J., Vandatta W., "An investigation on surface defects produced during the extrusion of some aluminum alloys", Applications of surface science 1982, 15:307 - 320.

10. Reiso O., "The occurance of surface defects during extrusion from a metallurgical point of view", Hydro Aluminium, Metallurgical R&D Centre, 1990.

11. Wright R.N., Usta M., Bartolucci S., "A modern view of the thermodynamics and kinetics of the magnesium silicide presence in 6xxx alloys", 8th international aluminum extrusion technology seminar, 2004:67-75.

12. Scharf G., "The influence of alloying elements and homogenizing treatment on the extrudability of wrought aluminum alloys", 1st international aluminum extrusion technology seminar, 1969.

13. Dons A. L., "The Alstruc homogenization model for industrial aluminum alloys", Journal of light metals, 2001, 1:133-149.

14. Reiso O., "Extrusion of AlMgSi alloys", 9th international conference on aluminium alloys, 2004, 32-46.

15. Lassance D., "Modelling of damage mechanisms in AlMgSi alloys", Catholic Univesity of Louvain, 2006.

16. Lefstad M., "Metallurgical speed limitations during the extrusion of AlMgSi-alloys", PHD thesis, University of Trondheim, 1993.

17. Zajac S., Gullman L., Johansson A., Bengtsson B., "Hot ductility of some Al-Mg-Si alloys", Materials Science Forum, 2005, 217-222:1193-1198.

18. Pridgeon J.W., Langer,E.J., Metals Handbook, 1985.

19. Callister W.D., "Materials science and engineering - An introduction", 2003.

20. Reiso O., "The effect of composition and homogenization treatment on extrudability of AlMgSi alloys", 3rd international aluminum extrusion technology seminar, 1984, 31-40.

21. Lassance D., Dille J., Delplancke J.L., Pardoen T., Ryelandt L., Delannay F., "Effect of homogenization conditions on the extrudability and high temperature fracture resistance of AA6063 alluminium alloy", Materials science forum, 2005, 426-432:447-452.

22. Bartolucci S. F., "Effect of thermal cycles on microstructure and extrudability of AA6xxx alloys", PHD thesis, Rensselaer Polytechnic Institute, 2001.

23. Reiso O., "The effect of billet pre-heating practice on extrudability of AlMgSi alloys", 4th International aluminum extrusion technology seminar, 1988, 287-295.

24. Parson N.C., Hankin J. D., Bryant A.J., "The metallurgical background to problems occuring during the extrusion of 6xxx alloys", 3rd international aluminum extrusion technology seminar, 1984, 13-23.

25. Castle A.F., "Temperature changes in the extrusion of aluminum alloys", 3rd international aluminum extrusion technology seminar, 1984, 101-106.

26. Li L., Zhou J., Duszczyk J., "Prediction of temperature evolution during the extrusion of 7075 aluminium alloy at various ram speeds by means of 3D FEM simulation, "Journal of Materials Processing Technology", 2004, 145:360-370.

27. Saha P.K., "Influence of plastic strain and strain rate on temperature rise in aluminum extrusion", 6th international aluminum extrusion technology seminar, 1996, 355-360.

28. Minoda T., Hayakawa H., Matsuda S., Yoshida H., "The mechanism of pick-up formation on 6063 aluminum alloy extrusions", 7th international aluminum extrusion technology seminar, 2000, 23-29.

29. Abtahi S., "Interface mechanisms on the bearing surface in extrusion", 6th International Aluminum Extrusion Technology Seminar and Exposition. 1996, 125-133.

30. Bjork T., Westergard R., Hogmark S., "Wear of surface treated dies for aluminium extrusion - a case study", Wear, 2001, 249:316-323.

31. Chen Z. W., "Formation and progression of die soldering during high pressure die casting", Materials Science and Engineering A, 2005, 397:356-369.

32. Qi Y., "Friction stir welding", Masters thesis, AUT University, 2006.

33. Nilsen K.E., Koenis P.T.G., Boal B.V., "Quantitative analysis of the homogenizing heat treatment by means of AlFeSi particle analysis and the effect on productivity", 7th international aluminum extrusion technology seminar, 2000, 2:69-75.

34. Matsuoka H., Kato Y., Sakaguchi M., "Effect of intermetallic compound distribution on extrusion surface in 6061 alloy", 7th international aluminum extrusion technology seminar, 2000, 99-104.

35. Sheppard T., "On the relationship between extrusion conditions, mechanical properties, and surface acceptability in some hard aluminum alloys, 7th international aluminum extrusion technology seminar, 2000, 307-321.

36. Matweb Material Property Data, Aluminum 6060 Composition Spec, 2006 [cited; Available from: http://www.matweb.com/search/SpecificMaterial.asp?bassnum=MA6060n

7 Appendix – Ram speed and ram pressure data

Pre-heat Temperature	Extrusion Speed	$T_{initial}$ (s)	T_{final} (s)	$RS_{initial}$ (mm/sec)	RS_{stable} (mm/sec)	RP_{stable} (PSI)	RP_{final} (PSI)
430°C	25m/min	25.1	108.8	1.05	4.2	3500	2500
430°C	25m/min	35	112	1.2	4.2	3500	2600
430°C	25m/min	47.2	119	0.8	4.3	3500	2600
430°C	25m/min	44.2	114.9	0.5	4.2	3500	2600
430°C	25m/min	48.9	115.0	1	4.2	3500	2600
430°C	30m/min	48.9	110.6	1	4.7	3500	2600
430°C	30m/min	52.7	106.8	0.5	4.7	3500	2700
430°C	30m/min	49.1	104.7	0.9	4.7	3500	2700
430°C	30m/min	41.7	102.2	1.2	4.7	3500	2800
430°C	30m/min	41	98.4	0.8	4.7	3500	2700
450°C	25m/min	39.3	118	1.1	4.2	3500	2500
450°C	25m/min	29.5	118	0.8	4.1	3500	2500
450°C	25m/min	21.1	108.9	1.1	4.1	3500	2500
450°C	25m/min	17.6	117.6	1.3	4.1	3500	2400
450°C	25m/min	21.4	119.9	1.4	4.2	3500	2400
450°C	30m/min	23.1	104.5	1.1	5.3	3500	2500
450°C	30m/min	22.1	108.5	1.9	5.3	3500	2500
450°C	30m/min	48.2	118.3	0.8	5.3	3500	2500
450°C	30m/min	35.5	109.2	1.1	5.3	3500	2500
450°C	30m/min	25.1	106.9	1.8	5.5	3500	2500
450°C	25m/min	26.5	111.8	1.7	4.2	3500	2600
450°C	25m/min	21.8	116.3	1.7	4.2	3500	2500
450°C	25m/min	23.3	111.5	1.4	4.2	3500	2500
450°C	25m/min	25.4	103.9	0.9	4.2	3500	2500
450°C	25m/min	20.5	113	1.1	4.2	3500	2500
450°C	35m/min	20	88.6	1.8	5.5	3500	2500
450°C	35m/min	23.3	89.9	2.3	6	3500	2500
450°C	35m/min	20.3	88.1	2.8	5.7	3500	2500
450°C	35m/min	21.2	88.2	2.8	5.7	3500	2500
450°C	35m/min	17.1	92.5	2.7	5.4	3500	2500
450°C	25m/min	22.4	109	1.7	3.7	3500	2500

450°C	25m/min	20.3	107.6	1.5	4.2	3500	2500
450°C	25m/min	20.8	109.2	1.8	3.9	3500	2500
450°C	25m/min	24.5	109	1.3	4.1	3500	2500
450°C	25m/min	19.4	106.9	2.1	4.3	3500	2500
450°C	40m/min	36	90	1.5	6.2	3500	2600
450°C	40m/min	29.2	76	1.7	6.7	3500	2600
450°C	40m/min	25.7	74.2	2	7	3500	2600
450°C	40m/min	21.5	70.7	2.9	6.8	3500	2600
450°C	40m/min	17.5	70.1	2.7	7	3500	2600
450°C	25m/min	21.5	93.3	1.1	3.7	3500	2600
450°C	25m/min	20.3	91.5	1.4	4	3500	2600
450°C	25m/min	26.6	106.6	1.1	4	3500	2600
450°C	25m/min	24.8	107.5	1.5	3.7	3500	2600
450°C	25m/min	19.2	109	1.3	4.2	3500	2600
450°C	45m/min	27.7	73.8	1.6	7	3500	2600
450°C	45m/min	15.4	58.5	2.5	7.5	3500	2600
450°C	45m/min	16.4	59.2	3.2	7.8	3500	2600
450°C	45m/min	25.2	64.3	2.5	6.7	3500	2600
450°C	45m/min	25.2	64.3	2.5	7.2	3500	2600
470°C	25m/min	22.8	119.9	1.2	4.1	3500	2500
470°C	25m/min	18	110.4	1.8	4.1	3500	2500
470°C	25m/min	18.5	117.5	1.8	3.6	3500	2500
470°C	25m/min	16.4	114.6	2	4.4	3500	2500
470°C	25m/min	17	112	1.8	4.1	3500	2500
470°C	30m/min	14.1	112.9	2	4.5	3500	2400
470°C	30m/min	17	97	1.9	4.6	3500	2400
470°C	30m/min	16.4	94.9	1.6	4.8	3500	2400

Table 8 Ram speed and ram pressure data